FFI-RAPPORT

16/00869

External man-made radio noise measurements

–

Bjørn Skeie
Bjørn Solberg

External man-made radio noise measurements

Bjørn Skeie
Bjørn Solberg

Norwegian Defence Research Establishment (FFI) 4 October 2016

Keywords

Radiostøy
Målinger

FFI-rapport
FFI-RAPPORT 16/00869

Prosjektnummer
1294

ISBN
P: 978-82-464-2726-3
E: 978-82-454-2727-0

Approved by
Nils Agne Nordbotten, *Research Manager*
Anders Eggen, *Director*

Summary

This report is the result of the work carried out at Forsvarets forskningsinstitutt (FFI) to evaluate the external man-made radio noise at different locations in Norway.

To solve the task, a measurement campaign was carried out in Norway from 2013 to 2014. The measurement results from the campaign were compared to the noise levels in the categories; city, residential and rural, given in ITU Recommendation, “ITU–R P.372 Radio noise”.

To our knowledge there are no data covering the external man-made noise in Norway, and the main source of the underlying data for ITU man-made noise model is from measurement campaigns in the late 1960s and early 1970s. The question is how the ITU model compares with today’s external man-made radio noise in Norway. One may expect an increase as there is more electronic equipment and devices in use today than there were 40 – 50 years ago.

During the FFI measurement campaign, radio noise in the frequency range 30 – 200 MHz was measured at several locations in Norway. We used dipole antennas with an omnidirectional radiation pattern and measured the external man-made radio noise at four selected frequencies. The noise samples were post-processed to estimate the median noise power, which was converted to an external noise figure with the ITU model reference antenna.

In general, the measured median external noise figure in Norway showed up to be lower than predicted by the ITU-R P.372 man-made noise model.

For the city category the measured external noise figure is within the variability of the ITU data. For the residential category the measured external noise figure is lower than the ITU prediction. For the rural category the measurements indicate that the measured external noise figure is lower than the ITU prediction.

Sammendrag

Denne rapporten er resultatet av et arbeid utført av Forsvartes forskningsinstitutt (FFI) for å evaluere den eksterne menneskeskapte radiostøyen på forskjellige steder i Norge.

For å løse oppgaven er det gjennomført en målekampanje fra 2013 til 2014. Måleresultatene har blitt sammenliknet med støynivåene i kategoriene “city”, “residential” og “rural” gitt av ITU i “Recommendation ITU-R P.372 Radio noise”.

Etter det vi vet, finnes det ikke data som dekker den eksterne menneskeskapte radiostøyen i Norge, og hovedkilden til de underliggende dataene til ITU støymodellen er fra målekampanjer fra seint 1960- og tidlig 1970-tallet. Spørsmålet er hvordan ITU støymodellen er i forhold til dagens eksterne menneskeskapte radiostøy i Norge. Man kan kanskje forvente en økning fordi det er flere elektroniske enheter og utstyr i bruk i dag enn det var for 40 – 50 år siden.

Under FFIs målekampanje ble radiostøyen målt i frekvensområdet 30 – 200 MHz på flere steder i Norge. Vi har brukt rundstrålende dipolantenner og målt den eksterne menneskeskapte radiostøyen på 4 utvalgte frekvenser. Støysamplene har blitt etterbehandlet for å estimere median støyeffekt, som er omregnet til et støytall for den eksterne støyen med ITU modellens referanseantenne.

Generelt kan vi si at medianen av støytallet til den målte eksterne radiostøyen i Norge viste seg å ligge lavere enn hva som ble prediktert av ITU-R P.372 støymodellen.

For ITU-kategorien “city” er støytallet fra den målte eksterne radiostøyen innenfor variasjonsområdet til ITU-dataene. For ITU-kategorien “residential” er støytallet fra den målte eksterne radiostøyen lavere enn prediktert av ITU støymodellen. For ITU-kategorien “rural” indikerer målingene av den eksterne radiostøyen at støytallet er lavere enn prediktert av ITU støymodellen.

Content

Summary **3**

Sammendrag **4**

1 Introduction **9**

2 Fundamentals of man-made radio noise **10**
2.1 External radio noise 10
2.2 The ITU Man-made noise model 13

3 Measurements of the external radio noise figure **18**
3.1 Scope of the measurement campaign 18
3.2 Considerations for the measurement setup 19
3.2.1 Receiving system 19
3.2.2 Measurement of the external Gaussian noise level 20
3.2.3 Antenna considerations 21
3.2.4 Choice of measurement frequencies 22
3.3 Estimating the median and its statistical variability 23

4 Results **24**
4.1 General 24
4.2 Measurement results 25
4.2.1 Presentation 25
4.2.2 On the accuracy of the estimated median values of the external noise 26
4.2.3 Results for the City category 27
4.2.4 Results for the Residential category 29
4.2.5 Results for the Rural category 30
4.2.6 Summary of measurement results 31
4.3 Temporal variability of the man-made noise level 32

5 Conclusions **35**

References **37**

Abbreviations **39**

Appendix **41**

A Supplementary data on man-made radio noise **41**
A.1 Man-made noise model for frequencies above 200 MHz 41
A.2 A survey of post-1974 man-made noise measurements 42
A.2.1 Background 42
A.2.2 ITS measurements in the 136-138 MHz band (1996) 42
A.2.3 ITS measurements at 137,5 MHz and UHF frequencies (1999) 43
A.2.4 ITS wideband noise measurements in VHF and low UHF band (2009) 43
A.2.5 UK Man-made noise measurements - AIMS 44
A.2.6 ITU-R P.372 information on measurements in Europe 2006/2007 46
A.2.7 Man-made noise measurements - UK 2003 47
A.2.8 Montreal/Ottawa measurements 1993 49
A.2.9 Summary of comparisons of measurement data with ITU–R P.372 predictions 50

B Measurement setup and preparations **53**
B.1 Overview of the man-made noise measurement system 53
B.2 Antennas 54
B.3 Tripod 55
B.4 Cables 55
B.5 Filters 56
B.5.1 Low-pass filter 56
B.5.2 Band-pass filters 57
B.6 Low noise amplifier 57
B.7 Spectrum analyser 57
B.8 Power 57
B.9 Laptop 58
B.10 NSM Noise Measuring System 58
B.10.1 Hardware configuration 59
B.10.2 Transducer 60
B.10.3 Frequency sweep 60
B.10.4 Noise measurement 62
B.11 Running the measurements 65
B.11.1 Finding a location 65
B.11.2 Finding available measurement frequencies 65

C Post-processing procedures **67**
C.1 Definitions of reference points 67

C.2 Estimating the RMS value of the Gaussian noise component at reference point E 69
C.3 Estimate of the external Gaussian noise contribution at reference point C 72
C.4 Estimating the external noise figure referred to a half-wave dipole antenna 74
C.5 Conversion of the external noise figure to the ITU-R P.372 reference antenna 76

D Antenna VSWR and gain 78
D.1 SRS 25 – 2000 MHz 78
D.2 Comrod VHF30108VM 79
D.3 Comrod VHF108185VM 81
D.4 Amphenol Jaybeam 7177010, 100 – 500 MHz 83

E Filter responses 84
E.1 Wavetek BP-filter 31 – 62 MHz 84
E.2 Mini-Circuits LP-filter NLP-250 86

F System attenuation and gain 87
F.1 Measurement frequency 30,45 MHz 87
F.2 Measurement frequency 84,5 MHz 88
F.3 Measurement frequency 114 MHz 89
F.4 Measurement frequency 194 MHz 90
F.5 Measurement frequency 203 MHz 91
F.6 Cable attenuation 92
F.7 System gain, all frequencies 92

G Frequency sweeps 94

H Intermodulation distortion 96

I Listing of locations 100

J Maps and photos of locations 104
J.1 Location_2 104
J.2 Location_3 105
J.3 Location_4 105
J.4 Location_5 106
J.5 Location_6 106
J.6 Location_7 107
J.7 Location_8 107
J.8 Location_13 108

J.9 Location_16 109
J.10 Location_17 109
J.11 Location_18 110
J.12 Location_19 110
J.13 Location_20 111
J.14 Location_23 111
J.15 Location_24 112
J.16 Location_34 112
J.17 Location_35 113
J.18 Location_36 113
J.19 Location_37 114
J.20 Location_43 114

1 Introduction

The sensitivity and range of radio receiving systems are ultimately limited by noise signals that are present in the receiving system. Noise contributions originating from the circuitry or components of the receiving system are always present, and these are collectively referred to as *internal noise*. The total amount of the internal noise power of the receiver is commonly characterised by its noise figure in dB (or, by its noise factor, which is the linear equivalent). Alternatively, the internal noise power can be expressed by an equivalent noise temperature at the input of the receiving system.

However, another type of noise contribution is generated by noise emissions from external sources. The electromagnetic field density caused by radiation from such sources will be converted to an electric noise power by the receiver antenna and is delivered to the input of the receiving system. This type of noise contribution at the receiver input is termed *external radio noise*. Such external noise will add to the internal noise of the receiver. At frequencies below about 100 – 200 MHz, the external radio noise may easily be the dominant noise contribution of the receiving system.

Hence the operating sensitivity of a radio receiving system depends on the sum of the internal and external noise power. Whenever the external noise is the dominating contribution, a receiver with a lower noise factor will not improve the operational sensitivity. In this case the external noise will limit the range of the radio communication system.

ITU–R P.372 (1) is a key document on external radio noise and provides noise prediction models on various categories of external noise sources. One of these categories, man-made noise, is quite special in the sense that its noise levels depend on human-made activities or processes thereof. For this reason the man-made noise level will vary with location and with time. ITU–R P.372 offers a man-made noise model based on historical recordings of man-made noise levels, and this model is commonly used as a general framework and as a tool for predictions of man-made noise levels. However, the statistical data of the noise levels on which the ITU–R P.372 man-made noise model relies, are based on a US measurements program that was carried out approximately 40 years ago.

The nature of, and as well as the number of, possible sources of radio noise that may contribute to man-made noise have probably changed considerably during this 40 year period. Hence the validity of the ITU–R P.372 man-made noise model as a tool for current and future predictions of radio noise could be questioned. Moreover, we are not aware that there exists any measurement data on man-made noise levels for locations in Norway; hence the full validity of the ITU–R P.372 man-made noise model in this country does not seem to have been explored. For these reasons it has been found useful to update our knowledge base on man-made noise by carrying out a measurement program on the man-made noise created at selected Norwegian locations.

This is the background for the noise measurement project that is documented in this report, the main objective of which is to measure external radio noise levels in the VHF band at some selected locations and to relate these measurements to the predictions according to the ITU–R P.372 man-made noise model. The actual noise measurements were done at various locations in Norway by FFI personnel, who also performed the post-processing and the reporting. The work was carried out on behalf of the Norwegian National Security Authority (Nasjonal sikkerhetsmyndighet - NSM).

2 Fundamentals of man-made radio noise

2.1 External radio noise

Electromagnetic noise power from external sources is converted to electrical signals by the antenna of a receiving system, where it is combined with the internal noise power of the receiving system. Man-made noise, which is the main topic of this report, is one specific type of external radio noise. Some other sources of external radio noise are:

- Radiation caused by lightening discharges (atmospheric noise)
- Galactic noise (also called cosmic noise), originating from the sun or other celestial radio sources
- Radiation from the ground or other obstructions within the antenna beam

The noise from the various external noise sources are additive. As a guideline, and somewhat depending on location, the man-made noise may be considered to be the dominating external noise source at frequencies from (high) HF up to the low UHF frequency range. Atmospheric noise can be considered to dominate at low frequencies up to the low HF frequency range. Galactic noise may dominate at high HF and VHF/UHF frequencies, but only at locations where the man-made noise is very low.

The level of the external radio noise in a reference bandwidth can be expressed quantitatively by different measures, the most common of which is:

- the RMS value of the electric field strength of the external noise.
- the available electrical power received by a lossless reference antenna.
- an “external noise figure” (or an “external noise factor”), which is based on a normalization of the available electrical power of the external noise from the lossless

reference antenna relative to the fundamental noise level defined by Boltzmann's constant, temperature, and bandwidth.

- an "effective antenna temperature" of the external noise, easily calculated from the external noise factor by the standard conversion formula.

The ITU–R P.372 expresses most of its external noise power data, and all of its data on man-made noise, by means of the "external noise figure". Therefore, all measurement results of this project will also be quoted as the external noise figure according to the definitions of the ITU–R P.372 recommendation.

ITU-R P.372 gives parameter definitions as well as equations for how the external noise factor and the internal noise factor of various components combine to an overall system noise factor. The following nomenclature and definitions, which are used by the ITU–R P.372, are introduced for the receiving system:

p_n : the available noise power from an equivalent lossless antenna,

t_0 : the reference temperature, (usually) taken as 290 K,

b : the noise power bandwidth of the receiver,

f_c : the noise factor associated with the antenna circuit loss,

f_t : the noise factor of the transmission loss (i.e. cable loss) between the antenna and the receiver,

f_r : the noise factor of the receiver,

f : the system noise factor referred to the equivalent lossless antenna

The *external noise figure* is defined as

$$F_a = 10log(f_a) \qquad (1)$$

Where the *external noise factor*, f_a, is defined by

$$f_a = \frac{p_n}{kt_0b} \qquad (2)$$

k is Boltzmann's constant. Since the available noise power from the equivalent antenna depends on the actual type of antenna being used, the value of the external noise figure also depends on the specific antenna type used as reference. The noise figures quoted in the ITU–R P.372 man-made noise model presumes the use of a short vertical lossless grounded monopole antenna receiving a surface wave signal.

The *system* noise factor, f_{system}, defines the combination of external and all internal noise contributions referred to a (hypothetical) lossless antenna. When the equipment and ground temperatures are equal to t_0, the system noise factor can be expressed as

$$f_{system} = f_a + f_c f_t f_r - 1 \qquad (3)$$

According to these ITU parameter definitions, an antenna introducing a loss (called "antenna circuit loss" in the recommendation) will influence the total system noise factor by both the value of parameter f_a (i.e., its external noise factor) as well as by f_c (i.e., the internal noise factor caused by its losses).

The relationship between the RMS electromagnetic field strength of the composite external noise and the available externally generated noise power from an antenna clearly depends on the receiving antenna parameters. Hence, the value of the external noise figure is dependent on the type of receiving antenna. This relationship is evaluated by Hagn in (2), where quantitative relationships are given for a few simple omnidirectional antennas.

For a short vertical monopole above a perfect ground plane, the vertical component of the RMS field strength in a 1 Hz bandwidth can be expressed as (1), (2):

$$E_n = F_{a,mono} + 20\log(f_{MHz}) - 95{,}5 \quad (\text{dB}\mu\text{V/m per Hz}) \qquad (4)$$

This equation assumes that the propagation mode of the noise field is the surface wave (2).

For a lossless half-wave dipole antenna in free space the relation is (1), (2):

$$E_n = F_{a,d} + 20\log(f_{MHz}) - 98{,}9 \quad (\text{dB}\mu\text{V/m per Hz}) \qquad (5)$$

$F_{a,mono}$ and $F_{a,d}$ are the external noise figure of the monopole and the dipole as defined by eq. (1). As mentioned, the ITU external noise figure values are in general referred to the short vertical monopole above a perfect ground plane, i.e. by $F_{a,mono}$ in equation (4). For short, it is simply termed F_a in this document.

In general, the external noise field strength is a statistical variable over space and time. This is reflected by the tools and the empirical models for external noise predictions, which tend to express the noise parameter F_a by statistical parameters relevant for a given frequency, geographic location and time. Man-made noise levels are dependent on the type of local environment, and the statistical data for F_a are offered for different environmental categories. The noise figure ($F_{a,m}$) or the noise factor ($f_{a,m}$) is commonly expressed by the *median* value of the statistical distribution that applies to the relevant category. The next section will give some more detail on the ITU man-made noise model.

Figure 2.1 shows graphics excerpted from ITU-R P.372 illustrating the presence of various types of external noise as a function of frequency. Note that the level of atmospheric noise in this figure is given not by the median, but by its extreme values (curves A and B) in order to

indicate its enormous variation range over time and location. Man-made noise normally plays a significant role at VHF frequencies. Depending on time of day and season, man-made noise may also be a major contributor at HF and even MF frequencies.

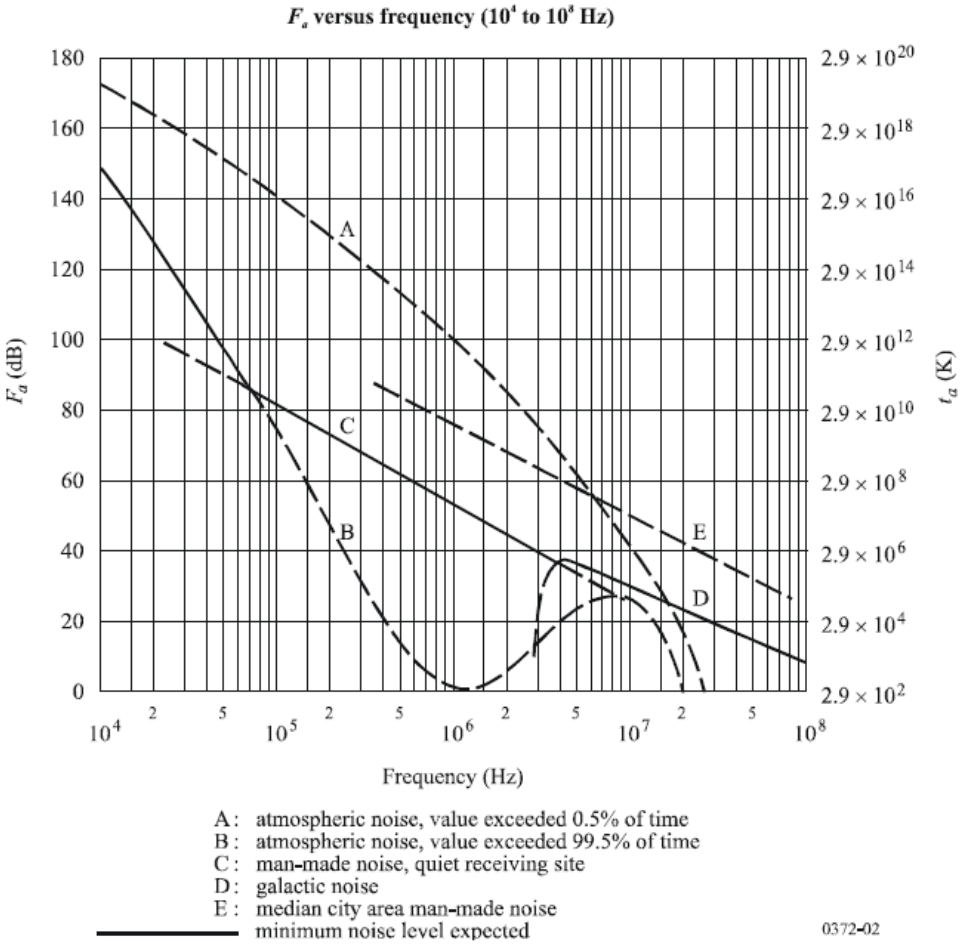

Figure 2.1 Examples of values of the external noise figure for various noise sources. Excerpt from ITU-R P.372 (1).

2.2 The ITU Man-made noise model

The most recognised source of data for man-made noise is that of the ITU-R P.372 recommendation (1). Its man-made noise model enables predictions of the median man-made noise level and offers some information of its statistical variability. Moreover, the CCIR Report 258-5 (3) discusses various aspects of man-made radio noise and, in particular, it offers a more detailed statistical description of its variation than what is found in ITU-R P.372 (1).

In general, man-made noise is considered to be composed mainly of two components, one which have a Gaussian distribution and a second component which has an impulsive character.

Both the above documents are concerned mainly with the Gaussian component of the man-made noise, which is generally considered to be the most important one. The above documents offer very limited treatment of man-made *impulse* noise, which in some special cases also needs to be taken into account. However, as we want to compare data to the ITU man-made noise model, this report will only be concerned with the Gaussian component of man-made noise.

Even though the latest version of the ITU-R P.372 is relatively new (edition 11 was issued in 2013), the main source of the underlying data for the ITU man-made noise model is rather old. This data was produced from man-made radio noise measurement campaigns taking place in the late 1960s and early 1970s. These campaigns were carried out under the auspices of the organization that preceded the current Institute of Telecommunications Sciences (ITS) in Boulder, Colorado[1], and will be referred to as the "ITS campaigns".

During these ITS campaigns, measurement data were simultaneously collected at ten frequencies during "mobile runs" through a measurement area. The results are documented in (4), which presents the measured noise data statistically according to the environmental category of the area in which the data was acquired.

Three main environmental categories were defined in (4): Business areas, Residential areas and Rural areas. These were, along with the database created from the ITS measurement campaign, adopted by the ITU-R P.372 recommendation for the man-made noise model. However, in the last editions of the latter recommendation the "Business" category has been renamed to the "City" category. The ITS measurement campaign and its database were based on explorations in 31 rural areas, 38 residential areas and 23 business areas in USA (5), (6). This ITS database is the basis for the statistical data of the man-made noise given by ITU in ITU-R P.372 (1).

The categorization used by ITS (4) and ITU (3), generally conforms to the following environmental guidelines:

- Business areas are defined as any area where the predominant usage throughout the area is any type of business (e.g. stores and offices, industrial parks, large shopping centres, main streets or highways lined with various business enterprises, etc.).

- Residential areas are defined as any areas used predominantly for single or multiple family dwellings with a density of at least five single family units per hectare and no large or busy highways.

- Rural areas are defined as areas where land usage is primarily for agricultural or similar pursuits, and dwellings are no more than one every two hectares.

- Quiet rural are defined as locations chosen to ensure a minimum amount of man-made noise. The data for these categories has been obtained from measurements at selected

[1] ITS is the research arm of the US National Telecommunications and Information Administration (NTIA)

receiving sites, such as sites previously used for measurement programs for atmospheric noise.

The ITS measurement campaign (4) also included some limited measurements of man-made noise at other types of areas, such as in parks and at university campuses as well as at interstate highways. However, these categories have been excluded by the ITU-R P.372 recommendation.

Based on the results of the ITS measurement campaign, a linear relationship between the *median man-made noise figure* of an environmental category and the logarithm of the frequency was suggested in (4). This has been directly adopted by the ITU–R P.372 man-made noise model, i.e.:

$$F_{a,m} = c - d\log(f_{MHz}) \qquad \text{(dB)} \qquad (6)$$

The values of the constants *c* and *d* for the different environmental categories are given in Table 2.1, ITU-R P.372 (1). Note that the values of *c* refer to the reception by a short lossless grounded monopole reference antenna.

Environmental category	*c*	*d*
City (Business)	76,8	27,7
Residential	72,5	27,7
Rural	67,2	27,7
Quiet rural	53,6	28,6
Galactic noise	52,0	23,0

Table 2.1 Values for the constants c and d for the different environmental categories, ITU-R P.372 (1).

The values for the median galactic noise figure, which follows a similar linear relationship with log (frequency), are included in Table 2.1 for comparison. Figure 2.2 presents an excerpt from recommendation ITU-R P.372 showing a graphical representation of equation (6).

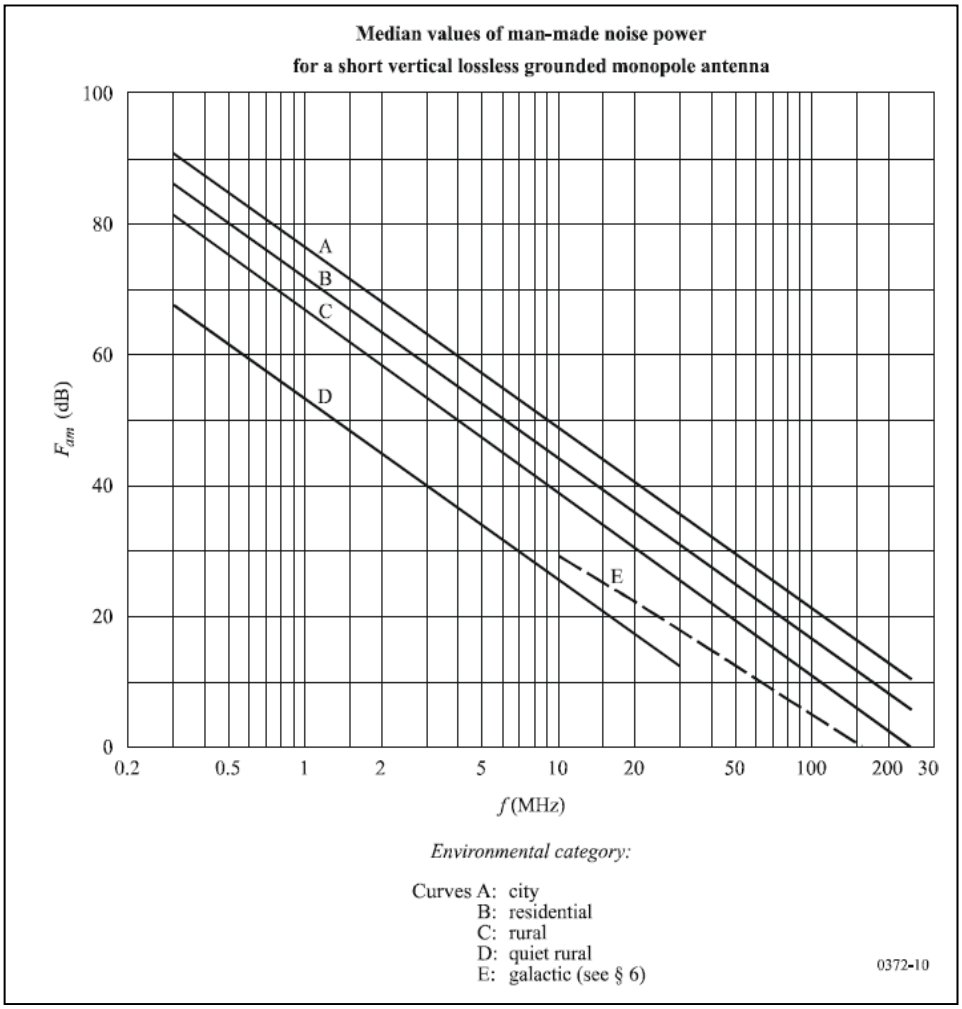

Figure 2.2 Excerpt from the recommendation ITU-R P.372 showing the median man-made noise figure for different environmental categories and for galactic noise.

Note that equation (6) gives the *median value* of the noise figure within a category, and that there may be a significant variation in the actual noise figure from site to site within an environmental category. This spatial variability within a category is normally assumed to follow a Gaussian distribution. It is expressed by the standard deviation, σ_{NL}, of the statistical distribution of the data within the given category, or alternatively, by its corresponding decile value. For each site, there may also be a temporal variation of the man-made noise power.

The temporal variation of the man-made noise figure has been found to have a quite unsymmetrical statistical distribution around its median. For this reason both the upper and lower decile values have been used to express the statistical variation with time for each environmental category. Reference (3), CCIR Report 258-5, presents a comprehensive overview of these noise variation parameters for spot frequencies within 250 kHz to 250 MHz for the three main environmental categories. The data for the temporal variations in (3) are measured within an hour about the hourly median value of the noise power at a specified location.

The ITU-R P.372 recommendation (1) provides a simplified version of the statistical parameters for the variability of the noise figure, disregarding any frequency dependence of these parameter values. This simplified data for the decile deviations is shown in Table 2.2. The overall variation space is very large. Consequently, even if the ITU man-made noise model may estimate the median value for a category with a reasonable accuracy, the large time and location variability does not allow accurate predictions of the man-made noise figure for a specific location or time.

Values of decile deviations of man-made noise

Category	Decile	Variation with time (dB)	Variation with location (dB)
City	Upper Lower	11.0 6.7	8.4 8.4
Residential	Upper Lower	10.6 5.3	5.8 5.8
Rural	Upper Lower	9.2 4.6	6.8 6.8

Table 2.2 Excerpt from recommendation ITU-R P.372, depicting the variability of man-made noise. Although not clearly stated in this recommendation, the background data in CCIR Report 258-5 (3) indicates that the time variation is defined to be variations about the median value within an hour at a given location.

The ITU-R P.372 man-made model can be used to make predictions of the median value of the man-made noise figure over time and locations of an environmental category. However, by using its statistical data on variability, it can also describe that noise figure at a given location in statistical terms, such as by a confidence interval around the median. However, this confidence interval will be quite wide.

Moreover, it is important to keep in mind that the ITU model is a wholly empirical model with its parameters matched to the fundamental measurements made more than 40 years ago. The number and the nature of the man-made noise sources may conceivably have changed significantly since then. There are more electric/electronic gadgets and equipment capable of producing unintended emanations (and hence contributing to radio noise) in use today than 40 years ago. On the other hand, the standards that apply for the control of unwanted emissions from equipment have improved with time. The influence of unwanted emissions from some major radio noise sources 40 years ago, such as ignition noise from engines and emanations from open-air power lines, probably have been greatly reduced since the 1960/70s.

For these reasons there is a significant uncertainty regarding how representative the man-made noise model of the ITU-R P.372 is for today's society. Even so, the man-made noise model of the ITU-R P.372 has maintained its role as the most authoritative and most widely used reference model for this type of radio noise as well as for other sources of radio noise.

A number of man-made noise measurement programs have been carried out in the 1990s and onwards, however, the scope of these has been much more limited compared with the ITS measurement program carried out more than 40 years ago. Appendix A reviews some results of these most recent measurements by comparing results with predictions according to the ITU-R P.372 man-made noise model. The results of these comparisons are somewhat diverging, however, there is no indication that the man-made noise level has increased significantly above predictions by the ITU-R P.372 man-made noise model. The results of all but one campaign were judged to be within the statistical variability of the ITU-R P.372 man-made noise model or below its predicted median noise level. In particular for the Residential environmental category, the material gives some indications that the median noise level might have decreased significantly during the years since the early 1970s.

The ITU-R P.372 man-made noise model claims a validity from 0,3 to 250 MHz. For frequencies higher than 200 MHz an alternative prediction model is proposed by Hagn (8). The latter model is briefly described in Appendix A.

3 Measurements of the external radio noise figure

3.1 Scope of the measurement campaign

The following guidelines were laid down for the man-made noise measurement campaign:

1. The main objective of the program should be to perform external noise measurements at different outdoor locations in the frequency range from about 30 MHz to about 200 MHz.

2. The measurement setup and procedures should be chosen to be compatible with the requirements of the ITU-R P.372 man-made noise model, and the results should be easily related to the predictions of this model.

3. The program should include measurements at a sufficient number of locations for each ITU environmental category (City, Residential, Rural) to estimate the median noise power with a reasonable statistical variance for a meaningful comparison with the ITU-R P.372 man-made noise prediction model.

4. The measurement setup should be portable and operable without access to local AC mains power.

3.2 Considerations for the measurement setup

3.2.1 Receiving system

The main tasks of the measurement system for Gaussian external noise are:

- to convert the external noise field strength into an electrical signal,
- to amplify and filter this received electrical noise signal,
- to record its amplitude statistics during a given measurement period at a given measurement location and to calculate the RMS value of the Gaussian noise.

The value of the received noise signal is recorded by amplitude sampling of the noise signal. The sampling rate is 10.000 samples per second. These samples are stored in a “capture file”, which typically contains data for a 10 minutes measurement period. This corresponds to 6 M samples, and constitutes the output of one specific measurement at a given frequency for a location. It will be subject to post-processing for the calculation of the external noise figure for that specific location and frequency. The noise figures for different locations are used to accumulate statistics and for the various types of the ITU environmental categories. From these statistics the median values for each category can be estimated and compared with predicted median values according to the ITU-R P.372 man-made noise model.

The measurement system comprises an antenna and a high-performance receiving system. The receiving system should operate with a low noise figure in order to be able to measure the low external noise levels that can be found in rural areas. It should not generate spurious responses or intermodulation products by any strong off-channel signals that might be presented to it by the antenna. This will require the use of pre-selection filters, and even with pre-selection filters, strong off-channel signals poses a minimum of linearity requirements to the components used by the receiving system.

Appendix B gives an overview of the measurement system, and describes some of its components. A key component is the NSM Noise Measuring System 1.1, which is a program for managing and executing the measurements and which assembles the noise capture file that comprises the output of each of the physical measurement.

Appendix C describes the post-processing procedures and explains the technical background for the methods used. These post-processing procedures concern the methods applied for conversion of the data of the capture file for a specific measurement into a corresponding final value of the external noise figure that is directly compatible with the ITU-R P.372 man-made noise model. Appendix D to F gives more details of components of the measurement setup including some performance data.

The external noise from the antenna will be superimposed on the internal noise generated by the receiving system. The samples of the capture file will reflect the sum of these two contributions. The best measure of the level of the external noise component is achieved by subtracting an estimate of the internal noise level from the total noise recorded. The internally generated noise level can be determined from a calibration process by replacing the antenna with a 50 ohm termination. This process is described in (15) and is also explained in Appendix C.3. This method will enable measurements of external noise levels below the internal noise level. However, at very low external noise levels the measurement accuracy will be reduced.

3.2.2 Measurement of the external Gaussian noise level

The ITU-R P.372 man-made noise model is concerned only with the Gaussian component of man-made noise. Hence it is preferable to use a measurement system that is able to measure the power of only the Gaussian component while rejecting any power contribution of the impulse noise component that might be present.

A receiving system with a conventional true RMS measurement method gives the power sum of both components. The impulse noise component is, in most situations, present in a small fraction of the time. However it may exhibit a very high instantaneous power level during its time of presence. For this reason, the presence and the influence of impulse noise can be detected by collecting enough data to estimate the amplitude probability distribution (APD) of the received noise signal. This method is applied by the various ITS campaigns documented in (9), (10) and (11). The cumulative APD is expressed mathematically as

$$F(a) = P(X > a) \qquad (7)$$

Where *P( )* means probability, *X* is a function assigning a real number (i.e. the amplitude level) to every element of a sampled space, and *a* is an amplitude value.

An estimate of the APD of the measured noise can be obtained by sampling the complex-baseband signal of the receiving system N times and converting each of these samples to an amplitude value.

It is well known that the APD of complex Gaussian noise (i.e. the square of the sum of the In-phase and the Quadrature noise signal) follows a Rayleigh distribution. For this reason it is very instructive to display the cumulative APD in a so-called Rayleigh graph. The axes in a Rayleigh graph are transformed by functions that linearize the cumulative APD of the Rayleigh distributed amplitude function. This means that for complex Gaussian noise (which is representative of the noise modelled by the ITU-R P.372 man-made noise model), the cumulative as well as the complimentary cumulative APD, the CCAPD, will show up as a straight line in the Rayleigh graph. Such a Rayleigh graph presentation of the CCAPD is frequently simply referred to as the APD of the measurements; which is a terminology that will be used also in this report.

The RMS value of a Rayleigh distributed variable will be approximately equal to the 37th percentile of the complementary cumulative APD. Hence, the 37th percentile value of the measured CCAPD can be used as an estimate for the RMS value for the Gaussian noise component also in cases the received noise contains an impulse noise component. This will be a very good estimate for the RMS level of the Gaussian noise component as long as the channel is dominated by impulses for less than about 5 % of the time. The shape of the actual APD in the Rayleigh graph will reveal how well this criterion is met.

All our external noise figure calculations are based on using the 37th percentile of the APD of the capture file as an estimate for the RMS level of the Gaussian noise components. For comparisons, also the true RMS level of the received noise was calculated. In cases with very high levels of impulse noise, the discrepancy was found to be quite significant (the true RMS value being several dB higher than the 37th percentile). However, in most cases the impulse noise contribution was not significant, leaving the discrepancy between the 37th percentile and the true RMS value to be less than one dB.

The data for generating the cumulative APD for a given location/frequency was based on the capture file providing amplitude samples generated by a spectral analyser operating in the zero span mode. As already mentioned, the sampling rate was 10 k samples/s, and the measurement period was nominally 10 minutes. Hence, a capture file with the raw data comprises 6 M samples for each measurement frequency and location. The size of this capture file is about 82 Mbyte.

3.2.3 Antenna considerations

The ITU-R P.372 man-made noise model defines the external noise figure based on the available external noise power from a reference antenna, which is a short vertical lossless grounded monopole antenna. This antenna is omnidirectional in the azimuth plane. It is important that the measurement antenna maintains this omnidirectional characteristic in order to arrive at results that can be directly compared to ITU-R P.372 man-made noise model predictions in all emanating environments. However, it is not a requirement that the measurement antenna is a short monopole. Other antenna types may be used, as long as the relationship between the RMS noise field strength and the external noise figure of this (lossless) antenna is known. This relationship has the following general expression (2):

$$E_n = F_{a,x} + 20\log(f_{MHz}) - C_x \qquad \text{(dBµV/m per Hz)} \qquad (8)$$

C_x is a constant characteristic for the particular antenna type, and $F_{a,x}$ is the actual (measured) external noise figure referenced to this particular antenna type. We have already seen from equation (5) that the constant C_x is 98,9 dB for a half wave dipole. For dipole antennas of other length ratios but below about 3λ/4, the value of C_x will vary only quite slightly.

FFI decided to use dipole antennas for the measurement program. Tuned half-wave dipoles would have given the best sensitivity. However, for practical reasons we chose to make use of

available tactical dipole antennas for VHF communications, although these will introduce some losses compared to a tuned half-wave dipole. This approach enabled measurements from about 30 to 200 MHz by using two “broadband” antennas. One covers 30 – 108 MHz. The other covers 108 – 185 MHz nominally, while maintaining a good VSWR performance to above 200 MHz. The antennas have a built-in matching network providing an undesired but acceptable loss. Both of these antennas have an excellent omnidirectionality in azimuth. The vendor (COMROD) supplied calibration gain data as part of the antenna specification. This is helpful for estimating the antenna circuit loss, which is an important parameter for calculation of the external noise figure in the post-processing phase. Initially the post-processing was based on this data only. However, the values for the antenna circuit loss for the 30 – 108 MHz antenna was later revised because the post-processing indicated that the antenna had lower gain at 84,5 MHz compared to its specifications. The revised data includes the influence of the antenna tripod too, and was based on antenna measurements performed at FFI. This is explained in detail in Appendix C.4

Appendix D presents data for the antenna gain, as specified by COMROD, for the antennas as well as results of VSWR measurements performed for the individual antennas used during the measurement campaign.

The electrical length of the dipole antennas varies with frequency. Hence the directive gain and the constant C_x will vary slightly with frequency. However, during the processing to arrive at an external noise figure, this variation is disregarded, and the post-processing makes use of the parameters of a half-wave dipole antenna for all frequencies.

Appendix C.4 explains how the antenna parameters are used to estimate values of the antenna circuit loss that are used in the post-processing of the capture file in order to arrive at the value of the external noise figure.

3.2.4 Choice of measurement frequencies

The measurement campaign covers frequencies in the range of about 30 to 200 MHz, and measurements were carried out at spot frequencies at locations spread over a wide geographical area of Norway. It is essential that the external noise measurements take place on frequencies that is not disturbed by interference from “intentional” transmitters. For calculation of statistical median values, it is considered an advantage to keep the measurement frequencies identical at all measurement locations. For the measurements it was decided to measure noise on at least three, preferably four, frequencies spaced over the chosen frequency range. The measurement bandwidth was chosen to be 30 kHz.

Four measurement frequencies were selected after an initial spectral exploration phase, which was executed at a number of locations around the Oslo area. These were:

f_1 = 30,45 MHz

f_2 = 84,5 MHz

f_3 = 114,0 MHz

f_4 = 194,0 MHz (changed to 203,0 MHz during the campaign)

However, during the course of the noise measurements, it was discovered that weak interference signals could occur when measuring at f_3 and f_4 at some locations. To avoid that these signals were recorded as external noise, a spectral scanning process with improved sensitivity was introduced as part as the measurement procedures. At locations where an interference signal was detected at the nominal frequency in the spectral scanning phase, the measurement frequency of the external noise was offset by 50 or 100 KHz to avoid that it would influence the recording of the external noise. Moreover, the measurement frequency f_4 was permanently changed to 203 MHz, since this frequency was found to have a lower probability of interference than 194 MHz.

3.3 Estimating the median and its statistical variability

Even if guidelines 1 and 2 of section 3.1 could be carried out with perfection, our estimate of the median noise of each category/frequency will exhibit a statistical error. The ITU-R P.372 man-made noise model is a statistical model predicting the median power level of the noise at a given frequency and environmental category. As explained in section 2.2 the actual noise level at a specific location within a category can only be described by a statistical distribution.

The ITU-R P.372 states that the location variability within an environmental category may be described by a log-normal distribution around the median. This means that on a dB scale the noise level variability for locations can be considered to follow a Gaussian distribution around the predicted median with a given standard deviation (σ) in dB. As shown in Table 2.2, the ITU-R P.372 characterises the variability the decile variation D rather than by the standard deviation σ. However, in a Gaussian distribution these two parameters are related by the following expression:

$$\sigma = {}^{D}/_{1,28} \qquad (9)$$

The median is the numerical value separating the higher half of data values of a population (or in a probability distribution) from the lower half. If a population comprises M observations, the values are arranged in a list from the lowest value to the highest value. The median value of the M observations is defined as:

- When M is an odd number, the median is defined as the middle element of the sorted list.
- When M is an even number, the median is defined as the mean of the two middle values of the sorted list.

In cases where the parameter observed has a large statistical variation, M needs to be high if a good estimate of the median is needed. The standard deviation of the distribution of external

noise factor within an ITU environmental category is quite large, which is evident from Table 2.2 and equation (9). For example, the upper and lower decile location variation for the City environment is 8,4 dB.

The estimate of the population median from a population of *M* Gaussian (*m, σ*) variables will, asymptotically (i.e. for large *M*), follow a Gaussian distribution with a mean value *m* and with a standard deviation of σ_{med} :

$$\sigma_{med} = \sigma * \sqrt{\frac{\pi}{2*M}} \qquad \text{(dB)} \qquad (10)$$

Using this simple expression with a population of 10 different location measurements of the City category with a decile location variation equal to 8,4 dB, the standard deviation for the estimated median is 2,6 dB. The corresponding decile variation of the median will be 3.3 dB. Hence, this population size would yield an accuracy for the estimate of the City median of approximately ±3,3 dB of its true value with an 80 % confidence level.

Equation (10) overestimates the value of σ_{med} when the population size *M* is small and particularly when *M* is an even number. More accurate expressions for σ_{med} , that are applicable for low values of *M* can be found in p. 271, (17). We will use the calculated values of σ_{med} to assess the statistical significance of the deviations between our calculated median value of the external noise figure and the ITU-R P.372 predicted one. Table 4.2 offers the estimated values for σ_{med} for the number of locations tested during the measurement campaign.

4 Results

4.1 General

The measurement campaign primarily aimed at exploring the external noise level at different outdoor locations. The measured external noise level is converted to an external noise factor with the same reference antenna as the ITU-R P.372 noise model as part of the post-processing. The campaign relied on a static measurement setup with observations of the noise level during a fixed time interval, usually 10 minutes, for each of the measurement frequencies used. Each measurement location was assessed with respect to conformation to environmental categories as defined in the ITS (4) and ITU (3) guidelines, and the results were grouped accordingly. At some locations this was not a clear-cut decision, leaving some room for uncertainties. Appendix I and Appendix J give some practical information of the measurement locations of the campaign.

According to the objectives of the measurement campaign, the radio noise measurements have been done measuring the external noise at various outdoor locations. In total 20 locations according to the ITU categories were covered, with a fairly large geographic spread.

The temporal variability of the external noise factor was not given much attention during the measurement campaign, and it was subject to observation only at one location. However, some impression of the variability of the external noise level was gained by real-time observation of colour-coded graphical output of the sampled noise levels.

4.2 Measurement results

4.2.1 Presentation

Following the philosophy of the ITU-R P.372 man-made noise model, the presentation of the external noise measurement results are organized in groups of locations belonging to the same environmental category. The measured external noise figure at a given location/frequency is calculated according to the post-processing procedure described in Appendix C. This allows easy comparison with the predictions by the ITU-R P.372 model.

The measurement campaign results are documented in tables for each ITU category. The tables give the external noise factor on a per location basis, and also give a few key statistical parameters for the population of each ITU category. The most important of these parameters is the median value of the population, as this is the parameter predicted by the ITU-R P.372 man-made noise model. The calculated median of the measured external noise can be compared with ITU-R P.372 predictions for the same environmental category. Table 4.1 provides an overview of the ITU-R P.372 predictions at the measurement frequencies.

Frequency (MHz)	30,45	84,5	114	203
F_{am} City (dB)	35,7	23,4	19,8	12,9
F_{am} Residential (dB)	31,4	19,1	15,5	8,6
F_{am} Rural (dB)	26,1	13,8	10,2	3,3
F_{am} Galactic (dB)	17,9	7,7	4,7	-1,1

Table 4.1 ITU-R P.372 predictions of the median man-made and galactic noise figures at the measurement frequencies of the campaign.

However, the accuracy of the estimated median must be taken into account when doing this comparison. As will be seen, the standard deviation of our median estimate is relatively large. This is due to the high location variability and the relatively small number of locations

measured per category. This statistical error, which will be discussed in the next section, will add to the normal measurement errors of each measurement.

4.2.2 On the accuracy of the estimated median values of the external noise

The locations are selected first and foremost because they comply fairly well with the characteristics defined for one of the three ITU categories, while at the same time allowing for the parking of the vehicle and offering enough open space for establishment of the antenna with only a minimum influence on its omnidirectionality. Such practical problems in some cases proved to be a general limitation with regard to finding suitable measurement sites, in particular for the City category of locations. Such good compliance with the ITU definitions of the ITU environmental categories is necessary to reach trustworthy conclusions of the campaign. As one can see from the location numbering, a lot of measurement locations have been registered, but only 20 of these falls into the ITU categories. The other measurement locations are for experimental purposes, or measurement locations that do not qualify to the ITU definitions of the categories, and are not the scope of this report.

The campaign comprised 20 locations according to the ITU categories. A median noise figure is estimated for each environmental category. Since the external man-made noise level exhibits a relatively large stochastic variation for locations within an environmental category (confer Table 2.2), the number of independent locations measured in each category will influence the accuracy of the estimate of the medians that are provided for this category. Altogether, measurements at 9 Residential locations, 6 Rural locations and 5 City locations were carried out.

According to the ITU-R P.372 the location variability may be assumed to follow a log-normal distribution. Using the location decile variations of Table 2.2 as a basis, an assessment of the expected accuracy of the estimated median of each category can be made. This is shown in Table 4.2.

Category	ITU-R P.372 Decile variation	ITU-R P.372 standard dev. σ	Number of locations	Expected std. dev. of median σ_{med}	Expected decile variation of median	Expected 95-percentile of median	Expected 97,5-percentile of median
City (dB)	8,4	6,6	5	3,5	4,5	5,8	6,9
Residential (dB)	5,8	4,5	9	1,8	2,3	3,0	3,5
Rural (dB)	6,8	5,3	6	2,6	3,3	4,3	5,1

Table 4.2 Assessment of statistical errors in the estimate of the median of the environmental categories, assuming that the location variations follow a Gaussian distribution.

Column 2 of Table 4.2 simply repeats the ITU-R P.372 data on decile deviation on location variations from Table 2.2. Column 5 shows the expected standard deviation of the estimated medians, taking into account the actual number of locations measured by category. This standard deviation is calculated not by using equation (10), but by using expressions given in (17) that give better accuracy for small populations.

The last three columns give the 90th percentile (i.e. the upper decile), the 95th percentile and the 97,5th percentiles of the distribution of statistical errors of the estimate of the median, assuming that these statistical errors follow a Gaussian distribution even for small population sizes.

It is seen from Table 4.2 that the statistical errors of the estimate of the median for a category are quite large. This standard deviation can only be reduced by increasing the number of locations measured per category.

The 95th percentile column of Table 4.2 indicates the ± accuracy (i.e. the "confidence interval") of the estimates of median noise figures with a 90 % confidence level, provided that location variations are the only contributions to estimation errors. It is also assumed that the ITU-R P.372 data on the decile location variations is still a valid representation.

However, there are other effects that may cause variations, such as the temporal variation of the external noise at a location. Table 2.2 shows the ITU-R P.372 statistical data on time variations. This data shows very large decile variations, which would contribute significantly to the percentile values for the influence of the combined location and temporal variations. However, we did not observe any signs of such large temporal variations during the measurement campaign. For this reason we suspect that the ITU-R P.372 data on temporal variations in Table 2.2 may be somewhat outdated.

It is necessary to keep these statistical considerations in mind when comparing the campaign results with the ITU-R P.372 man-made noise model. For example, if the difference between the estimated median for a category and its ITU prediction is smaller than the 95th percentile added with some extra margin to cover for time variations and errors introduced by the measurement setup, the campaign results may be regarded as supportive of the ITU-R P.372 man-made noise model with a probability of 90 %.

On the other hand, if the difference between the estimated median for a category and its ITU prediction is larger than the 95th percentile added with some extra margin, the campaign results will be regarded as an indication of a real deviation from the ITU-R P.372 man-made noise model.

4.2.3 Results for the City category

Table 4.3 shows the results of the external noise figures measured at City locations. The estimated population median is lower than the ITU-R P.372 predictions at three of the four frequencies measured. At 84,5 MHz the measured median is the same as the prediction.

			F_a (dB) @ Frequency				
Loc. Num.	Location Name	Date	30,45 MHz	84,5 MHz	114 MHz	194 MHz	203 MHz
Loc 7	Horten, industrial area	5.8.13	28,2	16,1	11,8	7,4	
Loc 34	Bodø, shopping area	25.11.14	35,4	23,9	13,7		3,9
Loc 36	Tromsdalen, shopping center	26.11.14	27,9	10,3	7,8		2,4
Loc 37	Tromsø, shopping area	27.11.14	28,7	23,4	15,9		8,5
Loc 43	Lillehammer, shopping area	13.12.14	34,2	27,9	20,1		14,1
Population median			28,7	23,4	13,7	7,4	
Population mean			30,9	20,3	13,9	7,3	
Standard deviation of mean			3,6	7,0	4,6	4,6	
ITU-R	P.372 City F_{am} prediction of median		35,7	23,4	19,8	12,9	

Table 4.3 Results of measurements at City locations.

The difference between the measured and the predicted median is {-7,0; 0,0; -6,1; -5,5} dB at the four frequencies. The average difference is about 4,7 dB, which is about the same magnitude as the expected 90th percentile of the expected statistical median location variation, as shown in Table 4.3.

However, we are unsatisfied with both the number and the composition of the City locations measured. As is explained in section 2.2 the City category embraces a multitude of sub-categories, such as stores and offices, industrial parks, large shopping centres, main streets or highways lined with various business enterprises, etc. A good choice would be to have selected campaign locations that mirror this composition of sub-categories.

However, for entirely practical reasons we were unable to find sites that mirrored this composition. For example, 4 of the 5 City locations of the campaign were associated with shopping malls. This obviously represents a somewhat skewed composition of locations relative to the original ITS data. Consequently, some additional uncertainties are introduced when comparing the ITU-R P.372 City predictions with the median estimate for the City category of our campaign. For this reason some additional margins should be taken into account in the assessment of this comparison.

The campaign measurements may be interpreted as an indication of a reduction of the external median noise figure at City locations at three of the four frequencies measured. However, we do not consider that this reduction is large enough to have a statistical significance. For this reason we do not consider that data of the measurements challenges the validity of the ITU-R P.372 man-made noise model data for the City environment.

4.2.4 Results for the Residential category

			F_a (dB) @ Frequency				
Loc. Num.	Location Name	Date	30,45 MHz	84,5 MHz	114 MHz	194 MHz	203 MHz
Loc 2	Lillestrøm, close to Skedsmohallen	3.7.13	17,0	8,0	2,8	1,9	
Loc 3	Lillestrøm, Volla school	5.7.13	17,1	7,1	5,0	1,9	
Loc 4	Drammen, Toppenhaug	8.7.13	20,2	4,4	7,4	3,3	
Loc 5	Tønsberg, Slottsfjellet	9.7.15	27,9	17,5	14,8	15,0	
Loc 6	Borre, close to sports area	30.7.13	19,0	4,8	12,7	5,4	
Loc 18-2	Sørum, Lørenfallet	7.11.13	26,2	15,6	9,1	6,7	
Loc 19	Aurskog, Aursmoen	8.11.13	19,6	5,1	5,7		3,0
Loc 24	Løten	22.11.13	27,8	7,2	6,4		3,1
Loc 35	Tromsø, Prestvannet	27.11.14	24,4	6,6	6,6		5,5
Population median			20,2	7,1	6,6	3,3	
Population average			22,1	8,5	7,8	5,1	
Standard deviation of mean			4,5	4,8	3,8	4,1	
ITU-R	P.372 Residential F_{am} prediction of median		31,4	19,1	15,5	8,6	

Table 4.4 Results of measurements at Residential locations.

The Residential category was given priority with respect to the number of locations measured in order to reduce statistical errors when comparing to the ITU-R P.372 predictions. Table 4.4 shows the results of the external noise figures measured at 9 locations.

The population median is much lower than the ITU-R P.372 predictions at all frequencies; the difference varying with frequency from 4,5 dB to 9,7 dB. The average difference is 7,9 dB. As indicated by Table 4.2, this is more than 2,5 times as much as the expected 95th percentile for the median residence location distribution. Therefore, we consider that this difference is too large to be caused by statistical variances. We consider that it truly reflects that *the median value of the external noise figure for Residential locations in Norway is below what is predicted by the ITU-R P.372 man-made noise data.*

We are not aware of results of prior measurements of the man-made noise figure in Norway. Hence it is not possible to determine with certainty whether this low value of man-made noise has developed over the last decades, or if the Norwegian Residential noise levels was lower than that of the ITU-R P.372 man-made noise data already at the time when the background data for this data was generated in the USA nearly fifty years ago.

4.2.5 Results for the Rural category

			F_a (dB) @ Frequency			
Loc. Num.	Location Name	Date	30,45 MHz	84,5 MHz	114 MHz	203 MHz
Loc 8	Vestfold, road crossing	5.8.13	19,2	10,2	4,1	NA
Loc 13-2	Sørum, Hammeren	30.10.13	20,5	5,3	2,3	-0,6
Loc 16	Sørum, Såkroken	30.10.13	21,4	4,8	1,4	-0,6
Loc 17	Skar, Maridalen	31.10.13	15,8	3,8	2,2	-2,6
Loc 20	Aurskog, Aursmoen	8.11.13	19,1	6,3	3,6	1,1
Loc 23	Budorveien	18.11.13	20,0	4,9	1,4	-2,1
Population median			19,6	5,1	2,3	-0,6
Population mean			19,3	5,9	2,5	-0,9
Standard deviation of mean			1,9	2,3	1,1	1,4
ITU-R	P.372 Rural F_{am} prediction of median		26,1	13,8	10,2	3,3

Table 4.5 Results of measurements at Rural locations.

Table 4.5 shows the external noise figures measured at the 6 locations measured of this category. The external noise measured at the three highest frequencies is similar to or below the

internal noise of the measurement setup, and has been estimated using the subtraction method described in the section C.3 of Appendix C. As explained, this leads to a somewhat reduced measurement accuracy in F_a for these low-level results at Rural locations.

The population median for Rural locations is much lower than the ITU-R P.372 predictions at all frequencies; the difference varies with frequency from 3,9 dB to 8,8 dB and the average difference is 6,9 dB. As depicted by Table 4.2 the expected 95th percentile for the statistical variation of the median location variability is 4,3 dB. This indicates that there is a high confidence that the median man-made noise figure for Rural locations in Norway is lower than the ITU-R P.372 model predictions. However, we consider that more measurements should be made before a firm conclusion can be drawn.

The measurement setup that captures the external noise cannot discriminate between galactic noise and the Gaussian component of the man-made noise. The RMS value measured is simply the sum of the RMS value of both contributions.

Comparing our results for median F_a of the Rural category measurements with the ITU-R P.372 model predictions for galactic noise that is shown in Table 4.1 there is quite a good match at the lowest and the highest frequency. At 84,5 MHz and 114 MHz the measured median is more than 2 dB below ITU prediction of galactic noise. This is well within the ITU statistical prediction, but it indicates that the galactic noise may be a non-negligible contributor to the F_a values presented in Table 4.5.

4.2.6 Summary of measurement results

Figure 4.1 summarizes the above discussions by showing graphically the median values of the external noise figure for each category, and also shows the ITU-R P.372 predicted median values for comparison.

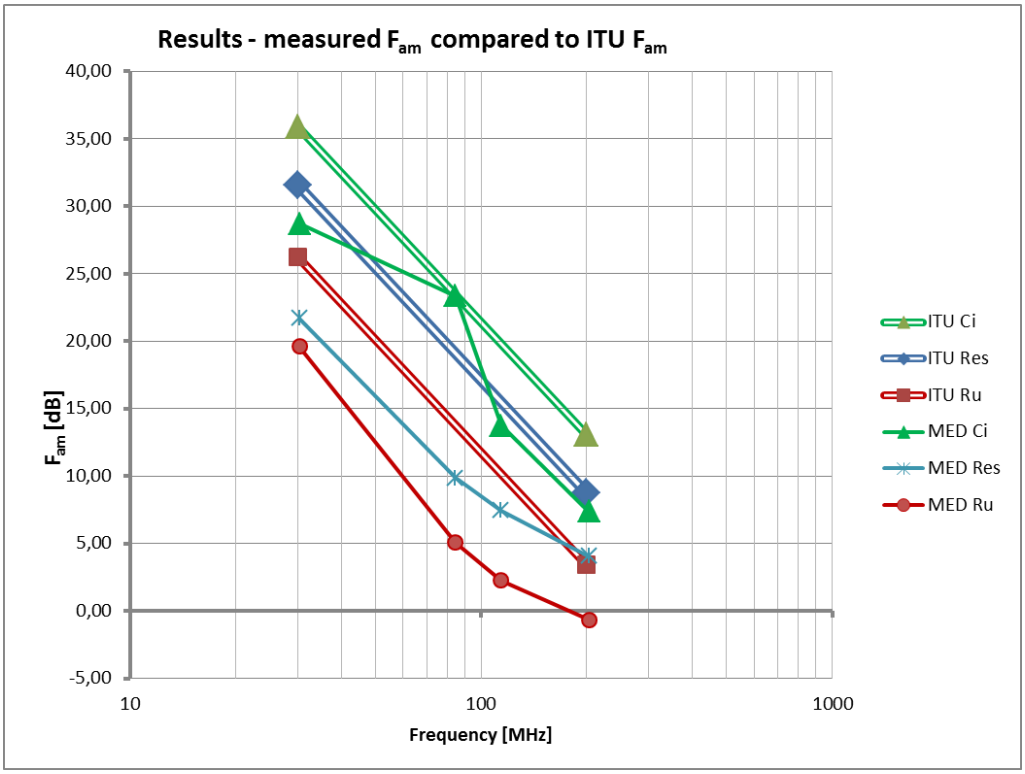

Figure 4.1 Summary of the median external noise figures of the measurement campaign versus the corresponding ITU-R P.372 predictions.

4.3 Temporal variability of the man-made noise level

The ITU-R P.372 data on time variation (confer Table 2.2) indicates a high variability. Contrary to that, the summaries of ITS measurements in 1999 of 24 hours periods in (10) indicates a much lower time variability of the man-made noise level than given by the data of the ITU-R P.372.

Our measurement campaign did not focus of providing statistical data on the temporal variations. However, a normal measurement series of the external noise figure at two locations were repeated with a delay of about two hours or more. Hence, the time variability of a total of eight independent noise figure estimates could be studied by comparing the two available noise figure estimates for the same location/frequencies. For all eight cases only a quite modest time variability was observed, typically one dB or less. This seems to indicate that the time variability seems to be far less important than the location variability of man-made noise.

This approach was extended by an experiment performing identical measurements of the external noise figure several times during an 11½ hour interval at a residential location. All measurement periods were 10 minutes. The purpose was to look for signs of diurnal variations of the external noise level.

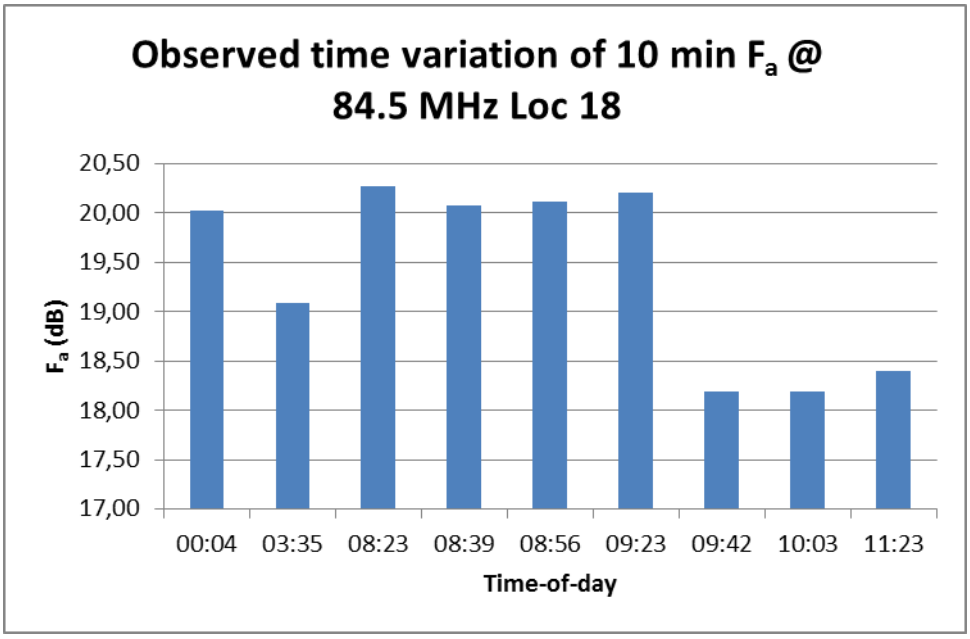

Figure 4.2 The measured external noise figure according to the time of measurement at a residential location. The measurement date was Nov. 7 2013. Note that the bars are not equispaced.in time.

As shown in Figure 4.2 the peak variation in F_a during the interval from midnight to nearly noon is only slightly higher than 2 dB. A very moderate sign of a diurnal variation seems to be present at this residential location. The lowest noise levels are measured in the hours before noon when, presumably, most people have left their homes for work or school.

The time variability parameter as used by ITU-R P.372 (confer Table 2.2) is not clearly defined. However, in (3) which is a CCIR document on man-made noise preceding the ITU-R P.372, the time variation parameter is defined as “the decile deviations from the median value within an hour at the given location”. We interpret the definition of the time variation parameter used in ITU-R P.372 and hence in Table 2.2 to be according to that of (3). Although the definition is not fully non-ambiguous, it seems to be clear that the time variability parameter is meant to quantify only relatively short term variations, and not diurnal ones.

In order to estimate an approximate value of the time variation according to this latter definition, we made a new experiment using our standard measurement setup. We generated 12 different capture files at a given Residential location and frequency, each covering one minute of noise samples. This process lasted for 28 minutes due to the manual handling of the capture process. This gave us a record comprising 12 values of the external noise figures each valid for a one minute period.

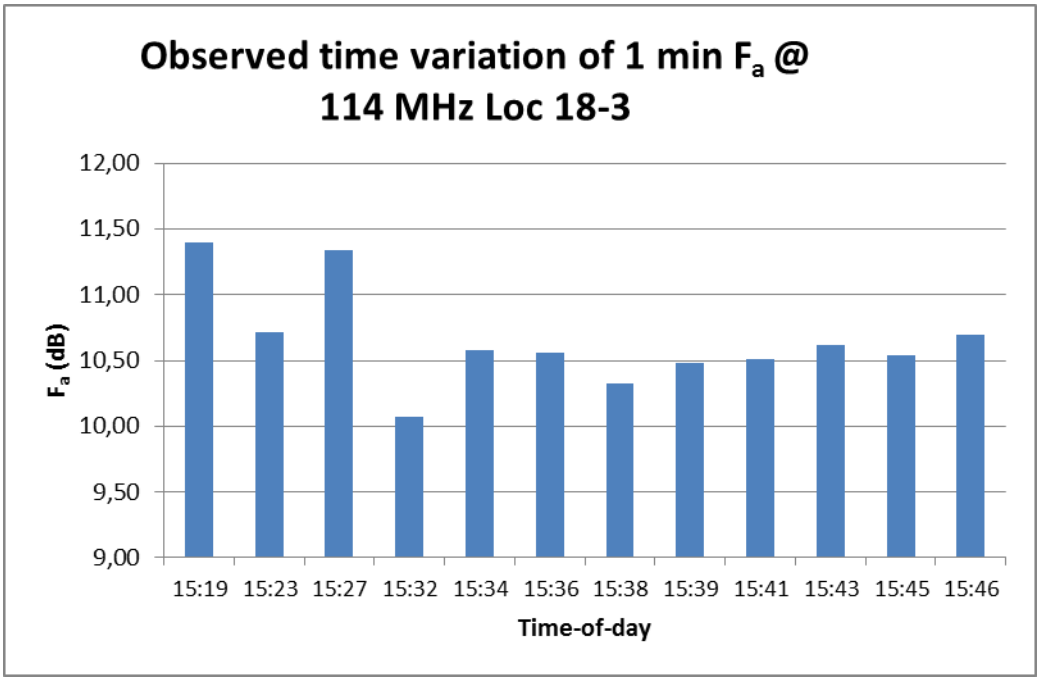

Figure 4.3 The short-time variations of the external noise measured at a Residential location.

The results are shown in Figure 4.3. The data enables us to give a rough estimate of the short term variability based on similar principles as used in ITU-R P.372. The median value of the external noise during the 28 minute interval is estimated by calculating the median of the 12 independently measured noise figures, which is approximately 10,6 dB. This is assumed to be a fair estimate for the median value within the hour.

The difference between the extreme (i.e. max, min) values of the 1 minute noise figures and the one-hour median is 0,8 dB and -0,5 dB, respectively. The upper decile of the difference between the 1 minute noise figure and the hourly median is estimated to D_u = 0,8 dB, while the estimate of its lower decile is about D_l = 0,3 dB. These decile values are vastly lower than the corresponding values given in Table 2.2, which are 10,6 dB for the upper decile and 5,3 dB for the lower decile for Residential locations.

No firm conclusion can be made based on only one measurement series. However, it is considered that the measurement represents an indication that the ITU-R P.372 data of man-made noise time variability may not give a representative description of its current characteristics.

5 Conclusions

FFI has conducted a campaign for measuring the radio noise with the objective of exploring how well the ITU-R P.372 recommendation on man-made noise emanations describes the current conditions in Norway.

The ITU-R P.372 recommendation on man-made noise offers statistical data for three different environmental categories. These are the City, Residential and Rural categories. This recommendation gives its data on noise levels as the median values of the external noise figure for each environmental category as well as information on the statistical variability with location and time.

The FFI campaign covered measurements at 20 fixed locations that were selected as best effort according to the ITU definitions of the three environmental categories. Hence a fair comparison between the measurements and the predicted values from the ITU noise model can easily be achieved.

The measurement results are discussed in chapter 4. The following conclusions and considerations summarize the main findings or tendencies of the measurement campaign:

- The median external noise figure that was measured was in general somewhat lower than what is predicted by the ITU-R P.372 man-made noise model. However, the magnitude of this deviation varied between the different environmental categories.

- Although the measured median external noise figure for the City category was found to be on average 4,7 dB below the ITU predictions, we do not consider that the measurements are contrary the ITU-R P.372 man-made noise model. This is due to the very high location variability of the ITU data and a low number of different types of City locations measured.

- The measured median external noise figure for the Residential category is on average 7,9 dB below the ITU predictions. A total of 9 Residential locations were subject to measurements. We consider that this deviation is large enough to claim with a very high probability that the median man-made noise level at Residential locations in Norway is lower than the ITU-R P.372 prediction.

- The measured median external noise figure for the Rural category is on average 6,8 dB below the ITU predictions for this category. A total of 6 Rural locations were subject to measurements. We consider that this deviation is large enough to indicate that the man-made noise at Rural locations in Norway is probably lower than ITU predictions. However, measurements at more Rural locations are necessary to increase the confidence level of this statement.

- The temporal variability of the external noise was subject to only two simple tests, both of which indicated that the time variability of the man-made noise is much lower than what is depicted by the current ITU-R P.372 data. More measurements would be necessary in order to obtain statistical data.

References

(1) Recommendation ITU-R P.372-11 “Radio noise” 09/2013

(2) G.H. Hagn, “Selected Radio Noise Topics”, SRI International Final Report, Project 5002, Contract No NT83RA6-36001, 1984

(3) CCIR Report 258-5 “Man-made radio noise”, ITU, 1990

(4) A.D.Spaulding and R.T.Disney, “Man-made radio noise, part 1: Estimates for business, residential and rural areas”, Office of Telecommunications Report 74-38, June 1974’

(5) D.B. Sailors, “Techniques for Estimating the Effects of Man-made Radio Noise on Distributed Military Systems”, Proceedings of AGARD Conference, Oct. 1990

(6) G.H.Hagn, “Man-made Radio Noise and Interference”, Proc. of AGARD Conference No 420, Lisbon, Portugal, October 26-30th 1987, pp 5-1 to 5-15

(7) E.N.Skomal, “An Analysis of Metropolitan Incidental Radio Noise Data” IEEE Trans on Electromagnetic Compatibility, Vol EMC-15, No. 2, May 1973

(8) W.R.Lauber and J.M.Bertrand, Man-Made Noise Level Measurement of the UHF Radio Environment”, Symposium Record, 1994 IEEE National Symposium on EMC, San Antonio, TX, 14-26 April 1984

(9) R.J. Achatz, Y. Lo, P.B. Papazian, R.A. Dalke, G.A. Hufford: “Man-Made Noise in the 136 to 138- MHz VHF Meteorological Satellite Band”, NTIA Report 98-355, September 1998

(10) R.J. Achatz, R.A. Dalke, “Man-Made Noise Power Measurements at VHF and UHF Frequencies”, NTIA Report 02-390, December 2001

(11) J.A. Wepman, G.A. Sanders, “Wideband Man-Made Radio Noise Measurement in the VHF and the Low UHF Band, NTIA Technical Report TR-11-478

(12) A.J. Wagstaff, N.P. Merricks: “Autonomous Interference Monitoring System Phase 2”, Final Report Volume 1 – Summary Report, Issue 1, March 2007, MC/SC0585/REP016/1

(13) A.J. Wagstaff, N. Merricks: ” Man-Made Noise Measurement Program (AY4119)”, Final Report, Issue 2, September 2003, MC/CC025/REP012/2

(14) W.J. Lauber, J.M. Bertrand, P.R. Bouliane: An update on CCIR Business and Residential Noise levels, Symposium Record: IEEE International Symposium on Electromagnetic Compatibility, Chicago, 1994, pp 348-353

(15) Recommendation ITU-R SM.1753-2 “Methods for measurements of radio noise” 09/2012

(16) R.J.Achatz et al.: “Estimating and Graphing the Amplitude Probability Distribution Function of Complex –Baseband Signals”, IEEE P802.15-04-0428-00, 24.8.2004

(17) J.P. Patel, C.B. Read: “Handbook of the Normal Distribution”, Second Edition ISBN-13 978-0824793425

(18) Comrod, Specifications VHF30108VM, 15.02.2012

(19) Comrod, Specifications VHF108185VM, 27.03.2009

(20) Norgeskart: https://www.norgeskart.no/

(21) Norwegian Mapping Authority: http://www.kartverket.no/

Abbreviations

AIMS = Autonomous Interference Monitoring System

APD = Amplitude Propability Distribrution

CCAPD = Complimentary Cumulative APD

CCD = Complimentary Cumulative Distribution function

CCIR = Comite consultatif international pour la radio /

Consultative Committee on International Radio

dB = desiBel

dBm = dB ref 1 milliwatt

F_a = Noise Figure, external

FFI = Forsvarets forskningsinstitutt

GB = Giga Byte

HF = High Frequency

IF = Intermidiate Frequency

IMD = Intermodulation Distortion

ITS = Institute of Telecommunications and Sciences

ITU = International Telecommunication Union

ITU-R P = Radiocommunication Sector of ITU, P Series – Radiowave Propagation

JPG = Joint Picture Group

m = meter

LNA	= Low Noise Amplifier
NSM	= Nasjonal Sikkerhetsmyndighet
NTIA	= US National Telecommunications and Information Administration
RMS	= root of the mean of the square
RA	= Radiocommunications Agency of UK
RAM	= Random Access Memory
RBW	= Resolution Bandwith
RF	= Radio Frequency
R&S	= Rohde & Schwarz
SA	= Spectrum Analyser
SMF	= Sealed Maintenance Free
U.K.	= United Kingdom
U.S.A.	= United States of America
UHF	= Ultra High Frequency
US	= United States
V	= Volt
VBW	= Video Bandwith
VHF	= Very High Frequency

Appendix

A Supplementary data on man-made radio noise

A.1 Man-made noise model for frequencies above 200 MHz

The validity of the ITU-R P.372 man-made noise model as given by eq. (6), page 27, is limited to the frequency range 0,3 - 250 MHz for the three environmental categories (City, Residential and Rural). The equation for the median value of each environmental category was obtained by using the ITS data to calculate the least squares fit approximation assuming a linear dependency with log(frequency) over the frequency band 250 kHz - 250 MHz. The median values was found to decrement with log(frequency) at a rate of 27,7 dB/decade.

As far back as in 1973 Skomal (7) published a meta-analysis of radio noise measurements available at that time. His analysis indicated that the rate of noise power decrement with frequency was more moderate for frequencies above 100 MHz, compared to the rate of decrement with frequency at the lower frequencies. Measurements at high VHF and low UHF frequencies in Canada published in 1984 by Lauber and Bertrand (8) confirmed that the rate of decrement slowed down at high frequencies. Their measurements indicated that for frequencies above 200 MHz, the values for the constants *c* and *d* in equation (6) according to Table A.1 give more accurate estimates for the median man-made noise figure than what the ITU-R P.372 noise model does. This model, as suggested by Hagn (8), is in reasonable harmony with the measurements of Lauber (8) up to several hundred MHz.

Environmental category	*c*	*d*
City (Business)	49,4	15,8
Residential	45,2	15,8
Rural	39,2	15,8

Table A.1 Values for the constants c and d in eq. (6) for the prediction of median man-made noise for frequencies above 200 MHz, as suggested by Hagn (8).

A.2 A survey of post-1974 man-made noise measurements

A.2.1 Background

In the 1990s there were some growing concerns about the validity of the ITU-R P.372 man-made noise model, mainly due to the technological changes that had occurred during the 25 years that had passed since the database for this noise model was established by the ITS predecessor. For this reason some further measurements were initiated by ITS by performing two separate measurements campaigns during the late 1990s (9), (10). A third one was performed during 2009 (11). However, none of these were close to being equally comprehensive as the ITS measurement campaigns performed during the 1960/70s.

Additionally, there have been post 2000 projects on man-made noise measurements in the UK, and Germany, as well as a campaign in Canada during 1993. Results from the UK and Canada ones have been published, however, no available public documentation on the German project has been found.

A brief overview of the above measurement campaigns will be given in the following and the degree of compliance to the ITU-R P.372 man-made noise model predictions will be commented.

A.2.2 ITS measurements in the 136-138 MHz band (1996)

All measurements during this ITS campaign were conducted at a single frequency within the 136-138 MHz band, which is allocated for Meteorological Satellite services. Measurements were performed during 1996 at locations belonging to the rural, residential and business environmental categories. However, for each category measurements were apparently only performed at relatively few different locations. Hence, the total amount of measurement data seems to be rather limited as to generating statistics for good comparisons with the ITU-R P.372 man-made noise model. The measurements were made in a stationary situation, i.e. a non-moving antenna was used. The antenna construction was a quarter-wave monopole mounted on a rectangular ground plane, which is a reasonable approximation to the ITU-R P.372 reference antenna.

Measurement results of this campaign are documented in (9). For assessing whether the background data for the ITU-R P.372 man-made noise model might have changed over time, the following findings are most relevant:

- The median of the external noise figure ($F_{a,m}$) measured for the business and rural environmental categories was close to (within a couple of dBs) the median noise figure predicted by the ITU-R P.372 man-made noise model. However, for the residential category the measured median value was 7,3 dB lower than that predicted by the ITU model, indicating that an appreciable reduction of man-made noise at the measured frequency might have occurred.

- The within-the-hour variability of the measured $F_{a,m}$ was significantly reduced compared to the data on time variability in ITU-R P.372 (reproduced in Table 2.2). This was valid for all environmental categories.

- The measurement results of the influence of automobile noise suggest that automobiles are no longer a significant noise source at the measured VHF frequency. This is contrary to predictions based on Spaulding's measurement results of the radio noise at highway locations published in 1974 (4).

A.2.3 ITS measurements at 137,5 MHz and UHF frequencies (1999)

This second ITS campaign was conducted in 1999, and noise measurements were made at 137,5 MHZ, 402,5 MHz and 761 MHz. Vertical quarter-wave monopole antennas tuned according to frequency and mounted on a ground plane were used. The measurements were performed in two residential and two business locations in the area of Boulder/Denver, Colorado. No measurements were done in rural areas. The duration of the measurement at each location was 24 hours in order to observe the noise level variability over this period. Hence the focus of these measurements was primarily to explore time variability rather than the location variability.

The processing of the measured noise data presents the median, the mean and the peak values of the external noise (10) during the 24 hours period, giving indications of the non-stationarity of the man-made noise. This ITS campaign concludes that noise levels are correlated to working hours in that they rise in the morning and fall in the afternoon, and that high noise levels are not present during the middle of the day (10).

At the two highest frequencies the value of $F_{a,m}$ could not be determined with any accuracy because the total noise measured were too close to the internal noise generated by the measurement setup. However, since the noise figure of the setup was quite low, this implies that the measured man-made noise power was lower than what is predicted by the Hagn model (confer Table A.1).

At 137,5 MHz the results of the measurements confirmed the findings of the ITS 1996 campaign (9), showing a significantly lower man-made noise level for the residential area compared to predictions from the ITU Residential man-made noise model. In Business areas the measured data and the prediction by the ITU-R P.372 man-made noise model was in good agreement.

A.2.4 ITS wideband noise measurements in VHF and low UHF band (2009)

A third measurement campaign was conducted by ITS during the summer of 2009 (11), using a different test setup compared to the two preceding ITS campaigns. While the measurement bandwidth of the two previous campaigns was 30 kHz, the new setup was able to support measurement bandwidths of up to 36 MHz. This would, in principle, allow a more versatile use of the data collected by filtering to a narrower bandwidth in the post-processing. However,

because of the difficulties to find areas of the spectrum that was free from intentional radiators, the actual bandwidth used for the measurement campaign had to be lowered to 1,16 MHz.

The noise measurements data records were collected every 10 minutes during a 24 hours measurements period for each frequency and location. The noise power measurements were carried out at three frequencies, which were 112,5 MHz, 221,5 MHz and 401 MHz at each location. Only four different locations were selected; one business and one residential location in Boulder, Colorado and one business and one residential location in Denver, Colorado. However, according to (11), the residential locations were not strictly residential as defined in (3) and (4); they were residential with some nearby businesses or busy roads. Unfortunately, this may obscure a direct comparison between the residential $F_{a,m}$ of this study and the prediction based on the ITU-R P.372 man-made noise model.

A statistical summary data of the campaign is presented in (11). This includes the median, mean and peak noise power levels of a 24 hours period, characterizing the time variability of the external noise. Also, the median of all the hourly medians of the mean external noise power measured during business hours at the two locations belonging to the same environmental category are calculated. This value of the median antenna external noise figure $F_{a,m}$ was used to for comparison of the measured data with predictions from the ITU man-made noise model, the background data of which was also collected during business hours.

The conclusion of the result of this comparison was that for business locations the measured values of $F_{a,m}$ at 112,5 and 221,5 MHz were somewhat larger than predicted with the ITU model. However, the measured values were (marginally) within the standard deviation of the ITU predictions. At residential locations the measured values of $F_{a,m}$ at 112,5 and 221,5 MHz were found to be less than 2 dB larger than the ITU model predictions, which is clearly within the standard deviation of ITU predictions.

When assessing the results of this campaign, one should keep in mind that that data is based on two locations only, and that the residential ones may have had influences from noise originating from businesses or busy roads.

No value of $F_{a,m}$ at 401 MHz was produced by this campaign, since the external noise at this frequency was too low to be measured with a sufficient accuracy.

A.2.5 UK Man-made noise measurements - AIMS

Mass Consultants Limited of UK has reported (12) on a man-made noise measurement study made for Ofcom, which is the UK communications regulator. The test setup used was the Autonomous Interference System (AIMS), which is a multi-function tool for assessing spectrum quality and usage, and which had been specially developed for Ofcom by Mass Consultants.

This measurement campaign took place in 2006/2007, and measurements were performed at 25 different outdoor locations of various environmental categories as well as at 8 indoor locations. Wherever possible, 24 hours of activity was captured in order to study diurnal variations. Tuned

vertically polarised dipole antennas were used. Noise measurements were performed at two frequencies, 209,5 and 425 MHz.

The locations are sorted into the following categories: Urban, Industrial, Suburban and Rural, the nomenclature of which is slightly different than that of the ITU. However, no clear definition of categories is given in (12). We believe that it is fair to assume that the Urban and Suburban categories are equivalent to ITUs City and Residential categories, respectively.

			Average of Median *Fa*, dB above kTb	
Indoor/Outdoor	**Site Category**	**No. Sites**	**209.5 MHz**	**425 MHz**
Indoor	Urban	3	13.8	15.6
	Industrial	2	4.8	2.6
	Suburban	3	11.5	4.7
Outdoor	Urban	5	15.6	10.1
	Industrial	5	10.4	7.9
	Suburban	8	7.6	6.9
	Rural	7	4.6	3.4
	Total	33		

Table A.2 The estimates of $F_{a,m}$ for each location category of the AIMS man-made noise measurement campaign in 2006/2007. Excerpt from (12).

Table A.2 shows the median external noise figure calculated from the measurements at the various environmental categories during this AIMS man-made noise measurement campaign. The lowest noise levels, which are measured at the rural locations, were only just above the noise floor of the measurement system. The measurement setup did not seem to perform any processing compensating for the influence of internal noise, which probably means that the values for the rural noise figure in the table may be somewhat overestimated.

The ITU-R P.372 man-made noise model applies to outdoor conditions only, and is limited to frequencies below 250 MHz. Hence comparisons with the ITU model can only be done for the outdoor measurements at 209,5 MHz. At this frequency the ITU model predicts a median noise figure of {12,5; 8,2; 2,9} dB for {city; residential; rural} categories. This should be compared with the values {15,6; 7,6; 4,6} for the {urban; suburban; rural} categories in the above table. In other words, the measurements in urban area indicate a slight increase in the man-made noise figure, while the results of the suburban measurements matches the ITU model predictions very well. The estimated median noise figure at rural locations slightly exceeds the prediction of the ITU model, although this could easily be the result of influence of the internal noise of the measurement setup. However, the deviations between the measured and predicted noise figure seem to be within the statistical variance of the ITU model.

The AIMS measurement system has been successfully compared to the German Federal Network Agency's measurements system. Measurement results from both systems have been submitted to the ITU-R in 2007, and serve as a source of the tables with information on "man-

made noise measurements in Europe" that has been included in the recent editions of ITU-R P.372 (confer next sub-section). These results are considered to have generally confirmed noise figure predictions by the ITU man-man noise model.

A.2.6 ITU-R P.372 information on measurements in Europe 2006/2007

The ITU-R P.372 recommendation (1) quotes measurement results on man-made noise taken in Europe during 2006/2007. These are probably based on combined contributions from the UK (AIMS) and the German noise measurements. Table A.3 shows the quoted values for the measured median noise figure for measurement frequencies below 250 MHz along with the corresponding predictions of the ITU man-made noise model.

Frequency (MHz)	City environmental category		Residential environmental category		Rural environmental category	
	Median F_a quoted	ITU model prediction	Median F_a quoted	ITU model prediction	Median F_a quoted	ITU model prediction
35	23	34	17	30	16	24
140	12	17	8	13	6	8
210	16	13	8	8	5	3

Table A.3 The median value of the measured F_a in Europe 2006/2007 as quoted by ITU-R P.372 (1). The calculated median noise figure according to the ITU-R P.372 man-made noise model is shown for comparison.

The table shows values for three different frequencies below 250 MHz which is the highest frequency of the ITU-R P.372 man-made noise model. It is noted that the highest frequency, 210 MHz, has measured F_a values equal to those of the UK AIMS program, which is probably the source of this measurement data. As already concluded, the AIMS measurement data at this frequency is in good harmony with the ITU man-made noise model predictions.

However, the calculated median of the measured F_a values at 35 MHz is much lower than the values predicted by the ITU man-made noise model. The values are 11, 13, 8 dB below ITU predictions for City, Residential and Rural environments respectively. This difference is assumed to be high enough to be statistically significant, indicating that it cannot be explained only by the variance of the ITU noise model data.

The measured median F_a values at 140 MHz is up to 5 dB lower than predicted values. This difference may or may not have statistical significance depending on parameters that are not depicted, such as the number of locations per category on which the quoted median is based. At 210 MHz the agreement between the measurements and the prediction is good.

A.2.7 Man-made noise measurements - UK 2003

Mass Consultants Limited was involved in building a wideband measurement system, which it used to measure the levels of man-made noise at sites in the UK. This work was done on a contract with the Radiocommunications Agency (RA) of UK. These activities preceded the UK measurement campaign of 2006/2007 described above, and are documented in a report (13) issued in 2003.

The man-made noise measurements of (13) comprise recordings of one working day from 8 different measurement locations, each belonging to a chosen (non-ITU) category. Of the 8 locations, only one would translate into each of the residential and the rural environmental categories, providing an extremely low statistical baseline. Noise measurements were made at several different frequencies from about 40 MHz to about 3 GHz, but the selection seemed to vary from location to location. The measurement bandwidth was also varied, from a few hundred kHz and up to 10 MHz.

A receiving antenna with horizontal directivity was used, which is an unconventional choice that makes conversions to the ITU external noise figures difficult unless the external noise is composed of statistically equal contributions from all angles. The report (13) leaves an overall impression that these measurements were tailored more for the objective of gaining experience with the measurement system rather than to arrive at measurement data that could be compared to predictions of the ITU-R P.372 man-made noise model.

The report (13) does not give details as to how the measurements are transformed into an external noise figure that can be directly compared to those valid for the ITU-R P.372 reference antenna. It is stated in (13) that the number of observations are limited and that the F_a values presented is the estimate of the *mean* value at the locations while the ITU F_a value is the *median* for an environmental category.

A graph for comparison with the ITU-R P.372 model is presented in the report, and Figure A.1 shows a copy of this graph. It is evident that for most comparable location categories, the measured mean values of F_a are higher, and for some cases much higher, than the median values predicted by the ITU man-made noise model.

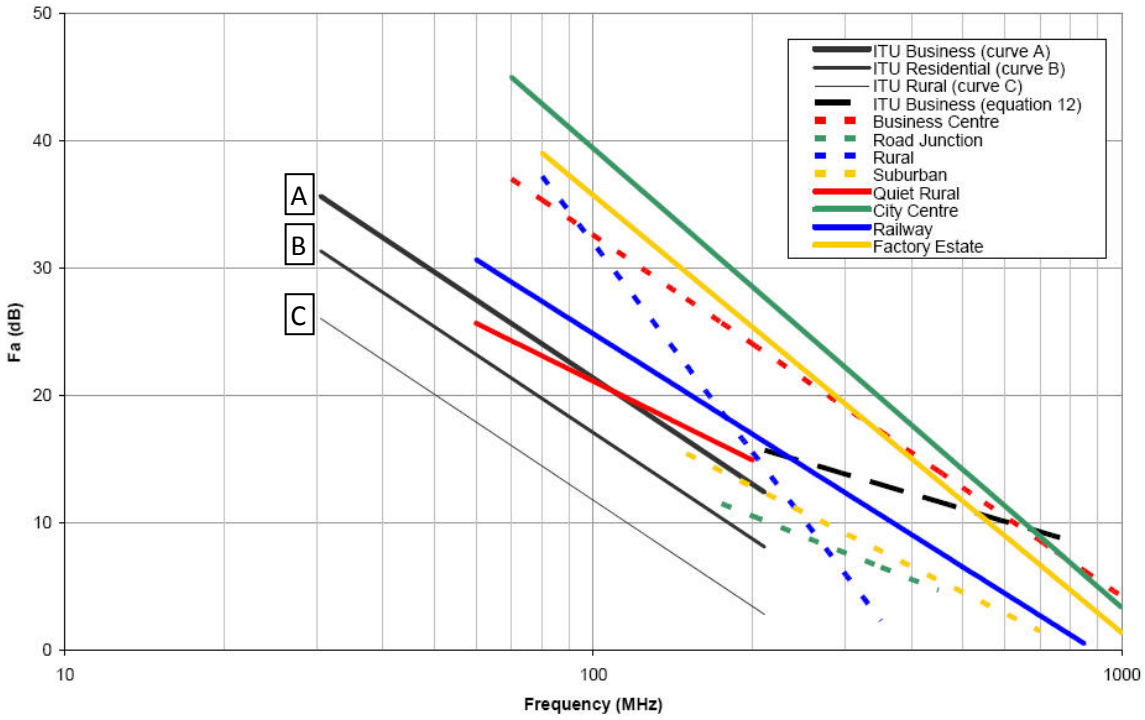

Figure A.1 Excerpt from (13) showing the measured F_a for each of the 8 location categories as defined by this study. Also shown are the curves for the ITU City (i.e. Business), Residential and Rural noise models.

For example, the curve for City Centre (green solid curve) at 100 MHz is approximately 17 dB higher than the value predicted for the ITU City category (curve A, called ITU Business in the figure). For the measured rural location (dashed blue line) the F_a value at 100 MHz is approximately 20 dB higher than the ITU rural value; moreover this rural curve has a very peculiar gradient. The results of these measurements indicate that the noise levels measured seem to be generally higher than the corresponding ITU F_a values, even though the statistical definitions of the noise figure are slightly different. This is also the conclusion given in (13).

It should be noted that the results of the UK 2006/2007 AIMS measurements (12) at 209,5 MHz give values for the external noise figure that is quite a bit lower than the results of these 2003 UK measurements. Importantly, the AIMS campaign makes use of a healthier measurement setup (omnidirectional vertical antennas) and offers a better statistical significance for comparison with the ITU model, because it covers more locations per environmental category. We believe that this makes the AIMS results the most reliable as source of UK measurements of man-made noise for comparison with the ITU man-made noise model. UK authorities seem to share this opinion; since only the measurement results of the AIMS campaign have been subject for submission to the ITU-R of UK man-made noise measurements data.

A.2.8 Montreal/Ottawa measurements 1993

Lauber et al (14) reports on a measurement campaign of man-made noise that was made in urban core areas of Montreal and Ottawa as well as in some residential areas of Ottawa. Measurements were made in the HF frequency range at 6 spot frequencies from 2,5 MHz to 25 MHz, using a short (9 foot) rod antenna.

Data from 37 urban locations in Montreal was recorded and analysed. Recordings from only 5 different urban locations were collected in Ottawa. However, several days of recordings were made at each site, providing all together 40 day-sites (an equivalent of 40 sites) of urban data.

The measurement data from residential areas were collected from 37 different locations in four residential areas of Ottawa. Two of these areas had buried power-lines, while the other two areas had overhead power-lines. This sampling strategy allows an assessment of the reduction of radio noise emissions from the power network that the development from overhead cables to underground power cabling has led to.

The results of Lauber's 1993 measurements indicate that there was no significant increase in the measured median man-made noise figure compared to the ITU man-made noise model. At frequencies between 15 and 30 MHz the measured data showed a good match with the ITU City noise model predictions. The median of the measured data at 10 MHz and below was around 4-5 dB below ITU city noise predictions. Interestingly, it was observed that at two of the 37 Montreal urban locations the measured noise levels were significantly above (by 20 dB or more) the measured median. This excess noise could be attributed to flashing nearby neon lights.

The measurements in urban Ottawa resulted in a median that was below the ITU City noise predictions at all frequencies measured. In fact, these locations had a median noise level that was in reasonably harmony with values predicted by the ITU Residential noise model.

The Ottawa residential measurements were analysed with respect to two subgroups of locations according to the type of power cabling used at the locations. The median of the location subgroup with overhead wiring tended to follow the predictions for the ITU Residential environment. However the median noise level at locations with buried cables was reduced by an average of about 6 dB compared to those with overhead power-lines. Consequently, the median noise level for Residential locations with buried cabling was found to be close to the levels predicted by the ITU Rural noise model.

This clearly suggests that an elimination of overhead electrical cables could lead to a general decrease in the man-made noise level for residential locations. According to (14), at the time when the background data for the ITU man-made noise model was collected, overhead power cabling was typical for the residential areas sampled (4). This indicates that the increased use of buried power cables could be an important contributing factor to the reduction of the man-made noise levels in some Residential areas relative to the ITU-R P.372 predictions, as is suggested by results of some measurement campaigns.

A.2.9 Summary of comparisons of measurement data with ITU–R P.372 predictions

It is not straightforward to give firm conclusions as to changes of the levels of man-made noise during the years since the background data for the ITU–R P.372 recommendation was collected. This is mainly caused by the statistical nature of the man-man noise levels, and in particular its high variance with locations and time compared to its median value. Unless a measurement campaign has a fairly wide selection of measurement sites within an environmental category, it takes a large difference between measured and predicted values to conclude that the measurement is caused by a real change in the median man-made noise level and not by the statistical variance of F_a over location and time.

Table A.4 shows a summary of the results from the seven referenced measurement programs described above, sorted according to the three ITU-defined environmental categories. Three of these seven programs address only City and Residential locations; hence we have 18 different results that can be used for comparison with predictions of the ITU–R P.372 man-made noise model. The green cells in the table indicate that the measured noise level was considered to be (statistically) significantly below the ITU model predictions, at least at one measurement frequency. The red cells indicate that the measured noise level was found to be (statistically) significantly above the ITU model predictions on at least at one measurement frequency.

Section/ (Year)	**Results trend for environmental categories explored:**			**Freq (MHz)**	**Comments**
	City	**Residential**	**Rural**		
A.2.2 (1996)	Median is in agreement with ITU	Median is below (7,3 dB) ITU	Median is in agreement with ITU	137,5	US/ITS. Very few residential and rural locations. Lower time variance than ITU.
A.2.3 (1999)	Median in agreement with ITU	Median is significantly below ITU	No locations measured	137,5	US/ITS. Focuses on time variation study and UHF frequencies. Only two location per category
A.2.4 (2009	Higher (4 – 8 dB) than ITU, marginally within the statistical variance	Higher than, but close to, ITU (within 3 dB)	No locations measured	112,5 and 221,5	US/ITS. Wideband measurements with focus on time variation study. Only two locations per category
A.2.5	Median is 3 dB higher than ITU; well within the	Median is very close to ITU	Median is close to ITU (within 2 dB)	209,5 (and 425)	UK. 5 – 8 locations per category. Results claimed to be in good compliance with a

(2006/ 2007)	statistical variance				German campaign performed at the same time.
A.2.6 (2006/ 2007)	Median significantly below ITU (11 dB) at 35 MHz	Median significantly below ITU (14 dB) at 35 MHz	Median significantly below ITU (8 dB) at 35 MHz	35, 140, 210	Deviation from predicted ITU value is very frequency dependent.
A.2.7 (2003)	More than 15 dB above ITU	A few dB higher than ITU, but within its the statistical variance	Up to appr. 20 dB above ITU and with a different frequency variation. Questionable validity?	Various, from 40 to > 250	UK. Only one location per category. Questionable measurements setup (directive antenna used).
A.2.8 (1993)	Median is slightly lower than ITU City.	Median is lower than ITU Residential, appr. corresponding to levels of ITU Rural	No locations measured	2,5 - 25	Canada. Many locations per category (≥37) measured. Analysis gives data for the influence of buried vs overhead power cabling.

Table A.4 Summary of measured F_a results of the measurement campaigns described, compared to ITU man-made noise model $F_{a,m}$ of the corresponding category. Uncoloured result cells indicate that the measurement results are assessed to be within the quoted variance of the ITU model. Green cells indicate that measured results are lower than the corresponding ITU prediction. A red cell indicates that the measured results are higher than the corresponding ITU prediction.

It is noted that only one measurement campaign measured noise levels significantly higher than those predicted by the ITU model. This is the UK 2003 campaign. However, we assess this particular campaign to be by far the least suitable one to be used for a meaningful ITU-R comparison. This is primarily related to its use of a measurement antenna with azimuth directivity. No discussion is made in the report (13) about how their evaluation and comparative ITU analysis is performed or about the effects that an antenna with horizontal directivity will introduce. For this reason we believe the validity of the results from UK 2003 campaign is highly questionable. We believe that it should be disregarded, in particular with respect to a comparison with the ITU–R P.372 noise model.

Based on the results of the six other measurements campaigns described above, the following coarse summary can be made:

For ITU City environments, one of the six quoted campaigns shows a noise level significantly below the level predicted from the ITU–R P.372 noise model. The five remaining campaigns give results that are more or less within the statistical variability of the ITU–R P.372 man-made noise for the City category. We consider that this indicates that the general level of man-made noise does not appear to have changed significantly for ITU City environments during the years from about 1970 to 1993-2009.

At ITU Residential environments four of the six campaigns found that the measured noise was lower than the predicted ITU–R P.372 man-made noise for the Residential category. Two of the campaigns measured the noise level to be in agreement with predictions. We consider that these results indicate that the man-made noise level for ITU Residential environments may have decreased during the years from about 1970 to 1993-2009. However, the indications are somewhat ambiguous.

Only three of the six campaigns performed measurements at rural locations. One of these three campaigns measured noise levels below the predicted ITU–R P.372 man-made noise for the Rural category, but only at one measurement frequency. The two other campaigns measured noise levels close to the predicted ITU Rural levels. Hence, there is no indication from the above campaigns that the man-made noise level for ITU Rural environments has increased during the years from about 1970 to 1993-2009. On the other hand, we consider that the above material is too sparse and inconsistent to conclude that the man-made noise level at ITU Rural environments has been generally reduced during this time period.

B Measurement setup and preparations

This chapter describes the measurements setup in more detail.

B.1 Overview of the man-made noise measurement system

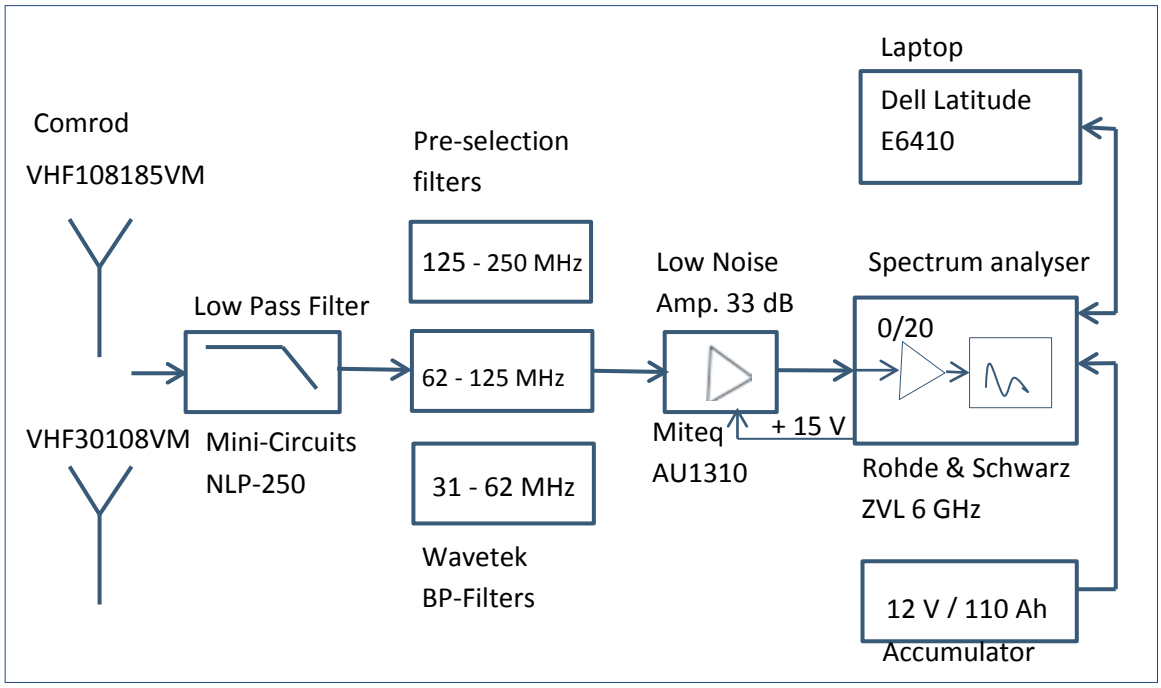

Figure B.1 Schematic of the external noise measurement system.

The external noise measurement system picks up noise with one of two antennas, and then feed the noise through a 20 – 25 m long antenna cable. The noise then enters a low pass filter which purpose is to minimize possible interference from the GSM-bands at 900 MHz.

Because of the simplicity of the spectrum analyser it doesn't have pre-selection filters, so these are supported as external band pass filters. The filters must manually be changed and tuned according to each measurement frequency. From the filters, the noise is amplified 33 dB by a Low Noise Amplifier (LNA) before entering the spectrum analyser. The spectrum analyser can amplify the noise by 0 dB or 20 dB, and gets its power from a 12 V / 110 AH accumulator. The spectrum analyser is usually under the control of the laptop running the "NSM Noise Measuring System" software.

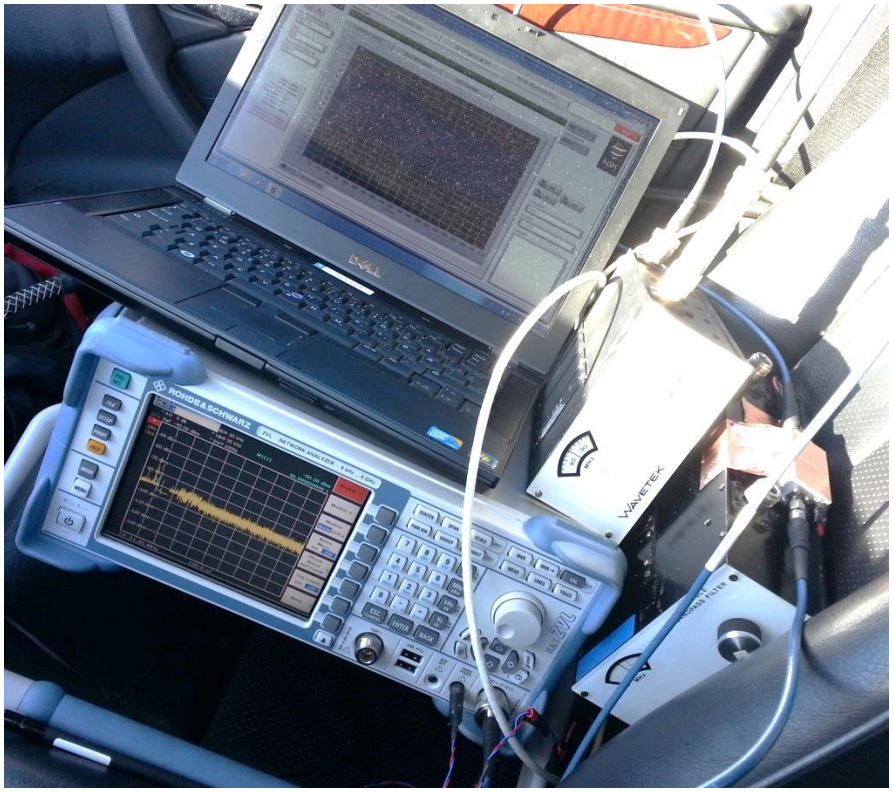

Figure B.2 The measurement system in action with laptop, filters, spectrum analyser, and cables.

B.2 Antennas

The external noise measurement system consists of the choice of two dipole antennas from the antenna manufacturer Comrod. These are VHF30108VM, that covers the frequency band from 30 to 108 MHz, and the VHF108185VM, that covers the frequency band from 108 MHz to approximate 200 MHz plus. Figure D.2 to Figure D.7 shows the performance of the Comrod antennas.

A couple of other antennas were considered too, the “Royale Discone” antenna from S.R.S. (Swedish Radio Supply) covering 25 – 2000 MHz, and the Jaybeam 7177010 antenna from Amphenol covering 100 – 500 MHz. The benefit with these antennas is that they cover the whole frequency range of interest, so we don’t have to change between several antennas to cover all measurement frequencies. The drawback is their size, which makes them difficult to handle and transport without disassembling. Another drawback with these discone antennas are their poor performance at low frequencies, typically below 100 MHz. Figure D.1 shows the VSWR of the S.R.S. discone, and Figure D.9 shows the gain of Jaybeam discone.

B.3 Tripod

During measurement the antennas are mounted on a tripod, one at a time. The tripod is a Gitzo G1228Mk2, made of carbon fibre.

Figure B.3 The Gitzo G1228Mk2 tripod. - To the left, the unmodified tripod. - To the right, the tripod during measurement, with counterweight, rod, and antenna adapter.

To the tripod we have added a counterweight of approximately 3 kg, a rod or shaft 55 cm long, and on top of that, an antenna adaptor. This gives a total height to the lower end of antenna of approximately 158 cm with the tripod legs extended two lengths. With the tripod made of carbon fibre, the rod and adaptor made of plastic, the assembly should not influence the antennas radiation pattern significantly, compared to an assembly made of metal parts.

B.4 Cables

During the first measurements we used a Belden H-1000 cable of 20 m as an antenna cable. This cable has low attenuation of 1 dB @ 100 MHz as shown in Figure B.4. During use the cable became more difficult to handle because of the unwinding and winding of the cable. It also showed some influence to noise when moved, and noise pickup in the cable, so we changed it for a more ruggedized cable, CellFlex. At 25 m this cable has an attenuation of 1 dB @ 100 MHz, and even better performance than the Belden H-1000 cable at higher frequencies, shown in Figure B.4. The CellFlex is used at measurements from date 30.10.2013. From the CellFlex cable we use Huber&Suhner Sucotest cables to the other connections in the measurement setup.

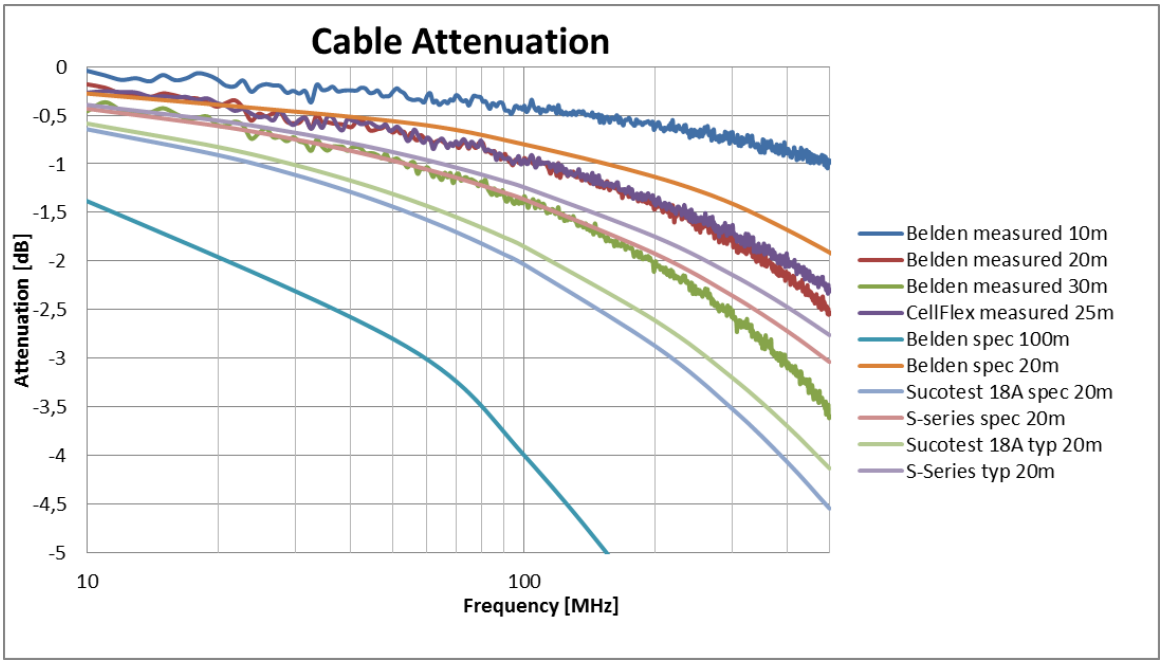

Figure B.4 Cable attenuation of some cables. CellFlex 25 m has the lowest attenuation.

B.5 Filters

B.5.1 Low-pass filter

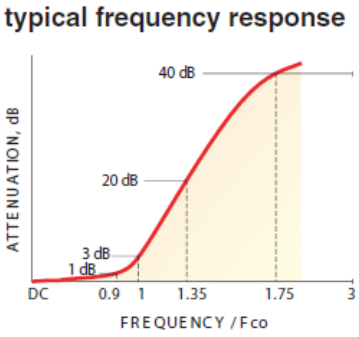

Figure B.5 Typical frequency response of the NLP-250 low-pass filter from Mini-Circuits. The 3 dB cut-off frequency is 250 MHz.

The low-pass filter has a 3 dB cut-off frequency at 250 MHz, and its main purpose is to minimize interference from the GSM bands at 900 MHz. It has N-connectors at both ends and fits directly to the Wavetek band-pass filters. The low-pass filter is used at all measurement frequencies covered by the antennas VHF30108VM and VHF108185VM. Its typical frequency response is shown in Figure B.5 and in the datasheet in Figure E.3.

B.5.2 Band-pass filters

The Wavetek band-pass filters act as pre-selection filters to the R&S ZVL spectrum analyser. The models cover the frequency bands:

1. Model 5201: 31 – 62 MHz
2. Model 5202: 62 – 124 MHz
3. Model 5203: 125 – 250 MHz

The purpose of these filters is to minimize strong interference outside the measurement frequency. Strong interference can bring the amplifiers out of the linear region or into saturation to produce distortion, either harmonic or intermodulation products. Some plots of the filters frequency response are shown in Figure E.1 and Figure E.2.

B.6 Low noise amplifier

The external low noise amplifier (LNA) that follows the band pass filter(s) is from Miteq, AU-1310, and covers the frequency band 0,001 – 500 MHz, with a typical gain of 33 dB and a noise figure of 1,3 dB. It gets its +15 V_{DC} power from the R&S ZVL Spectrum analyser. This amplifier compensates for the spectrum analyser's poor noise figure.

B.7 Spectrum analyser

The spectrum analyser is a 6 GHz ZVL from Rohde & Schwarz. It is primarily a network analyser, but the spectrum analyser and the 20 dB internal amplifier are included as options. Its noise figure is 30 dB. Unfortunately it lacks pre-selection filters. The instrument weighs about 7 – 8 Kg and is highly portable.

B.8 Power

The analyser has an internal Ni-MH battery pack that is charged from the mains or another power source. The internal accumulator can run the analyser for approximately 40 – 60 minutes on one charge. Charging time is between 5 and 9 hours. Due to this short work time from the internal accumulator, the analyser is powered from a SMF (Sealed Maintenance Free) accumulator of 12 V and 110 ampere hours, giving approximately 16 hours of work time.

We have two of these accumulators, so when the first one is discharged, we can continue measurements with the other accumulator. Charging the accumulator takes about 4 – 5 hours with a current of 25 A. If we charge the accumulator every night, we will never run out of power. The accumulators have the property to give moderate currents over long time, compared to a car battery giving high current in a short time. The laptop can also run on 12 V through a

converter, but primarily the laptop runs on its internal accumulator, which we have two of, and change it during a day of measurements. The drawback with the accumulators is their heavy weight of approximate 15 – 20 Kg each.

B.9 Laptop

The laptop is a Dell Latitude E6410 with a Core i7 processor, 4 GB RAM, and a 148 GB disk. During measurements the laptop is running the "NSM Noise Measuring System", a LabView program developed by NSM. When running the program, it controls the ZVL spectrum analyser through the different measurement phases conducted by the test person.

B.10 NSM Noise Measuring System

The NSM Noise Measuring System 1.1 starts from a shortcut on the desktop. The program's different modes are selected by clicking at the tabs. The main tabs are:

1. Hardware configuration
2. Transducer
3. Frequency sweep
4. Noise measurement (with sub tabs):
    a. Current sweep
    b. Spectrogram
    c. Histogram

B.10.1 Hardware configuration

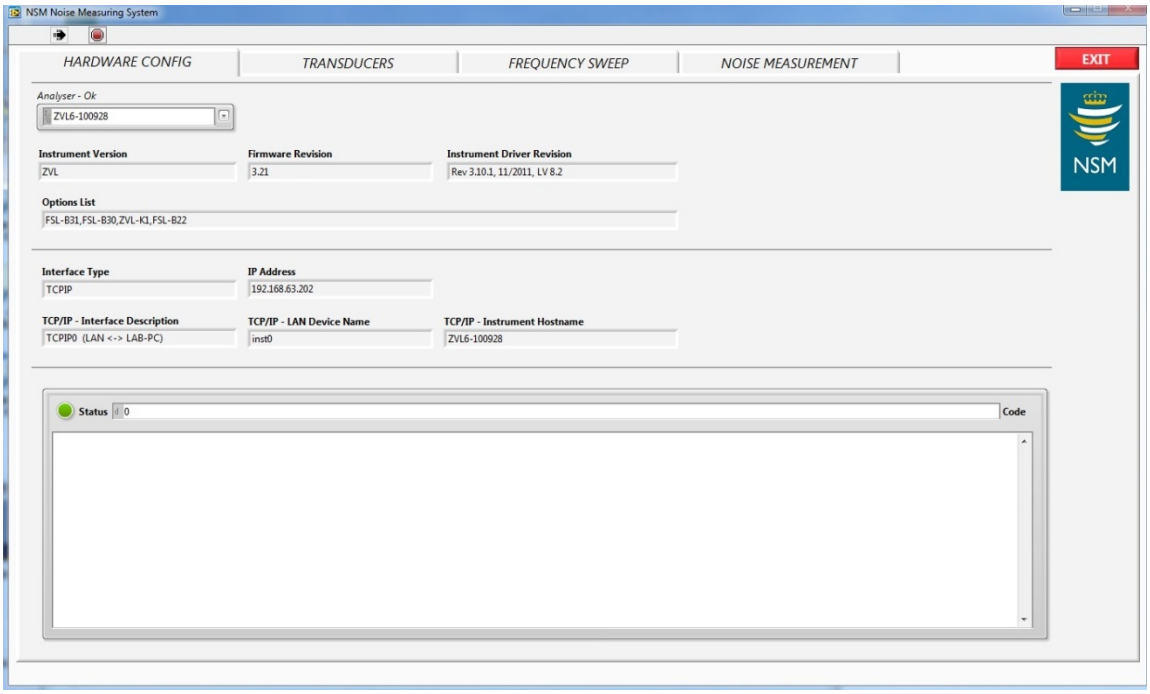

Figure B.6 The NSM Noise Measuring System startup screen showing the hardware configuration tab.

At start up the program displays the hardware configuration shown in Figure B.6. The hardware configuration tab displays several instrument parameters including a status field which lit green when everything is ok. At all screens there is a black arrow and a red bulb. Clicking the red bulb stops the Lab View program, and clicking the black arrow restarts it.

B.10.2 Transducer

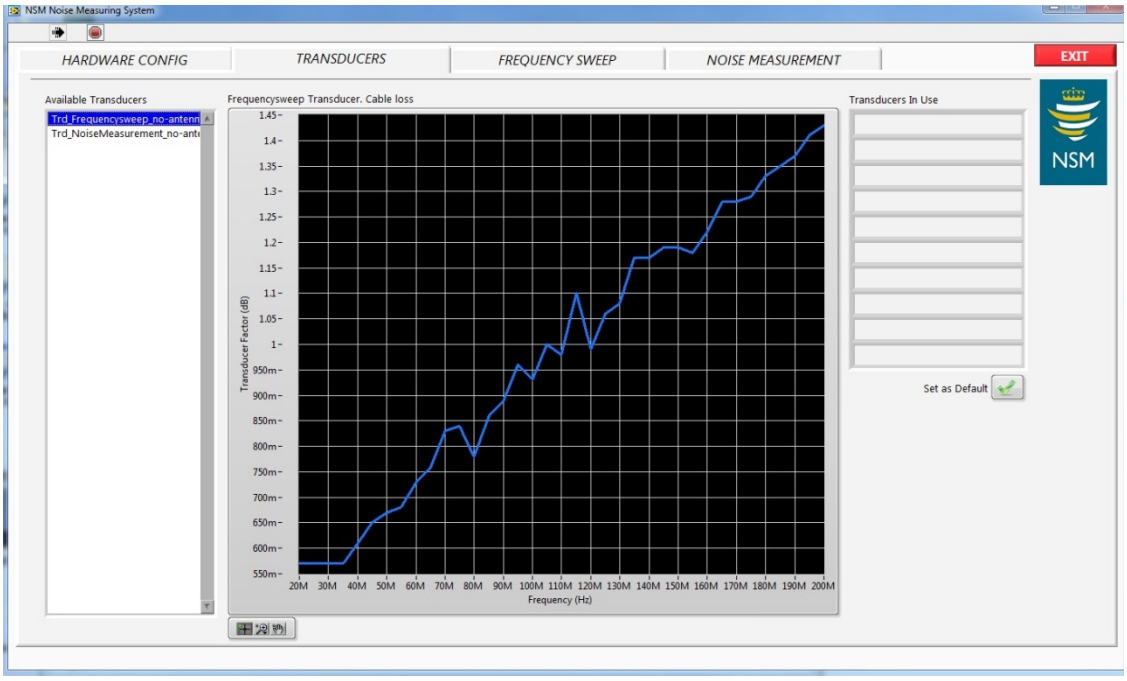

Figure B.7 Transducer screen.

The transducer tab displays a screen where you can select predefined transducer tables that will correct the measurement samples before saving. The transducer tables could for instance be the frequency response of the measurement chain. During noise measurements we have not used any transducer tables. Instead we have done the correction afterwards, based on system gain measurements through the chain for each of the noise sampling frequencies, as shown in Figure F.1 to Figure F.7. We do not use the transducers because if we have the undisturbed raw data, it is easier to do all kinds of corrections and calculations as post-processing.

B.10.3 Frequency sweep

In the frequency sweep mode we use the screen displayed in Figure B.8. Here we have buttons to start and stop a measurement, and a field with the analyser's default non-changeable parameters:

1. RBW = 30 KHz
2. VBW = 30 KHz
3. Detector = RMS
4. Sweep time = auto
5. PreAmp = ON

6. RF Atten = Auto
7. Reference Level = -40 dBm
8. IF overload > -20dBm
9. RF overload > -17 dBm

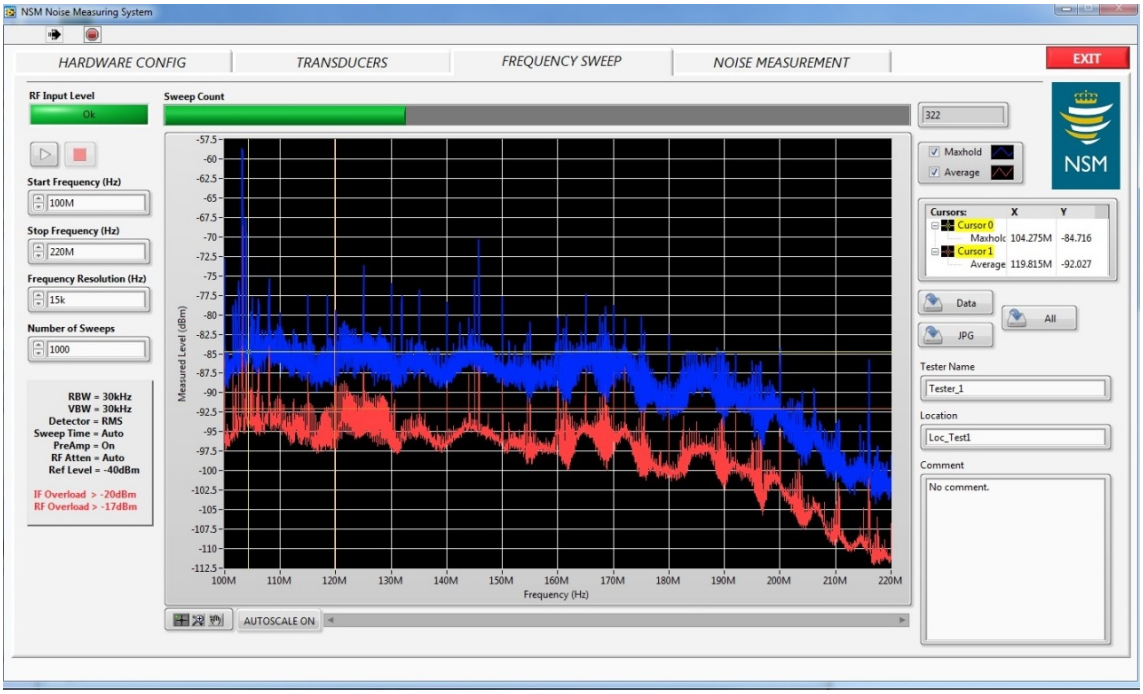

Figure B.8 Frequency sweep screen.

The user can change:

1. Start frequency
2. Stop frequency
3. Frequency resolution (bin size)
4. Number of sweeps

There is a relation between the frequency span and the frequency resolution, if out of range, an error message will occur until the parameters are in range. On the screens right side there are sweep counts, readouts from cursors, fields to put the tester's name, the location, and a comment field, usually commenting if the external preamp (LNA) is active. The location field is read by the Matlab post-processing program and should be in short form, like Loc-1, Loc-23.

The grid's vertical range can be changed by editing the tic mark values and/or turning the autoscale function off.

In the frequency sweep mode there are drawn one trace in "Max Hold" and one trace in "Average", both run over the number of sweeps set by the user. When the sweeps end, the "DATA", "JPG" and "ALL" – buttons highlights as active, and by selecting the right button, it is possible to save just the data (DATA), as ASCII, or just the grid with the traces plot (JPG), or both data and plot (ALL). Usually the "ALL" - button is used.

The frequency sweeps have been post-processed, and some results are given in Appendix G.

B.10.4 Noise measurement

The layout of the noise measurement screen is quite similar to the frequency sweep screen. We have the fields with the fixed parameters and the user selectable parameters to the left, and saving buttons and info fields to the right.

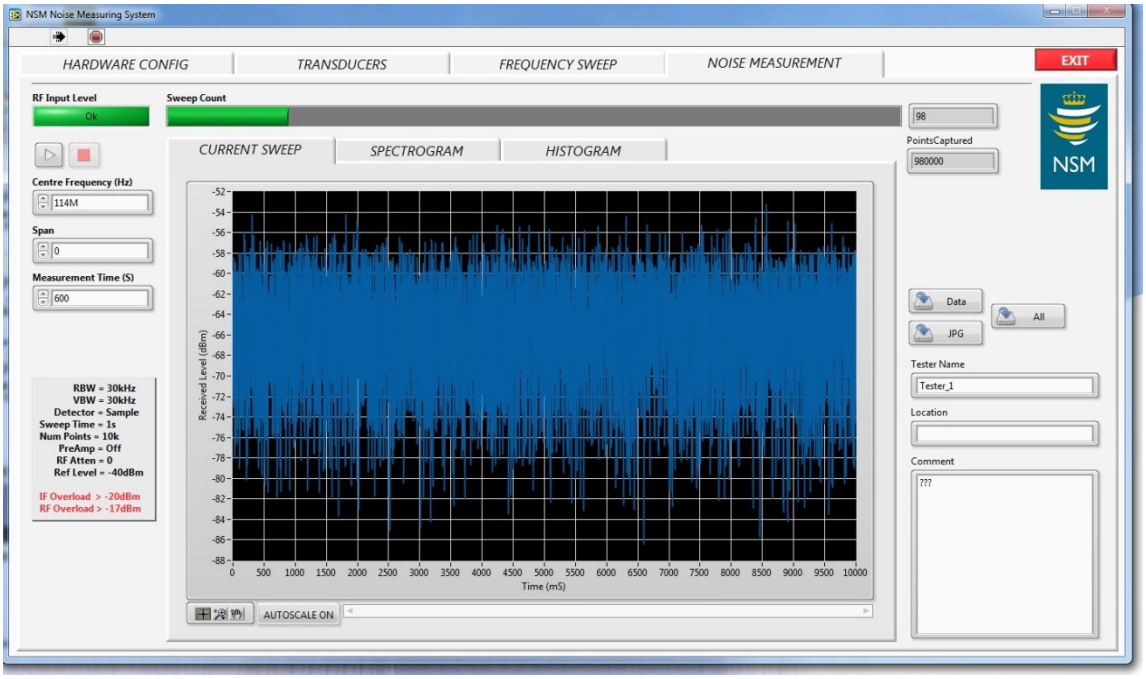

Figure B.9 Noise measurement screen.

In the noise measurement mode, the analyser's default non-changeable parameters are:

1. RBW = 30 KHz
2. VBW = 30 KHz
3. Detector = Sample

4. Sweep time = 1 s
5. Number of points = 10 K
6. PreAmp = OFF
7. RF Atten = 0 dB
8. Reference Level = -40 dBm
9. IF overload > -20dBm
10. RF overload > -17 dBm

The user can change:

1. Centre frequency
2. Span
3. Measurement time (s)

The span should be zero, or otherwise the noise measurement will be wrong. The noise measurement does 600 sweeps in the time domain, each lasting for 1 s, giving a total of 10 minutes and 6 million captured samples.

In “Current Sweep” the screen displays the noise samples taken during 1 s at a time, in near real time.

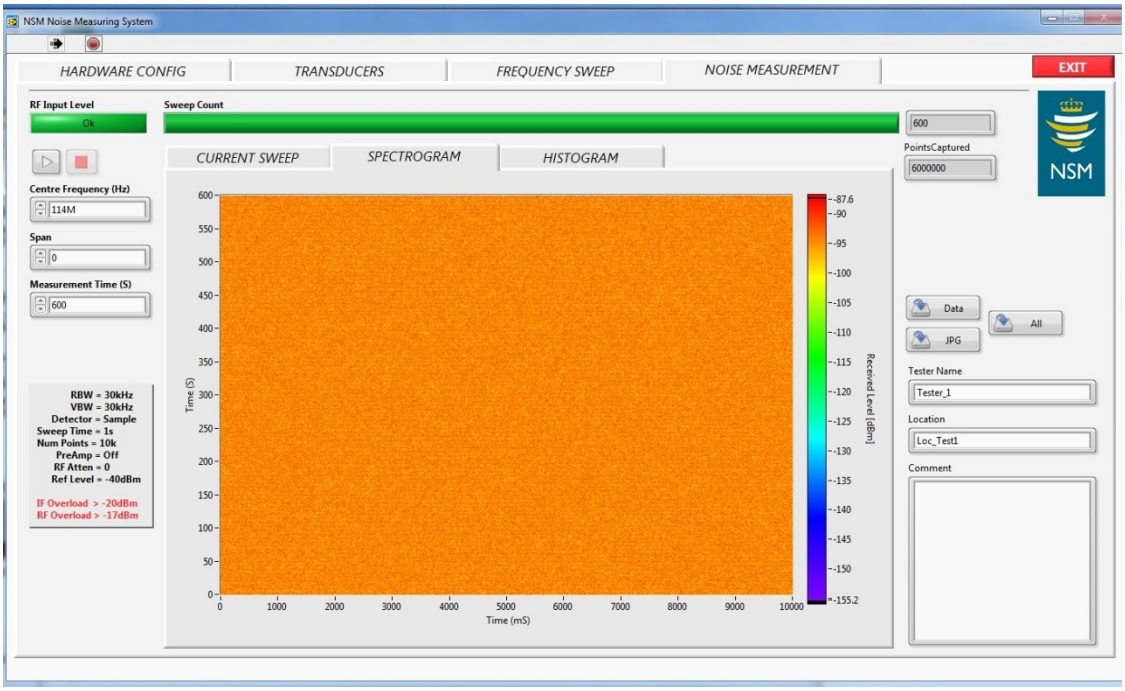

Figure B.10 Spectrogram of noise samples.

In “Spectrogram” the screen displays a spectrogram of the noise samples 1 s at a time, adding sweep for sweep to the screen. The noise levels are color-coded. The spectrogram helps to see regular or irregular changes in the noise level, as it appears as patterns in the spectrogram.

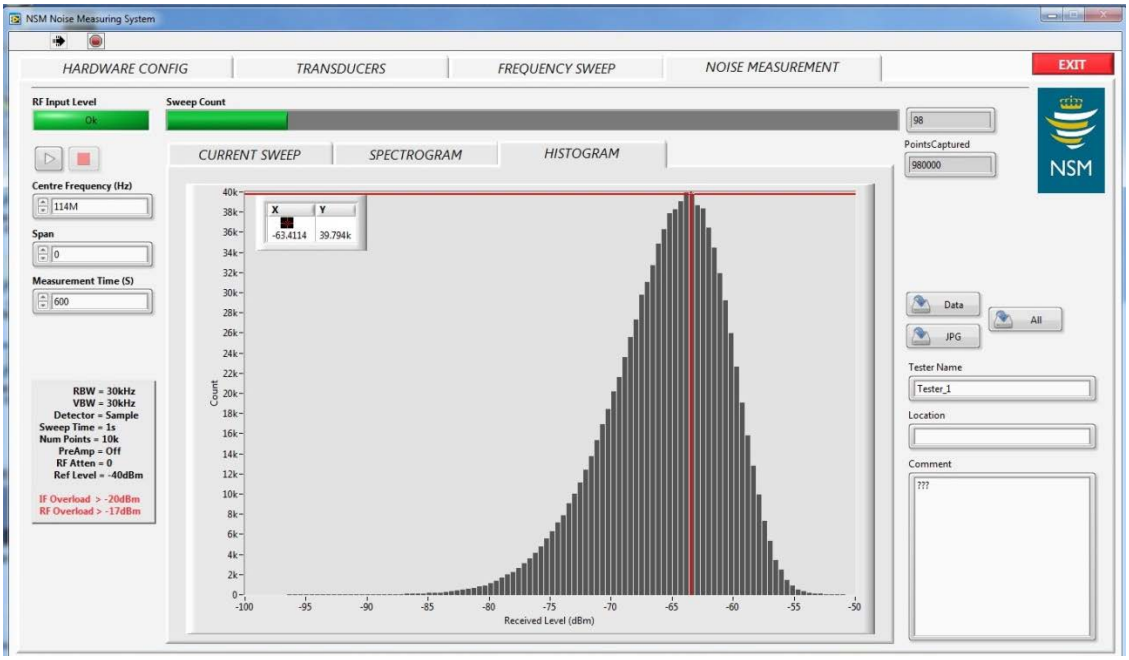

Figure B.11 Histogram of noise samples.

In “Histogram” the screen displays a histogram of the noise sample levels. The histogram is presented when the 600 sweeps are finished. Moving the cursor to the histogram’s highest point, and reading the corresponding noise level, gives an indication of the noise RMS value.

The three screens can be switched between during the noise measurement.

When the 10 minutes noise sampling is finished, the saving buttons become active. The “DATA” saves all the 6 million captured samples to a file, the “JPG” saves the graph of current (the last) sweep, the graph of the spectrogram, and the graph of the histogram to .jpg files. The “ALL” saves both the samples to a file, and the graphs to .jpg files. No data from current sweep, spectrogram or histogram is saved, just the graphs.

B.11 Running the measurements

B.11.1 Finding a location

When running the external man made noise measurements, the first task is to find a place to measure. This is done by using knowledge about local places that can be categorized according to the ITU “City”, “Residential”, and “Rural”. At more unknown places we have used Google Maps and Street View to select measurement locations. When selecting locations, we look for a place where we can park the vehicle, and place the tripod with the antenna some 10 – 20 meters away from the vehicle, without disturbing nearby traffic or activity. The antenna should, if possible, be placed in an open area, giving sight in most directions. Parking lots with “green” surroundings have shown to be good choices. To avoid noise pickup from the measurement system and the vehicle, we want to have the antenna some distance away from the vehicle.

B.11.2 Finding available measurement frequencies

Frequency [MHz]:	Antenna:	Low-pass filter:	Comments
20 - 120	VHF30108VM	NLP-250	
30 - 31			
84 - 85			
100 - 220	VHF108185VM	NLP-250	
113,5 - 114,5			
202,5 - 203,5			

Table B.1 Measurement setup during frequency sweep.

To cover the frequency span from some 10’s of MHz to about 200 MHz, we searched for one frequency in the lower end, and one frequency at the upper end of each of the two frequency ranges covered by the antennas, a total of 4 measurement frequencies. The first measurements were used to gain experience and find available frequencies.

Frequency [MHz]:	Antenna:	Low-pass filter:	BP-filter / Frequency	External Amplifier	Comments:
30 - 40	VHF30108VM	NLP-250	31 - 62	Miteq AU1310	Optional
30 - 31			30,45		
80 - 90	VHF30108VM	NLP-250	62 - 120	Miteq AU1310	Optional
84 - 85			84,5		
110 - 120	VHF108185VM	NLP-250	62 - 120	Miteq AU1310	Optional
113,5 - 114,5			114		
200 - 210	VHF108185VM	NLP-250	120 - 250	Miteq AU1310	Optional
202,5 -203,5			205		

Table B.2 Measurement setup during frequency sweep including filters and external amplifier.

Frequency [MHz]:	Antenna:	Low-pass filter:	BP-filter / Frequency	External Amplifier	Comments:
30,45	VHF30108VM	NLP-250	31 - 62	Miteq AU1310	
			30,45		
84,50	VHF30108VM	NLP-250	62 - 120	Miteq AU1310	
			84,5		
114,00	VHF108185VM	NLP-250	62 - 120	Miteq AU1310	
			114		
203,00	VHF108185VM	NLP-250	120 - 250	Miteq AU1310	
			205		

Table B.3 Measurement setup during noise sampling phase including filters and external amplifier.

At first a wide band scan is performed without any filtering, then a narrow band scan 1 MHz at measurement frequency. With both the low- and band- pass filters, and the external LNA in the chain, a 10 MHz, and a 1 MHz scan are performed. Table B.3 shows the noise measurement. The toggle between yellow and green cells means that a change in either settings or hardware is required.

C Post-processing procedures

C.1 Definitions of reference points

The purpose of the post-processing phase is to convert the raw noise measurement data of the capture file into a value of the external noise figure. This value of the noise figure is fully compatible with the definitions of the external noise figure in ITU-R P.372 and is based on the reference antenna of the ITU-R P.372 man-made noise model. The post-processing procedure is executed for each capture file generated, and gives a valid estimate of the external noise figure at the actual location, frequency and time in question.

Subsequent to the completion of this post-processing for all measurement frequencies and all locations within an environmental category, the values for the external noise factors are assembled in groups defined for each category. The median value of the external noise for each measurement frequency can be calculated from the statistics for each group.

A schematic of the practical realization of the measurement setup is described in Appendix B.

The post-processing executes the following tasks:

1. The capture file, which is generated by a spectrum analyser control PC, comprises sampled amplitude data with values referred to the spectrum analyser input. This is used to generate the APD of the (noise) signal of the input of the analyser. The APD is presented on the Rayleigh scale. As explained in section 3.2, this can separate impulse noise components in the measurements from Gaussian noise components. The power of the Gaussian noise component referred to the spectrum analysers input is estimated by the 37th percentile of the APD, which eliminates the influence of most impulse noise. However, this estimate presumes that there is no continuous or semi-continuous interference from radio transmitters present at the measurement frequency.

2. This value of the Gaussian noise power is converted to the external noise power at the antenna output by using pre-calibrated data from the components of the receiving system.

3. The latter noise power from the antenna is converted to an equivalent noise power of a loss-free half-wave antenna, which is used for the calculation of the external noise figure according to the ITU definitions.

4. In order to present the measured external noise figures on a format that is fully compatible to the ITU man-made noise data, the measured external noise figure of the half-wave antenna is converted to the equivalent value of the ITU reference antenna (short vertical grounded monopole antenna).

Figure C.1 shows a schematic that illustrates the post-processing process. The figure models the various elements of the measurement setup and defines the main parameters that are taken into account in the calculation of the external noise figure.

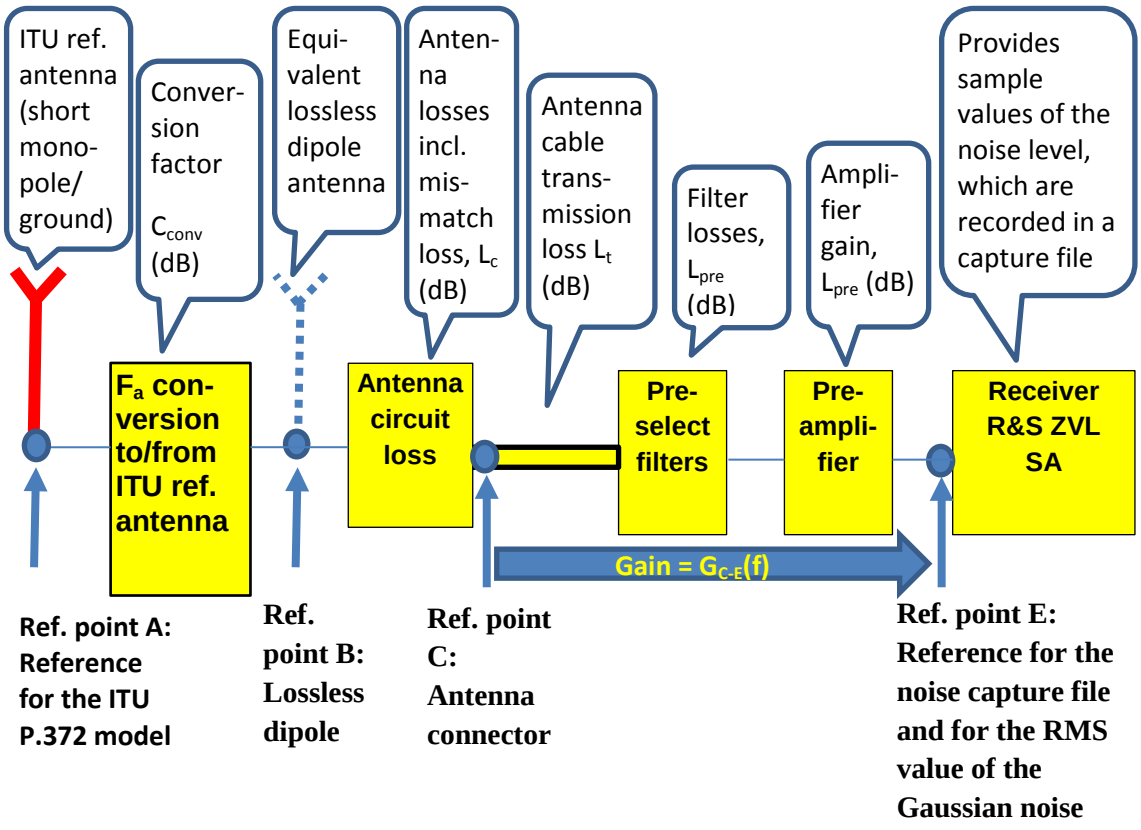

Figure C.1 The post-processing uses the data recorded in the capture file from the ZVL SA to calculate the value of the corresponding external noise figure of the equivalent reference antenna for the ITU-R man-made noise model.

The details of the methods applied during post-processing will be explained in the following sub-sections. In order to describe the various steps of this post-processing it is convenient to define the various reference points shown in Figure C.1:

- Reference point E is located at the input of the ZVL analyser and hence serves as the reference for the power levels of the captured sampled noise data file. Its RMS power level of the Gausssian noise component, P_E, is extracted from the APD of this capture file.

- Reference point C is located at the antenna connector which is, by definition, the input to the receiving system of the measurement setup. The RMS level of the external noise at this point is calculated from the noise power measured at reference point E, making use of calibration data of the part of the receiving system that precedes the SA.

- By definition, ITU-R P.372 relates the external noise factor to the external noise received by a *lossless* antenna. Hence reference point B is defined at the output of a hypothetical *lossless* dipole antenna of the same type and dimensions as our real antenna. The "antenna circuit loss" box between reference point B and C takes care of any loss of the real antenna, such as losses in its built-in matching network and losses due to mismatches. The calculated external noise figure at reference point B corresponds approximately to that of a half-wave lossless dipole antenna.

- Reference point A is a virtual point used for defining the available noise power that would have been received by a lossless short vertical monopole antenna above perfect ground, i.e. by the reference antenna for the ITU-R P.372 man-made noise model. This reference point is introduced only in order to be able to present the external noise figure measurements in a format which is directly compatible with and comparable to the predictions of the ITU-R P.372 man-made noise model. The monopole antenna reference of this model has a different relationship between the available noise power (and hence the noise figure) and the electromagnetic field strength of the noise compared to that of a dipole antenna. However, there is a simple mathematical relationship between the external noise figures of point A and point B; the difference in dB is defined by a constant conversion factor.

C.2 Estimating the RMS value of the Gaussian noise component at reference point E

In general, man-made noise is considered as having two main components, one component that has a Gaussian distribution and another component that has an impulsive characteristic. The ITU-R P.372 man-made noise model covers only the Gaussian component, which is generally considered to be the most important. A true RMS calculation of the received external noise will cover the power of both components. This is an adequate measure for the Gaussian noise component only in cases where the impulse noise is negligible.

A better method for estimating the power of the Gaussian component of the external noise in presence of impulse noise is based on using the characteristics of the APD of the received noise. Gaussian noise in the I and Q channel of a radio receiver will produce noise amplitude values (after demodulation) that follows a Rayleigh distribution. Hence the amplitude samples of the Gaussian component of the external noise are Rayleigh distributed. It is known that the complimentary cumulative distribution function (CCD) of a Rayleigh distributed variable will have a probability of $1\text{-}e \approx 0{,}368$ of exceeding the RMS value of the variable. Since the recorded capture file contains samples of amplitude values of the noise, the RMS value can be

estimated by calculating the 37th percentile of the CCD of the entries of the noise capture file. This gives a very accurate estimate when the noise is perfectly Gaussian. When impulse noise is added to Gaussian noise, the 37th percentile will maintain its role as a good estimator of the RMS value of the Gaussian component of the noise as long as the duty cycle of the impulse noise is reasonably low (disturbing the channel for up to a few per cent of the time). This is true even for noise impulses with very high power levels, the influence of which easily could dominate over the Gaussian noise component in a true RMS measurement.

Since the ITU-R P.372 man-made noise model only deals with the Gaussian noise component, eliminating any contribution from impulse noise in the measurements is desirable. Presenting the APD as a CCD of the capture file entries and calculating the 37th percentile value, secures an estimate of the Gaussian component that is fairly robust against the presence of additional impulse noise.

A graphical presentation of the APD using a so-called Rayleigh scaling provides the feature that a truly Gaussian distributed noise will be displayed as a straight line. An impulse noise component of the total noise can then be clearly identified as deviations from the straight line at low percentiles. A presence of an additive constant envelope interferer may also be identified by the APD plot on Rayleigh scale exhibiting distortion from a straight line. An explanation of the APD plots on Rayleigh graphs is given in reference (16), which also contains example Matlab code for creating such plots.

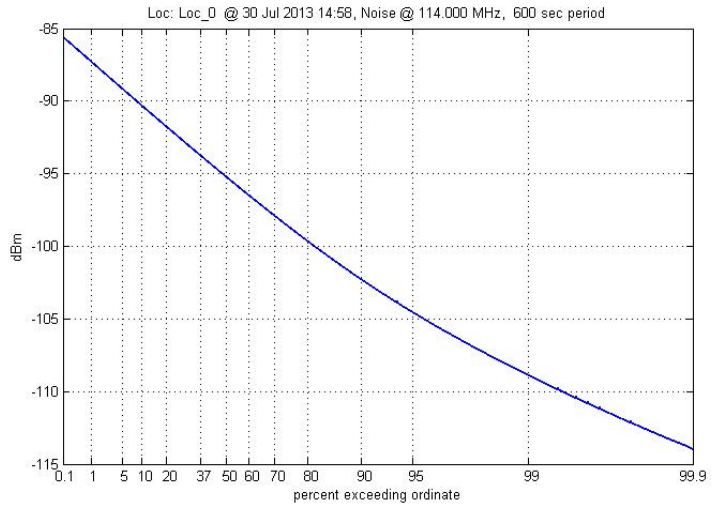

Figure C.2 ADP plot of the capture file data when the antenna is replaced by a 50 ohm termination. ZVL reception frequency = 114 MHz.

Figure C.2 to Figure C.4 show three examples of measured APD plots on Rayleigh scale. The frequency is 114 MHz. Figure C.2 applies for the case when the antenna is replaced by a 50 ohm termination. Hence it represents noise with a Gaussian distribution, and the ADP plot is expected to be a straight line. However, by contrast the APD displays a deviation from a straight line at low amplitude levels above about the 80th – 90th percentile value. This is attributable to

imperfections of the ZVL analyser and is probably due to some internally generated interference inside the ZVL instrument. However, because deviations occur only at low power levels, they do not significantly disturb the accuracy of the measured RMS power levels. The values of the calculated true RMS noise of the capture file are verified to be identical to the 37th percentile of the APD, which is to be expected from a Gaussian noise source.

A similar deviation from a straight line at the highest percentiles of the APD curve may also be present when measuring the external noise. However, as mentioned, this ZVL imperfection introduced at the lowest amplitude samples will not degrade the accuracy of the measurements of the external Gaussian noise power by its 37th percentile.

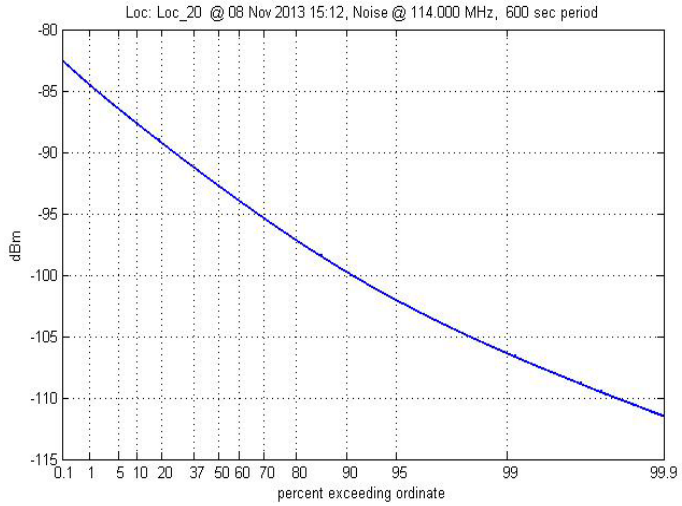

Figure C.3 Example of an APD plot of the capture file recorded at a location with negligible impulse noise.

Figure C.3 shows an ADP plot of the recorded external noise at a site with no detectable amount of impulse noise, while Figure C.4 shows an APD plot of the external noise at a site with a significant amount of impulse noise. In the latter and rather extreme case the impulse noise constitutes the dominating noise contribution. The true RMS power of all samples of the capture file in this case, i.e. the sum of the impulse noise and the Gaussian noise, are about 10 dB above the 37th percentile of the APD curve. In both cases the 37th percentile serves as a good estimate of the noise power of the Gaussian component, referred to point E.

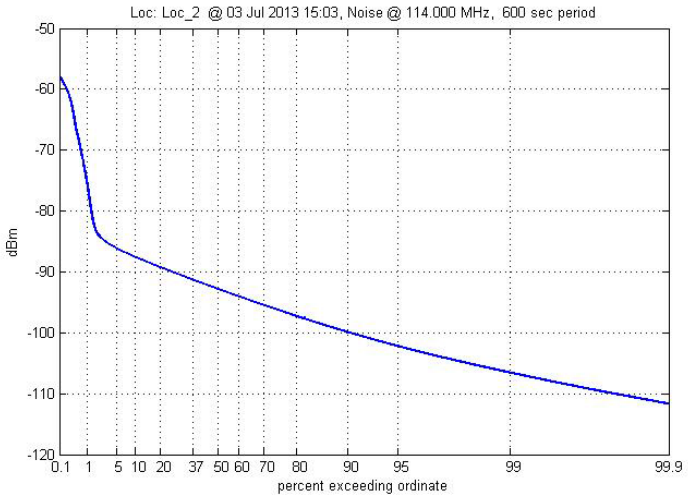

Figure C.4 Example of an APD plot of the capture file recorded at a location with a significant contribution of impulse noise.

For the purpose of calculating the external noise figure the estimate of the RMS power reference point E, P_E, is always based on the 37th percentile of the APD of the data of the noise capture file; thus supressing the influence of impulse noise. In most cases the RMS value of this Gaussian component will be within 1 dB of the true RMS value of the sum the Gaussian and the impulse noise contributions. However, in some extreme cases the difference between the RMS estimates that these two methods provide might be several dB (for example, the difference is about 10 dB in the case of Figure C.4).

C.3 Estimate of the external Gaussian noise contribution at reference point C

The RMS level of the Gaussian noise measured at reference point E, P_E, as calculated from the APD plot, is composed of the sum of the externally received Gaussian noise component and a noise component generated internally by the measurement receiving system. A measurement system for man-made noise aims at measuring the former component. Therefore, in order to increase the operational sensitivity of such a receiving system, a method is introduced to reduce the influence of the internally generated noise. This is done by subtracting an estimate of the internal noise contribution from the overall Gaussian noise measured. This operation can be done at reference point E, or, more suitably, at reference point C.

A measure of the internally generated noise is obtained by replacing the antenna with a 50 ohm termination and measuring the RMS noise level referred to point E, $P_{E50\Omega}$ (dBm), by the SA. This level can be converted to an equivalent internal noise level from the terminated receiving system referred to point C of:

$$P_{C50\Omega} = P_{E50\Omega} - G_{C-E} \qquad \text{(dBm)} \qquad \text{(C.1)}$$

In order to subtract power levels it is practical to convert from dB to linear units. Expressing a parameter in linear units (mW) is symbolized by starting the parameter name with a small letter (according to the ITU-nomenclature of (1), $p_{C50\Omega}$, $g_{C\text{-}E}$). Hence the linear equivalent of equation C.1 is expressed as

$$p_{C50\Omega} = p_{E50\Omega}/g_{C-E} = 10^{\left(\frac{P_{E50\Omega} - G_{C-E}}{10}\right)} \quad \text{(mW)} \quad \text{(C.2)}$$

The noise factor of the terminated receiving system referred to point C is defined as

$$f = p_{C50\Omega}/kt_0b \quad \text{(C3)}$$

where k is Bolzmanns constant, t_0 is the temperature (K) and b is the bandwidth (Hz). The internal noise contribution by *the receiving system* referred to point C is

$$p_{C,int} = (f-1)\cdot kt_0b = p_{C50\Omega} - ktb = p_{C50\Omega}\cdot(f-1)/f \quad \text{(C.4)}$$

Hence, in linear terms, the level of the *external* Gaussian noise referred to point C can be expressed:

$$p_{C,ext} = p_C - p_{C,int} = p_C - (p_{C50\Omega} - kt_0b) = p_C - p_{C50\Omega}\cdot(f-1)/f \quad \text{(C.5)}$$

Where p_C is the total equivalent RMS level of the Gaussian noise referred to point C, which is calculated from the RMS noise as measured at point E:

$P_C = P_E - G_{C-E}$ in dB, and

$$p_C = p_E/g_{C-E} = 10^{\left(\frac{P_E - G_{C-E}}{10}\right)} \text{ in linear terms} \quad \text{(C.6)}$$

Equation (C.5) is used during the post-processing in order to give a fair estimate of the external Gaussian noise level arriving from the antenna also in cases where the external noise level is comparable to, or even lower than that the internal noise level generated by the measurement setup. This has been the case particularly at rural locations. However, at low levels of the external noise, this estimate will have progressively lower relative accuracy compared to measurement of external noise level above the internal noise. This can be understood by inspection of eq. (C.5), where the difference between the two subtractive terms will become smaller for low values of the external noise level. If these two terms have uncorrelated errors, the linear subtraction process of eq. (C.5) will amplify the relative influence of the errors.

This effect can be illustrated by a practical example using data from our measurements. The measurement at 203 MHz at location 17 resulted in an estimate of the external noise figure of -1,5 dB (confer Table 4.5) using the values of P_C and $P_{C50\Omega}$ that we believe is nominally correct. However, what if the measured value of P_C for some reason contained a measurement error of 0.5 dB while $P_{C50\Omega}$ contained no such error? The effect of subtraction of eq. (C.5) will amplify

this 0,5 dB measurement error of P_C and the external noise figure would be reduced by 1,9 dB to a value of -3,4 dB.

Hence, although results of the external noise figure will be quoted even for cases when the internal noise of the measurement setup dominates, it should be kept in mind that these estimates are less accurate than the high values of the external noise figures.

C.4 Estimating the external noise figure referred to a half-wave dipole antenna

After having established the external Gaussian noise level at reference point C, the next step is to calculate the corresponding external noise figure or the noise factor of the antenna. The antennas used for the measurements are "wideband" tactical VHF dipole antennas from COMROD; VHF 30108VM and VHF108185VM. These are specified to cover a frequency range of 30 – 108 MHz and 108 – 185 MHz respectively; however, the latter antenna has a good performance up to frequencies above 200 MHz. The "widebanding" of the antennas is achieved by matching circuitry located inside the base of the antenna.

These antennas are treated as half-wave dipole in the post-processing. In reality the electrical length of the antenna varies across the operational frequency range of each antenna. However, this does not change its directive radiation pattern appreciably. Therefore, this simplification does not lead to unacceptable errors in the calculation of the noise figure.

One main effect of using the above "wideband" dipole antennas as compared with a tuned half-wave dipole antenna is that the former type of antenna has higher loss factor. This is mainly caused by losses in the built-in tuning network as well as the mismatch losses in a 50 ohm load. This loss will materialise itself in that the achievable effective gain of the antenna is lower than its theoretical directive gain. This type of loss is included in what is the termed "antenna circuit loss" in the ITU-nomenclature of (1), and is denoted l_c (linear) or L_c (dB). This antenna circuit loss is the only functional block that separates reference point B and C in Figure C.1. By definition the loss factor $l_c \geq 1$ and $L_c \geq 0$.

The available power from the hypothetical lossless antenna of reference point B is called P_B and can be expressed as

$p_B = p_c \cdot l_c$ in linear terms, or: $P_B = P_C + L_c$ (in dB scale) (C.7)

The effective gain of a lossless half-wave dipole antenna is 2,15 dBi. Alternatively it can be referred to as 0 dB above the theoretical gain of a half-way dipole, which is expressed as 0 dBd. Since our measurement antennas are treated like a half-wave dipole antenna, the antenna circuit loss can simply be calculated according to:

$L_c = -Measured\ Gain(dBd) = -(Measured\ Gain(dBi) - 2.15)$ (C.8)

Appendix D offers COMROD data for the two different antennas used during the measurement campaign. The antenna data for the post-processing is extracted from this COMROD data for the VHF108185VM as given in Appendix D. However, the COMROD data supplied for the VHF30108VM antenna was based on measurements on its sibling antenna (VHF3088VM), which has a narrower bandwidth.

Antenna	VHF30108VM		VHF108185VM	
Frequency (MHz)	30,45	84,5	114	203
Antenna Gain (dBi)	-7	-2,2	1,3	0,4
Tripod gain contr. (dB)	-0,1	-0,6	-0,8	-0,8
Antenna circuit loss, L_c (dB)	9,1	4,9	1,6	2,5

Table C.1 Estimates of the Antenna circuit loss, L_c, including the effects of the tripod, as calculated according to equation (C.8). The antenna gain for the VHF30108VM is estimated from FFI measurements, and COMROD data is used for the other antenna.

Moreover, the results after the initial post-processing indicated that our antenna gain at 84,5 MHz seemed to be lower than the value depicted by the COMROD data. This was confirmed by separate VHF30108VM antenna gain measurements performed by FFI, and the results from these measurements were used for estimating the antenna loss at the two lowest frequencies.

The antenna gain, and hence the antenna circuit loss is a function of frequency. The value of the L_c should account also for any loss attributable to the tripod antenna mount. The tripod loss contribution was measured by FFI in the frequency range of the VHF30108VM antenna, and estimated values are used at the higher frequencies. The value of L_c, calculated at the main measurement frequencies that are used in the campaign, is given by Table C.1. These are the values that are used for calculating P_B according to equation (C.7).

By definition, the external noise factor at reference point B is calculated according to

$$f_B = \frac{p_B}{kt_0 b} \qquad \text{(C.9)}$$

Hence the measured external noise figure referred to a half wave dipole antenna is calculated as:

$$\mathrm{F_B} = 10\log\left(\frac{p_B}{kt_0 b}\right) \quad \text{(dB)} \qquad \text{(C.10)}$$

C.5 Conversion of the external noise figure to the ITU-R P.372 reference antenna

As explained in section 2.1 the value of the external noise figure depends on the antenna type to which it is referred. The measured external noise figure at reference point B, F_B, is referred to a lossless half-wave dipole antenna. In order to make the measured noise figure directly comparable to the predictions of the ITU-R P.372 man-made noise model, F_B needs to be converted to the equivalent value that would have been measured if the ITU-R P.372 reference antenna were used. This is illustrated as reference point A in Figure C.1.

The noise figure at this hypothetical reference point A is denoted F_a, and its value is the output of the post-processing of a measurement at each location/frequency. The translation between the noise figure of reference point A and B can be expressed:

$$F_a = F_B - C_{conv} \quad \text{(dB)} \qquad \text{(C.11)}$$

The numerical value of the conversion factor C_{conv} can be found by combining equations (4) and (5). Recalling that $F_{a,mono}$ and $F_{a,d}$ are the external noise figures of the ITU monopole and a half-wave dipole, respectively, their relationship is given by

$$F_{a,mono} = F_{a,d} - 98{,}9 + 95{,}5 = F_{a,d} - 3{,}4 \quad \text{(dB)} \quad \text{(C.12)}$$

It can be concluded from eq. (C.12) that the numerical value of C_{conv} in eq. (C.11) is 3,4 dB. Substituting $F_{a,d}$ in (C.12) with the value of F_B given by equation (C.10) will translate our measured external noise figure to the antenna reference that is used by the ITU-R P.372 man-made noise model. Hence, (C.11) can be written

$$F_a = F_B - 3{,}4 \quad \text{(dB)} \qquad \text{(C.13)}$$

Applying this equation is the final step in the post-processing of each specific capture file and gives the measured external noise figure with identical antenna reference to that of the ITU-R P.372 man-made noise model. This calculated value is valid for the conditions of the capture file, i.e. for the specific location, the specific frequency and the actual time-of day of the capture recording.

Note that the noise figure that comes out from the processing is the external noise figure at a location, covering all sources of Gaussian noise. The external Gaussian noise at the frequency range measured may have contributions of both galactic and man-made noise. Decomposition of the measured external noise figure according man-made and galactic noise contributions cannot be done with any accuracy. However, the galactic noise will, in general, have a lower median level than the man-made noise at most locations except very quiet ones, as is indicated in Figure 2.2 of this report. We make the assumption that the external noise estimate can be considered as a reasonably good measure of the man-made noise level. This assumption is met for the

majority of the measurement locations except the quietest ones, where the galactic noise may be similar to or even higher than the man-made noise at high frequencies.

D Antenna VSWR and gain

D.1 SRS 25 – 2000 MHz

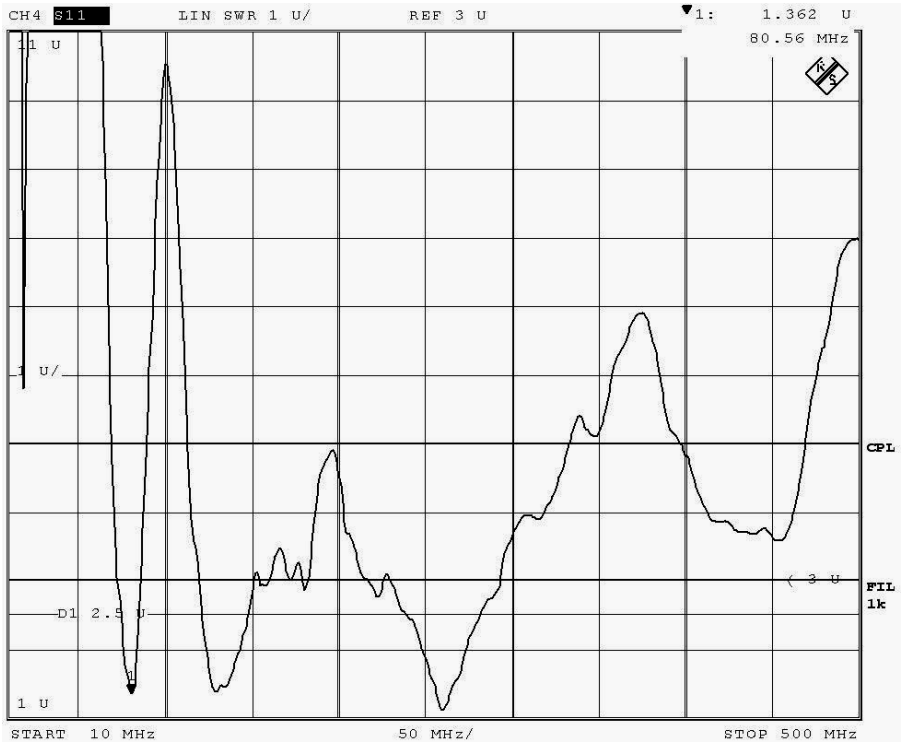

Figure D.1 Measured voltage standing wave ratio of the "Royal Discone" antenna from Swedish Radio Supply.

D.2 Comrod VHF30108VM

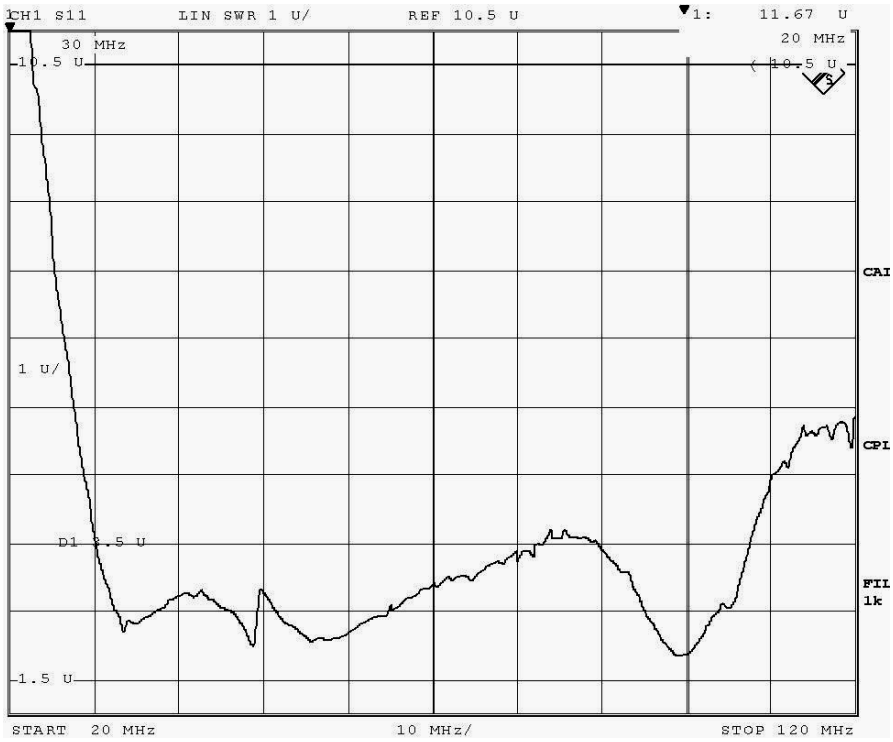

Figure D.2 Measured voltage standing wave ratio of the Comrod antennaVHF30108VM.

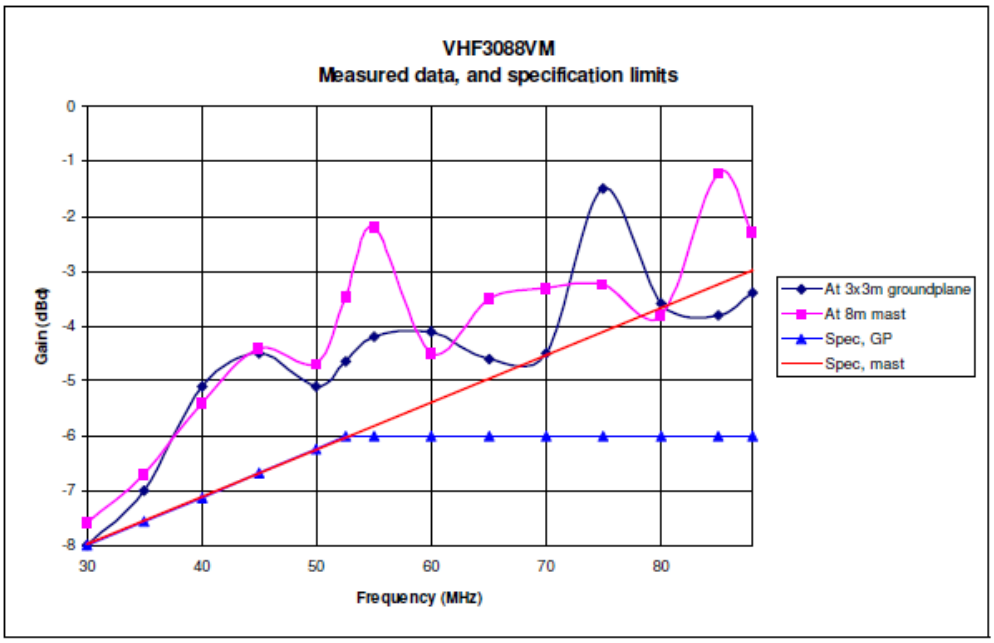

Figure D.3 The gain and pattern are measured with the antenna in free space, or in the centre of a 3x3m ground plane. These measurements were done on a VHF3088VM, but below 88MHz the VHF30108VM has similar performance. The antenna is at least 9m above ground, and the distance to the receiving antenna is at least 60m. For gain measurements the reference antenna is a resonant half wave dipole which is substituted for the antenna tested. Comrod specifications(18).

D.3 Comrod VHF108185VM

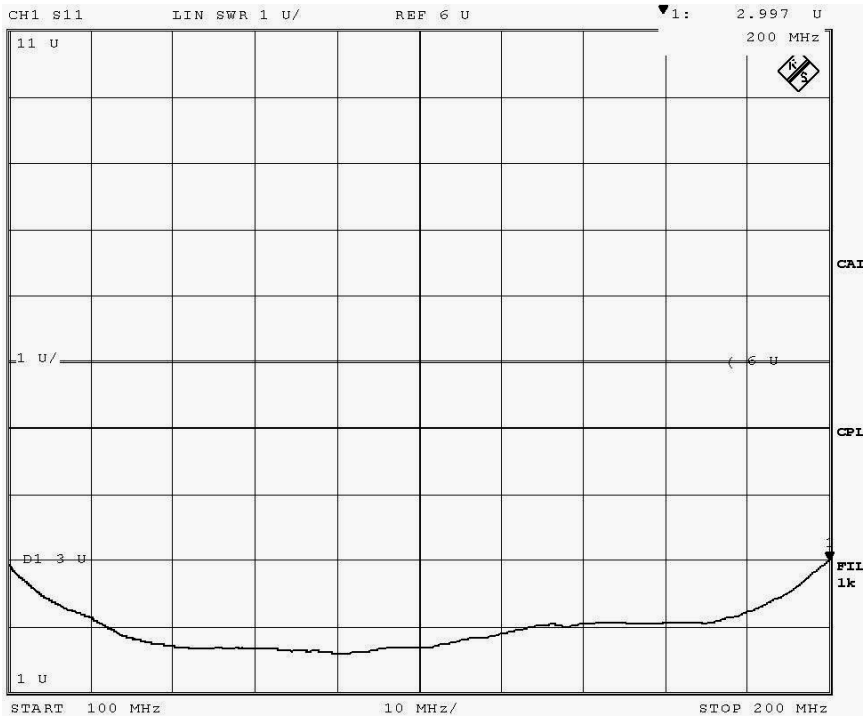

Figure D.4 Measured voltage standing wave ratio of the Comrod antenna VHF108185VM.

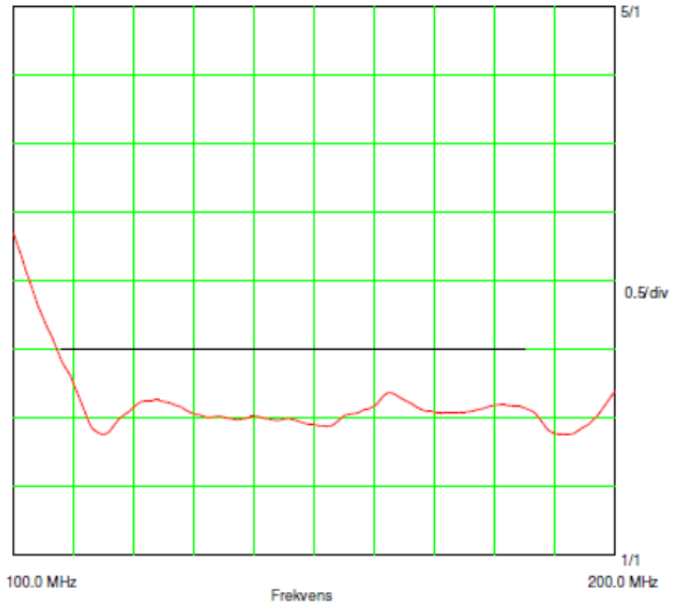

Figure D.5 This is tested with the antenna without ground plane. The lowest part of the antenna must be at least 1m above ground, and the antenna is in a vertical

position. The VSWR limit is 2.6/1, but may rise to 3/1 for less than 2 % of the frequency range. Comrod specifications (19).

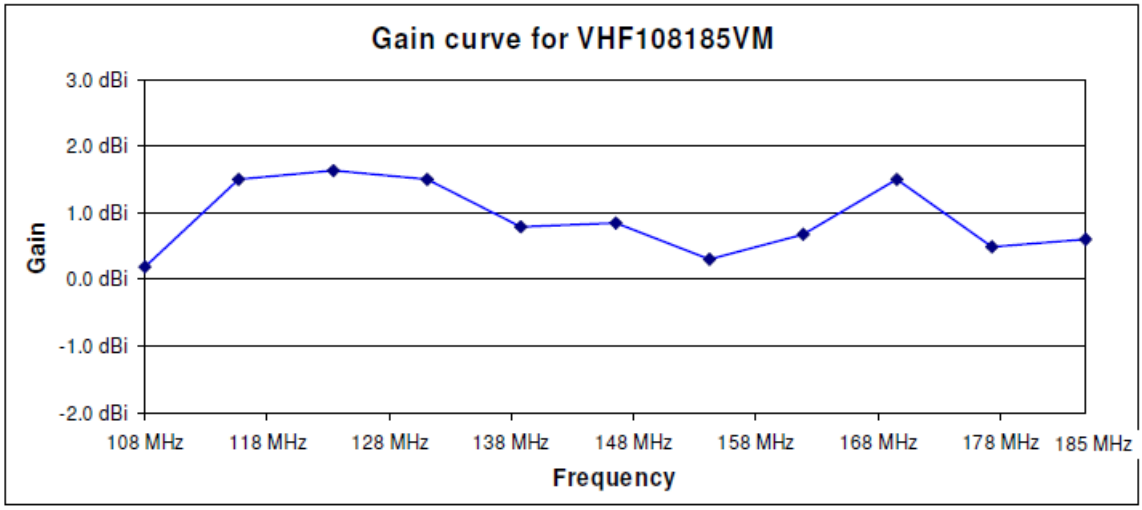

Figure D.6 The gain and pattern are measured with the antenna in free space on a ground reflection test range. The antenna was approximately 7m above ground, and the distance to the receiving antenna was around 68m. For gain measurements the reference antenna is a resonant half wave dipole which is substituted for the antenna tested. Comrod specifications (19).

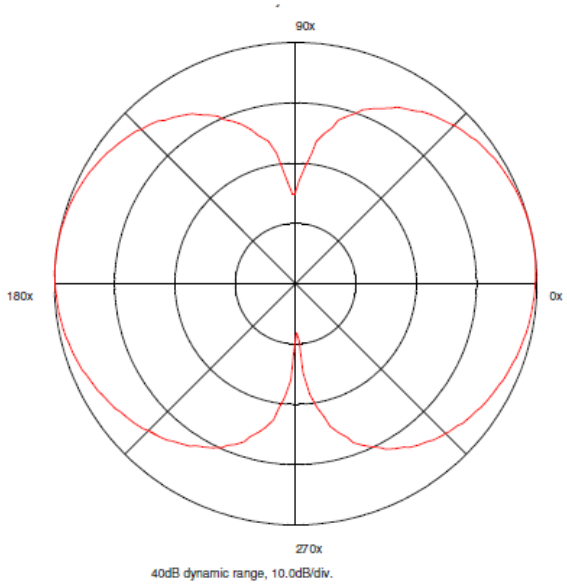

Figure D.7 Typical radiation pattern. Comrod specifications (19).

Figure D.8 Antenna test range. Measuring the tripod's influence on the Comrod VHF30108VM's gain.

D.4 Amphenol Jaybeam 7177010, 100 – 500 MHz

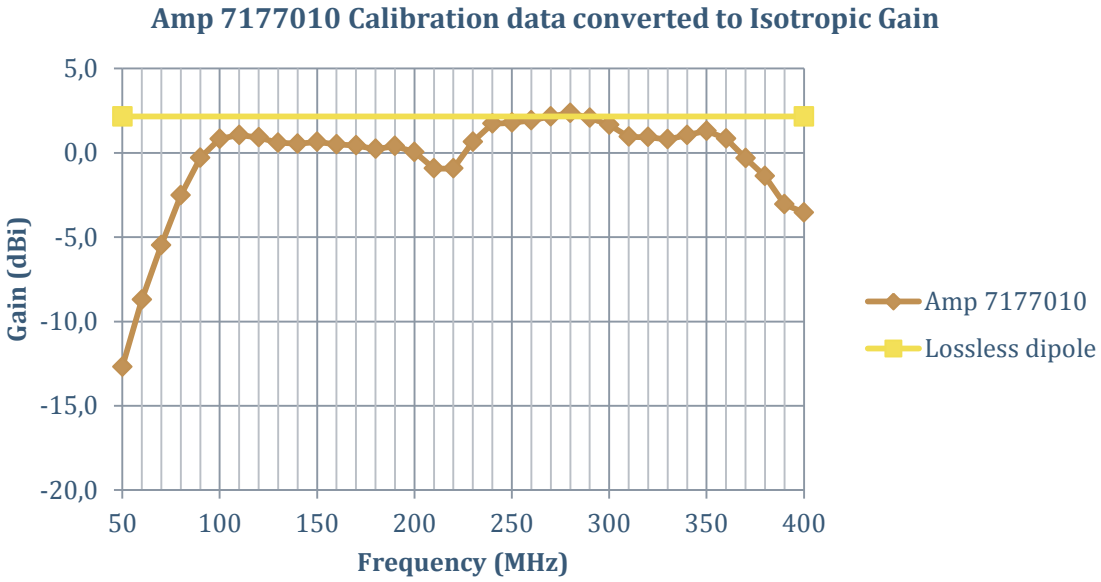

Figure D.9 Gain comparison between the Amphenol Jaybeam 7177010 antenna and a lossless dipole.

E Filter responses

E.1 Wavetek BP-filter 31 – 62 MHz

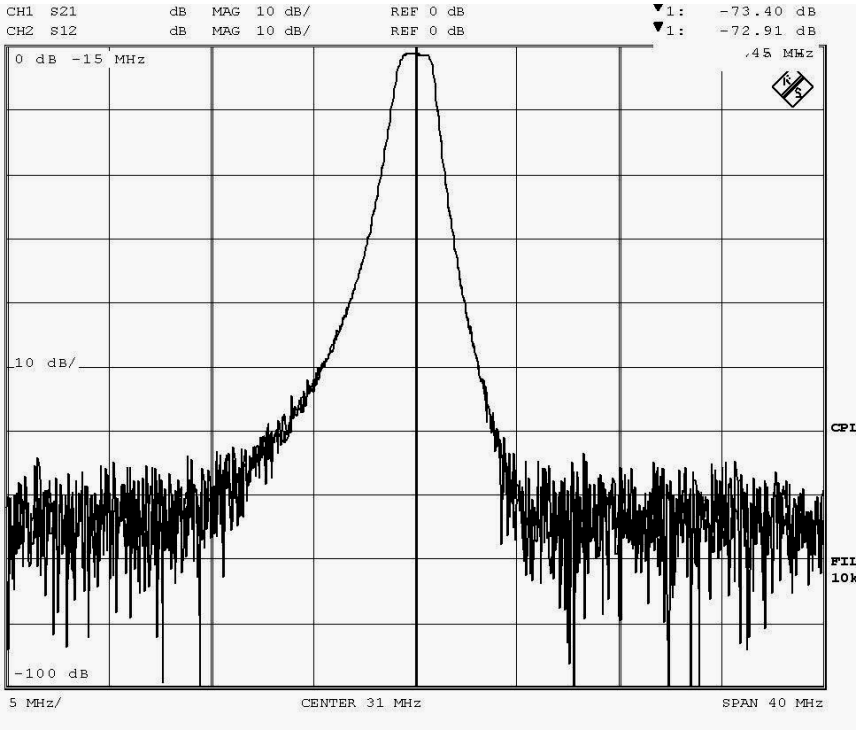

Figure E.1 Response of Wavetek band-pass filter tuned to 31 MHz.

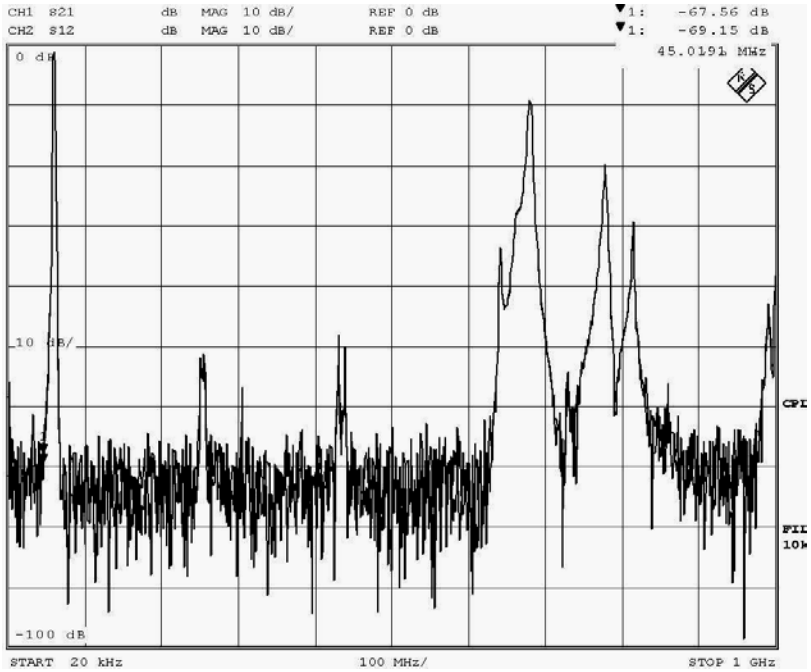

Figure E.2 Response of Wavetek band-pass filter tuned to 45 MHz showing spurious responses near the GSM Bands.

E.2 Mini-Circuits LP-filter NLP-250

Coaxial

Low Pass Filter

NLP-250+
NLP-250

50Ω DC to 225 MHz

CASE STYLE: FF57

Connectors	Model	Price	Qty.
N-Type	NLP-250(+)	$35.95 ea.	(1-9)

Maximum Ratings

Operating Temperature	-55°C to 100°C
Storage Temperature	-55°C to 100°C
RF Power Input	0.5W max.

Permanent damage may occur if any of these limits are exceeded.

Features

- rugged shielded case
- other NLP models available with wide selection of cut-off frequencies

Applications

- lab use
- test equipment
- video equipment

Low Pass Filter Electrical Specifications

PASSBAND (MHz)	fco (MHz) Nom.	STOPBAND (MHz)		VSWR (:1)	
				Passband	Stopband
(loss < 1 dB)	(loss 3 dB)	(loss > 20 dB)	(loss > 40 dB)	Typ.	Typ.
DC-225	250	320-400	400-1200	1.7	18

Outline Drawing

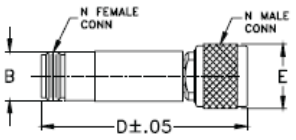

Outline Dimensions (inch / mm)

B	D	E	wt
.67	2.90	.82	grams
17.02	73.66	20.83	90.0

typical frequency response

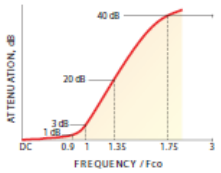

electrical schematic

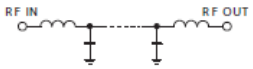

Typical Performance Data

Frequency (MHz)	Insertion Loss (dB) x̄	Insertion Loss (dB) σ	Return Loss (dB)	Frequency (MHz)	Group Delay (nsec)
10.00	0.03	0.1	28.7	10.00	3.54
20.00	0.03	0.1	24.7	20.00	3.66
80.00	0.20	0.1	16.1	80.00	3.78
100.00	0.28	0.1	14.8	100.00	3.80
165.00	0.27	0.1	24.4	165.00	4.63
217.50	0.60	0.1	16.4	217.50	6.37
225.00	0.64	0.1	20.4	225.00	7.25
240.00	1.59	0.3	8.3	230.00	8.00
250.00	3.87	0.6	3.6	240.00	9.42
260.00	7.27	0.9	1.6	245.00	9.37
280.00	14.62	1.0	0.5	250.00	8.91
300.00	21.27	1.1	0.3	260.00	6.90
310.00	24.28	1.2	0.3	270.00	5.18
315.00	25.71	1.2	0.3	280.00	3.91
320.00	27.12	1.3	0.3	290.00	3.02
330.00	29.77	1.3	0.3	300.00	2.66
350.00	34.87	1.6	0.2	310.00	2.33
370.00	39.35	1.9	0.2	315.00	2.14
380.00	41.63	2.0	0.2	320.00	1.98
390.00	43.91	2.3	0.2	330.00	2.13
400.00	46.09	2.7	0.2	340.00	1.53
580.00	69.80	3.0	0.1	350.00	1.30
682.50	69.02	1.5	0.1	360.00	1.37
785.00	69.27	2.4	0.1	370.00	1.15
890.00	69.72	4.5	0.1	380.00	1.78
992.50	70.16	5.1	0.1	390.00	0.46
1045.00	73.29	6.6	0.1	400.00	0.27
1097.50	70.40	5.6	0.0	580.00	0.25
1147.50	71.08	3.9	0.2	630.00	0.20
1200.00	71.31	2.1	0.2	682.50	0.20

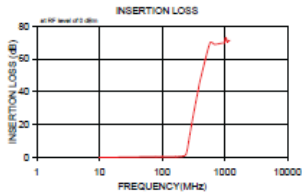

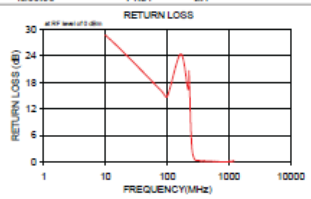

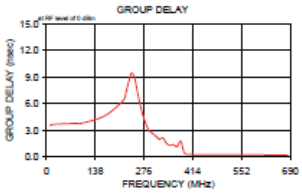

Mini-Circuits®
ISO 9001 ISO 14001 AS 9100 CERTIFIED

For detailed performance specs & shopping online see web site

P.O. Box 350166, Brooklyn, New York 11235-0003 (718) 934-4500 Fax (718) 332-4661 The Design Engineers Search Engine Provides ACTUAL Data Instantly at minicircuits.com

IF/RF MICROWAVE COMPONENTS

REV. A
M122594
NLP-250
100726

Notes: 1. Performance and quality attributes and conditions not expressly stated in this specification sheet are intended to be excluded and do not form a part of this specification sheet. 2. Electrical specifications and performance data contained herein are based on Mini-Circuit's applicable established test performance criteria and measurement instructions. 3. The parts covered by this specification sheet are subject to Mini-Circuits standard limited warranty and terms and conditions (collectively, "Standard Terms"); Purchasers of this part are entitled to the rights and benefits contained therein. For a full statement of the Standard Terms and the exclusive rights and remedies thereunder, please visit Mini-Circuits' website at www.minicircuits.com/MCLStore/terms.jsp.

Figure E.3 Mini-Circuits low-pass filter, NLP250 datasheet.

F System attenuation and gain

F.1 Measurement frequency 30,45 MHz

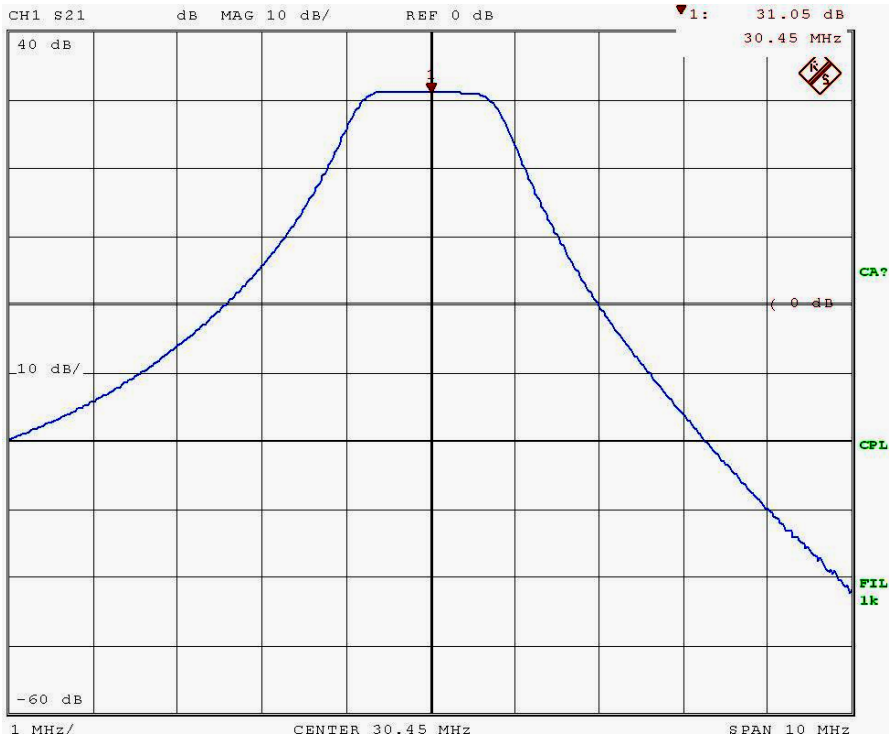

Figure F.1 System gain at measurement frequency 30,45 MHz.

F.2 Measurement frequency 84,5 MHz

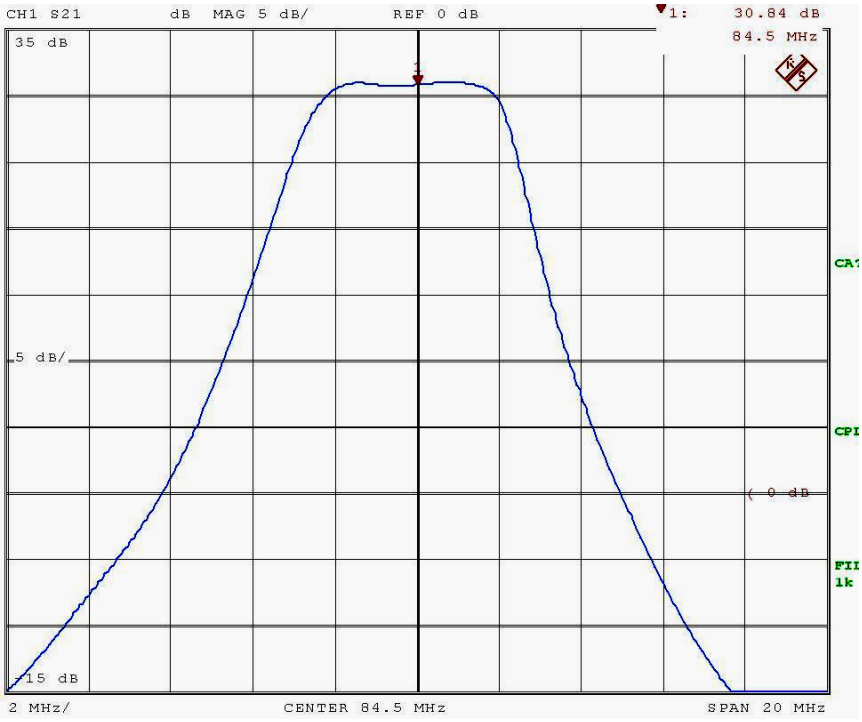

Figure F.2 System gain at measurement frequency 84,5 MHz.

F.3 Measurement frequency 114 MHz

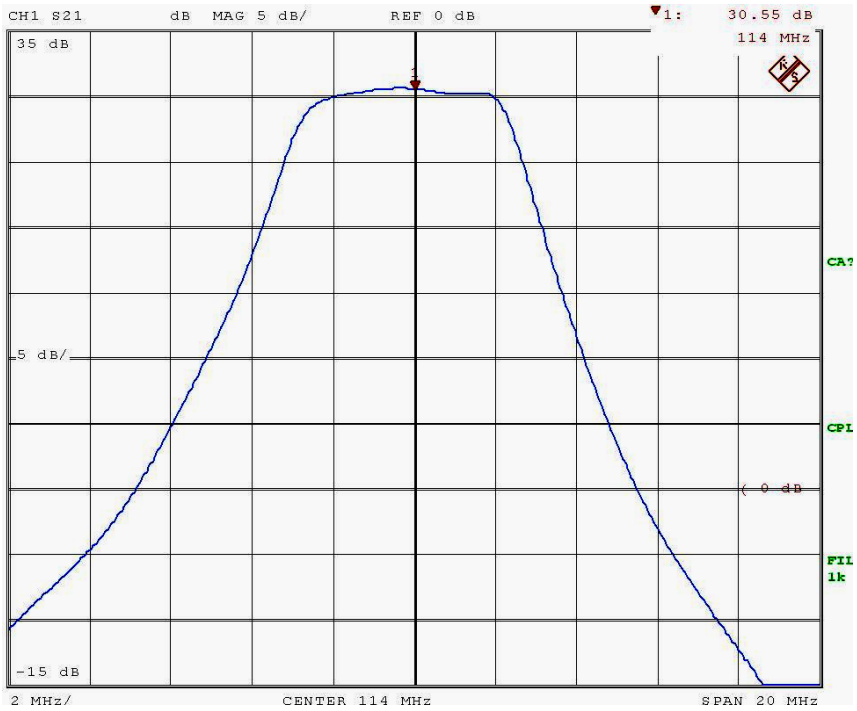

Figure F.3 System gain at measurement frequency 114 MHz.

F.4 Measurement frequency 194 MHz

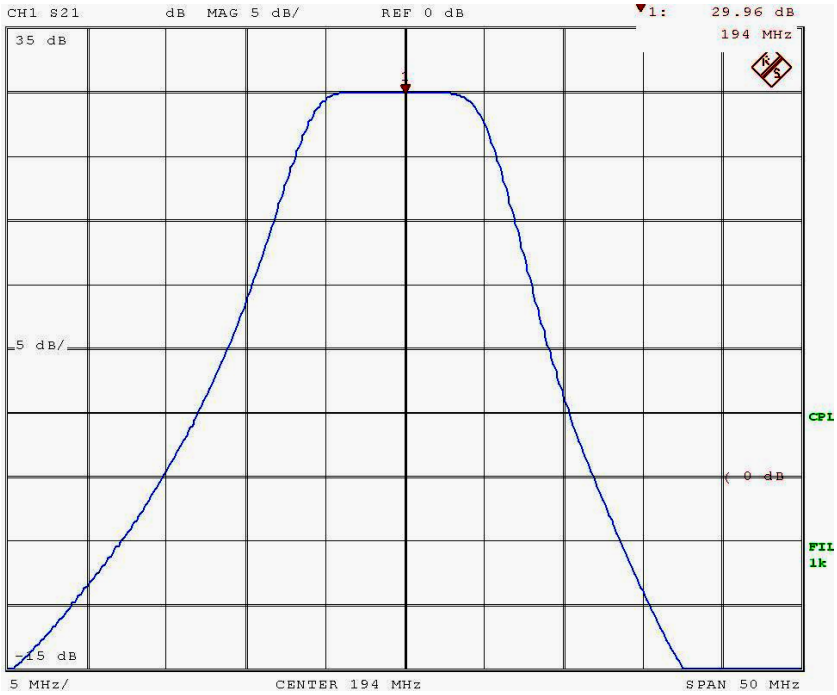

Figure F.4 System gain at measurement frequency 194 MHz.

F.5 Measurement frequency 203 MHz

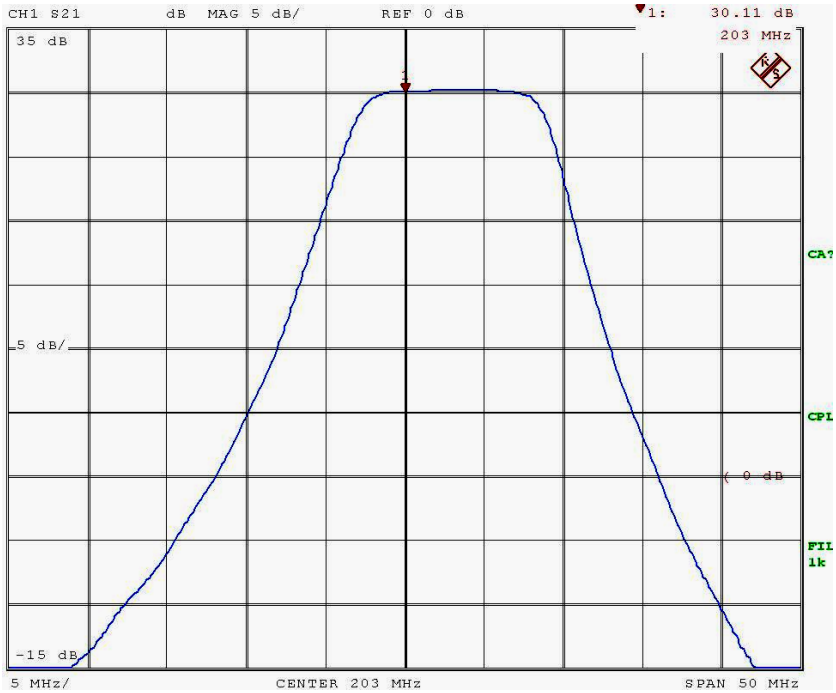

Figure F.5 System gain at measurement frequency 203 MHz, the filter is tuned to 205 MHz to filter out DAB – signals below 200MHz.

F.6 Cable attenuation

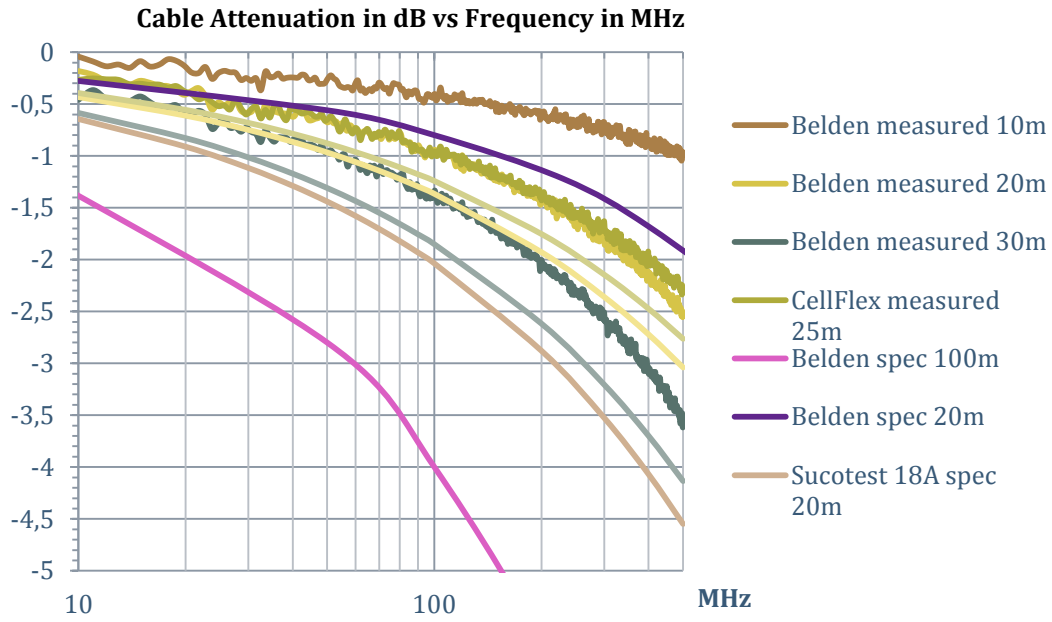

Figure F.6 Cable attenuation of some cables. CellFlex 25 m has the lowest attenuation.

F.7 System gain, all frequencies

	Gain throughout the measurement chain	
Frequency [MHz]	Cable; Belden-H1000 [dB]	Cable; CellFlex [dB]
30,45	30,74	31,05
84,50	30,53	30,84
114,00	30,28	30,55
194,00	29,96	30*
203,00	29,79	30,11

*Table F.1 Overall attenuation/gain measurement with network analyser throughout the measurement chain. *Estimated.*

Connection:	Antenna Cable:	Cable:	LP-filter:
Cable; Belden	Belden H-1000, 20m	Sucotest, 1m+	NLP250
Cable; CellFlex	CellFlex, 25m	Sucotest, 1m+	NLP250

BP-filter	Cable:	Low Noise Amp:	Cable:
Wavetek BP	SMA-Cable, 30 cm	Miteq AU1310	Sucotest, 1m
Wavetek BP	Sucotest, 1m	Miteq AU1310	Sucotest, 1m

Table F.2 The RF connections with Belden and Cellflex cables

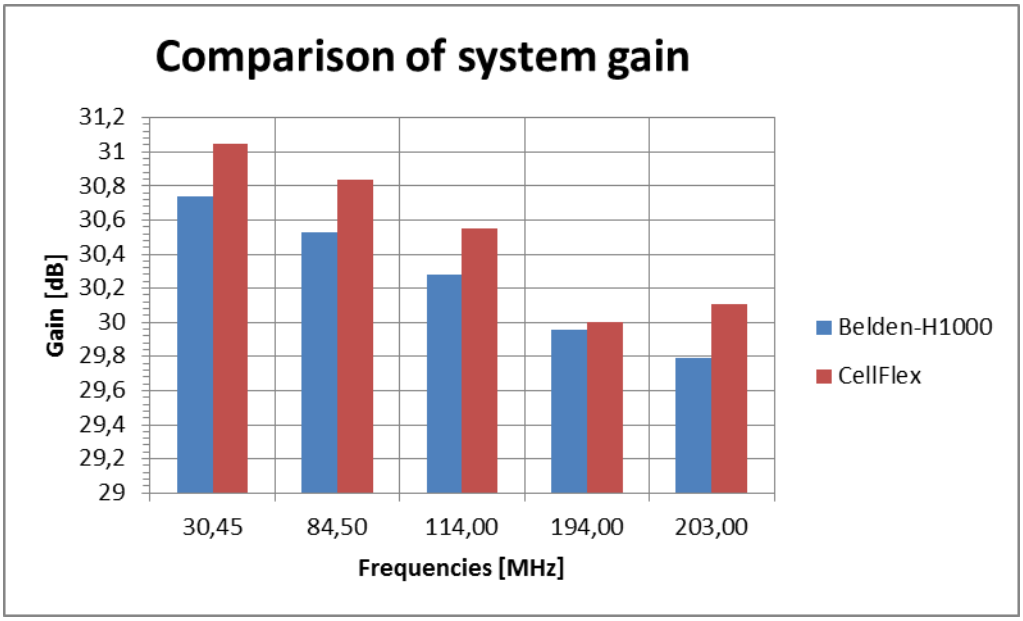

Figure F.7 Overall attenuation/gain measurement with network analyser throughout the measurement chain.

G Frequency sweeps

Together with the noise measurements, a lot of frequency sweeps have been made. These sweeps were intentionally made to find useful noise sampling frequencies. But, as they are saved as both graphical and ASCII files, we have imported the files to Excel and done some post-processing.

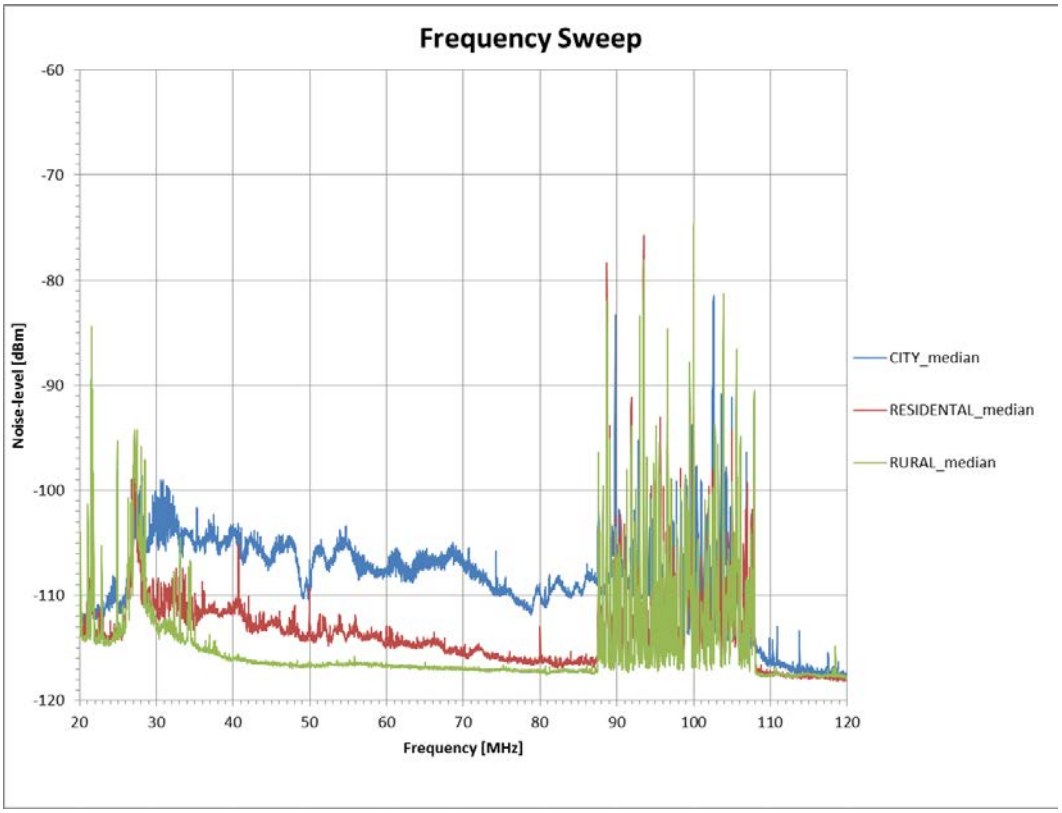

Figure G.1 Frequency sweeps of the three measured categories, median of all sweeps 20-120 MHz.

In Figure G.1 all relevant sweeps according to the measured ITU categories have been input to the median calculations. The median traces show a distinct difference between the “City”, “Residential” and “Rural” categories. At the lower end we have signals from the HF – band, and in the upper end we have FM –signals in the band 87,5 MHz – 108 MHz. Above the FM band, the traces roll off, much because of gain roll off from the Comrod VHF30108VM measurement antenna.

In Figure G.2 the median traces according to the measured ITU categories covers the frequency range 100 – 220 MHz. The “City” median noise level is clearly above the “Residential” and “Rural” noise level up to about 170 MHz, where the median noise differs less. From 190 MHz and up, the median noise of the three categories nearly merge at the same level.

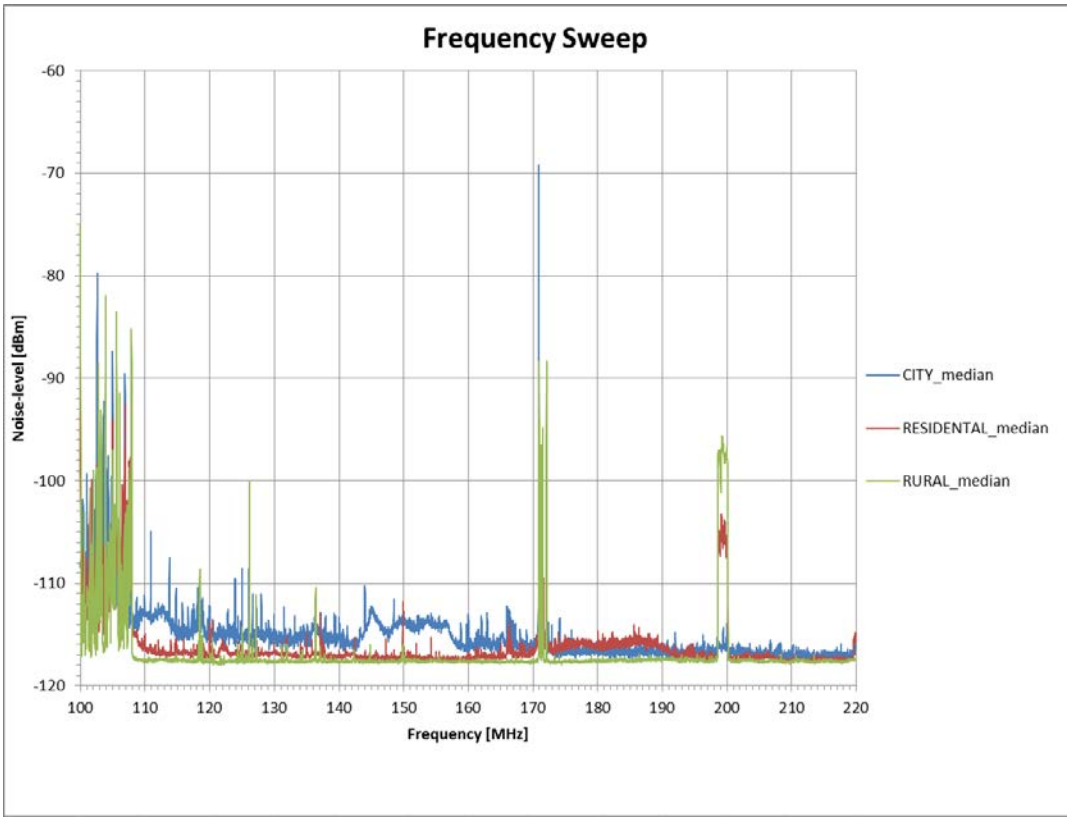

Figure G.2 Frequency sweeps of the three measured categories, median of all sweeps 100 – 220 MHz.

The data used for the sweep median calculations are not corrected according to the ITU model and reference antenna, but are the raw data output from the spectrum analyser measured with the dipole antennas.

H Intermodulation distortion

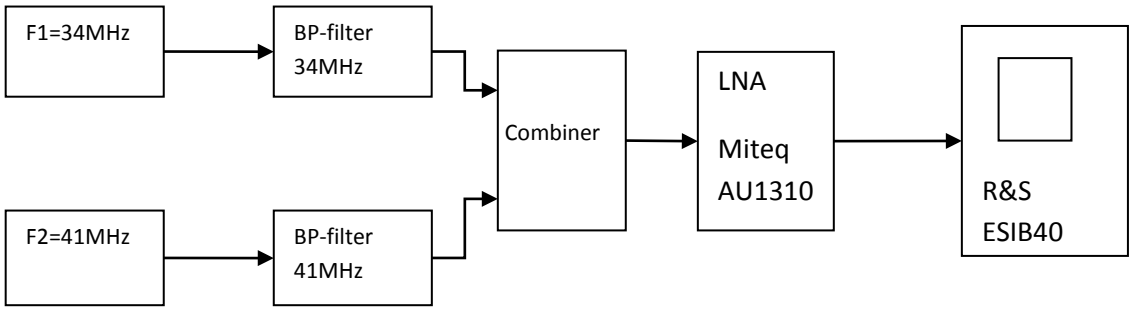

Figure H.1 Setup for measuring intermodulation distortion from LNA Miteq AU1310.

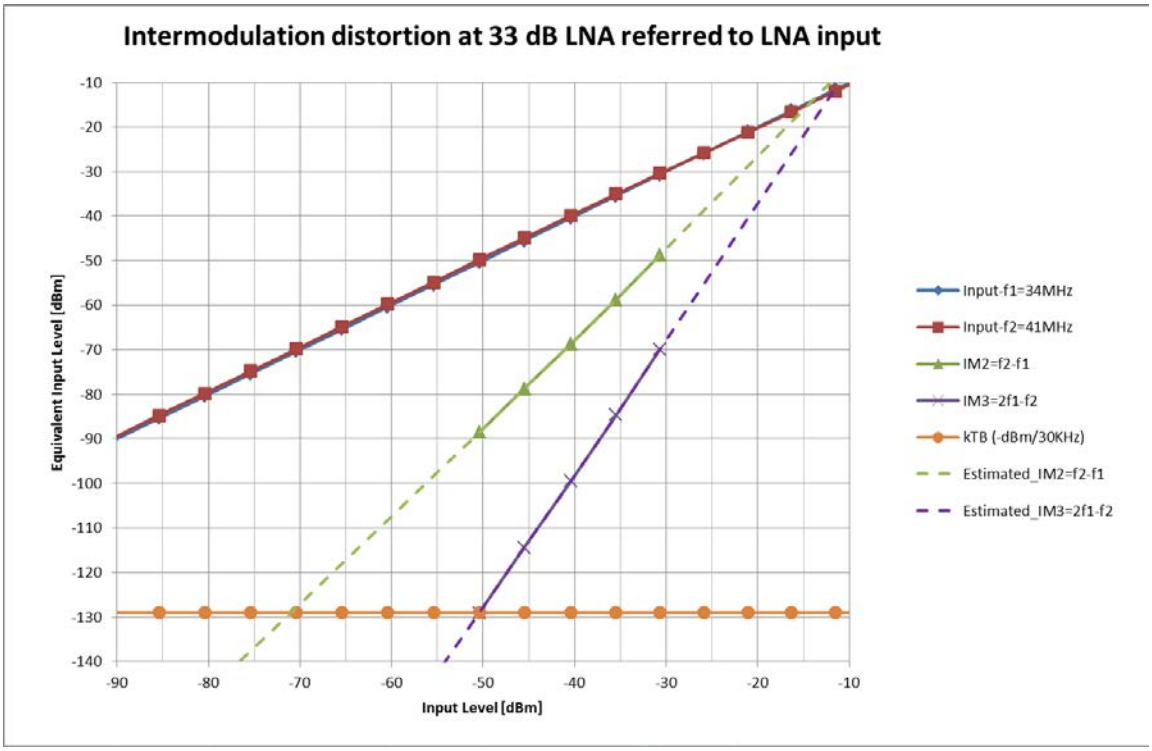

Figure H.2 Intermodulation distortion from LNA Miteq AU1310 with 33dB gain.

The intermodulation distortion (IMD), occur in devices when two or more signals at different frequencies at the device's input are strong enough. The IMD will reduce a receiver's ability to

receive weak signals. We can see where the IM traces cross the receiver's noisefloor. For instance, IM3 crosses the noisefloor at an input level of –50 dBm, then two signals at an input level of -50 dBm or higher, will generate IMD that reduces the receiver's sensitivity.

Even if the margins are quite good with -50 dBm, we must be aware that IMD may occur as interference in frequency sweeps and noise measurements.

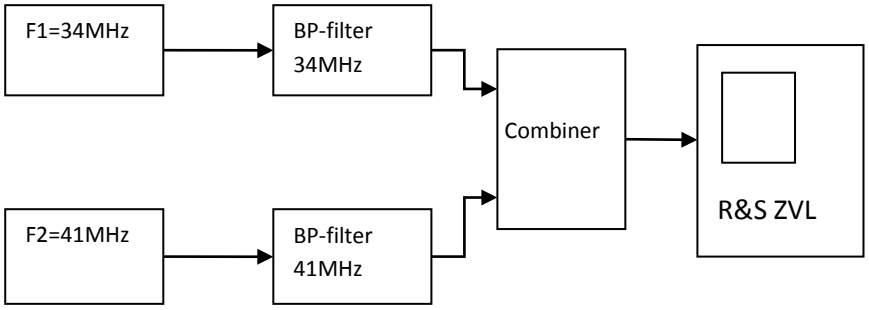

Figure H.3 Setup for measuring intermodulation distortion from spectrum analyser R&S ZVL.

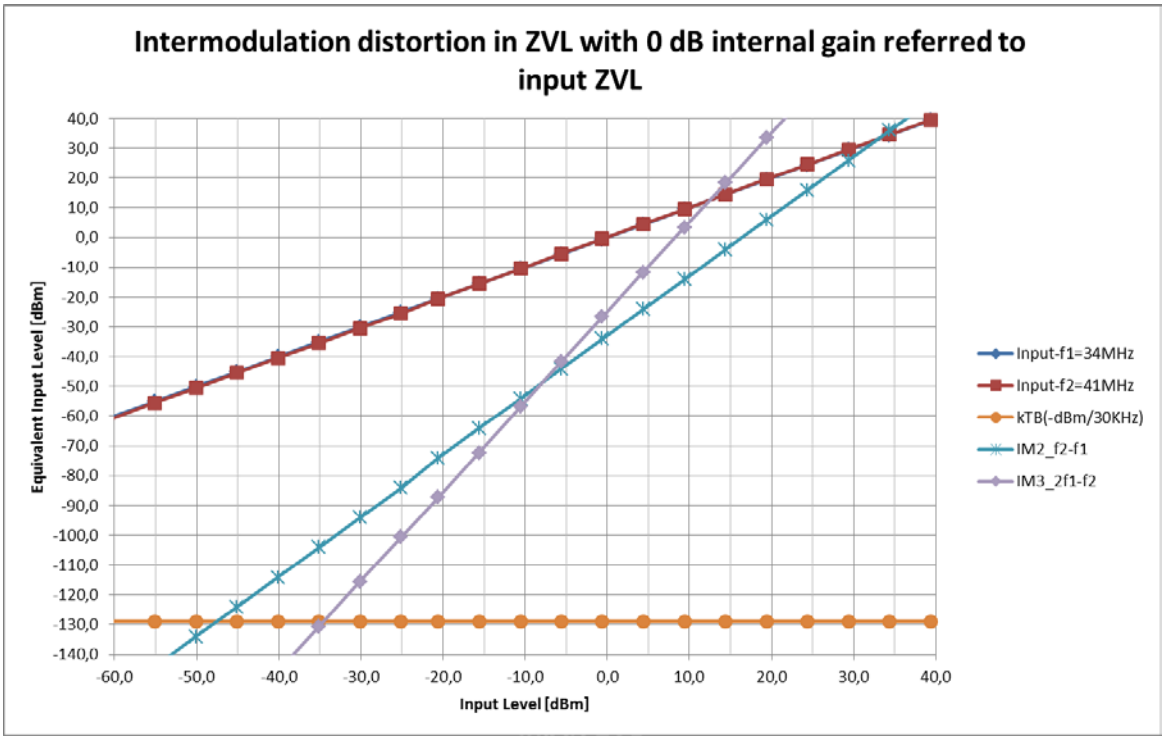

Figure H.4 Intermodulation distortion from spectrum analyser R&S ZVL without internal preamp.

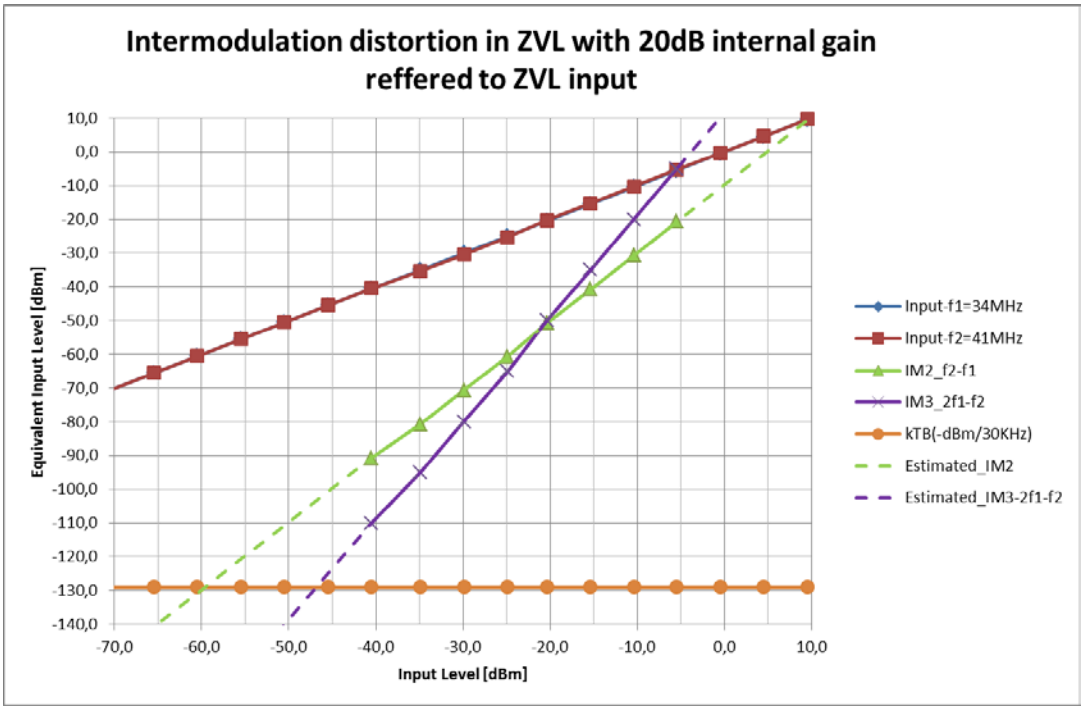

Figure H.5 Intermodulation distortion from spectrum analyser R&S ZVL with 20 dB internal preamp.

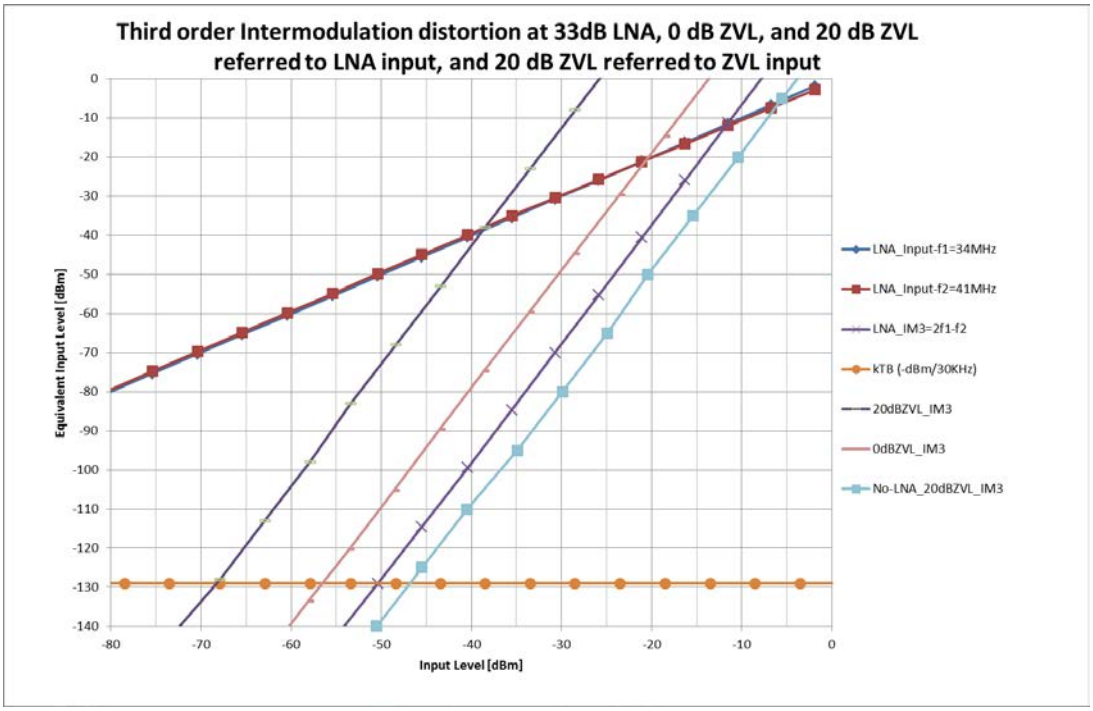

Figure H.6 Third order intermodulation distortion.

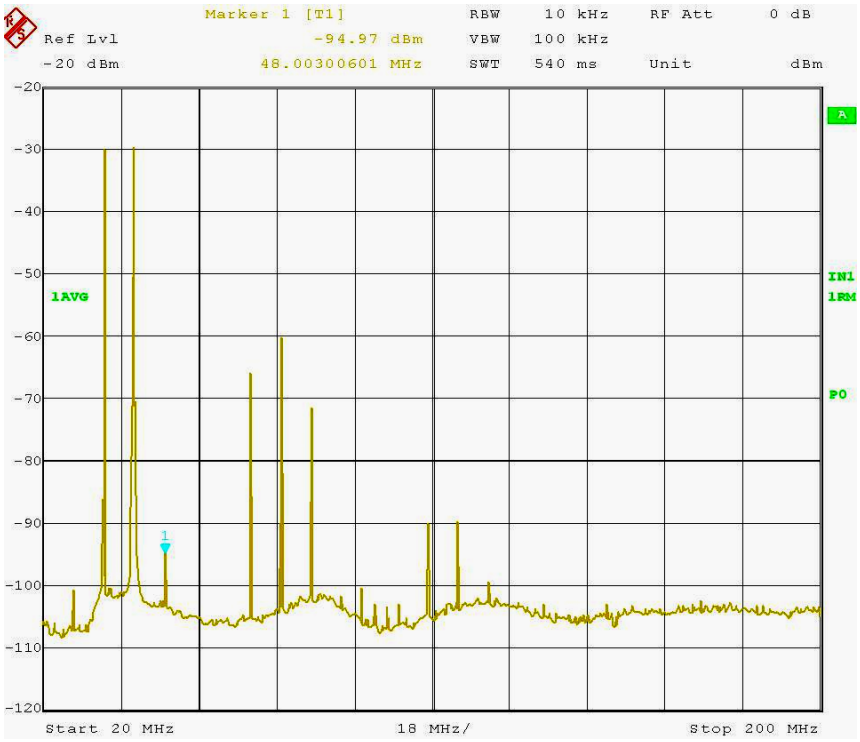

Figure H.7 Screen plot from measurement receiver and spectrum analyser ESIB40 showing intermodulation and harmonic distortion from LNA Miteq AU1310 with input frequencies at 34 MHz and 41 MHz. The output level from the sources is – 40 dBm.

I Listing of locations

Location	Date:	ITU - categori	Comments	Place	Address	Position	
						EPSG 4326 (NK) WGS84 - Desimal	
						Longitude	Latitude
2	03.07.2013	Residential	Parking lot, some trees, railway apprx 100m away, residential buildings apprx 200m away, open track and field area	Skedsmohallen, Lillestrøm	Leiraveien 2, 2000 Lillestrøm	59.96153	11.06549
3	05.07.2013	Residential	Parking lot, schools, at the edge of residentiall area, open field in 40% of area	Volla skole, Vestbygata, Lillestrøm	Vestbygata 59, 2000 Lillestrøm	59.96442	11.04289
4	08.07.2013	Residential	Open field in residential area, further down industrial/city areas and major roads and highways	Toppenhaug, Drammen	Lammers gate 22, 3014 Drammen	59.74765	10.22510
5	09.07.2013	Residential	Parking lot, hill, some open area, close to residential buildings/area, view to railway and citycenter	Slottsfjellet, Tønsberg	Slottsfjellet, 3111 Tønsberg	59.27267	10.40483
6	30.07.2013	Residential	Parking lot, mostly open area, larger residential areas apprx 100m	Borre track and field, Horten	Trimveien, 3188 Horten	59.40407	10.46135
7	05.08.2013	City	Parking lot, shipbuilding yard, industrial areas	Horten	Karljohansvern, 3190 Horten	59.42816	10.48879
8	05.08.2013	Rural	Crossing some km from E18 highway, farmland, apprx 500m to nearest farm and house, some traffic	Bruserudvegen, Vestfold	Bruserudveien / Kopstadveien, 3180 Nykirke	59.42085	10.34660

13-2	30.10.2013	Rural	Farmland, several 100m to nearest building, power lines near antenna, high power lines some 100m away. Complete measurement-series at new frequencies	Hammer'n, Sørum	Hammerenvegen, 1923 Sørum	59.99730	11.22423
16	30.10.2013	Rural	Farmland, open and flat, 300-500m to nearest bulidings, no powerlines	Såkroken, Sørum	Såkroken, 1923 Sørum	60.05918	11.23927
17	31.10.2013	Rural	Parking lot, recreation area, forest and (abandon?) buildings apprx 100m+ away, power lines	Skar, Maridalen	Skar, Maridalen, Oslo	60.02695	10.77859
18	6-7.11.2013	Residential	In the garden, 4-5m from the garage, 10-15m from the house, frequency-scans at lower frequencies, 10min noise capture at 84,5MHz several times to see variation with time, impuls noise, overload	Lørenfallet, Sørum	Lørenhagan 7, 1923 Sørum	60.02343	11.22479
18-2	07.11.2013	Residential	In the garden, 4-5m from the garage, 10-15m from the house, impuls noise, overload	Lørenfallet, Sørum	Lørenhagan 7, 1923 Sørum	60.02343	11.22479
18-3	07.11.2013	Residential	In the garden, 4-5m from the garage, 10-15m from the house, frequency-scans at lower frequencies, 1min noise capture at 114MHz several times to see variation with time, impuls noise, overload	Lørenfallet, Sørum	Lørenhagan 7, 1923 Sørum	60.02343	11.22479
19	08.11.2013	Residential	Open area, apprx some 10m+ to nearest buildings, flat, powerlines	Aursmoen	Falkeveien, 1930 Aurskog	59.92294	11.44813
20	08.11.2013	Rural	Parking at gravel road, 50-100m to nearest buildings, powerlines	Aursmoen - Tævsjøen, parking lot	Tævsjøveien, 1930 Aurskog	59.90992	11.45798
23	18.11.2013	Rural	Gravel road, small hilly terrain, farmland, apprx 150m+ to nearest buildings	Budorveien / Nordbygdveien	Budorveien / Nordbygdveien, 2340 Løten	60.86809	11.30617

24	22.11.2013	Residential	Open area, apprx some 10m+ to nearest buildings, flat	Løten	Bjørkerudvegen, 2340 Løten	60.81133	11.34434
34	25.11.2014	City	Shopping area, parking lot, traffic cross	City Nord/ Nordlandshallen, Bodø	City Nord, Stormyra, 8008 Bodø	67,27776	14,41859
35	26.11.2014	Residential	Recreation area, homes and offices	Prestvannet, Tromsø		69,66107	18,93648
36	26.11.2014	City	Shopping center, mobil basestation 30 - 50m, power, traffic at main road (E6) some 100m away. Some overload and non-white gaussian noise.	Pyramiden Amfi, Tromsdalen		69,64111	18,97274
37	27.11.2014	City	Shopping area, parking lot, Tromsø Airport ca 500m - 2km. Apprx 09.00 - 11.00. Traffic.	Europris, Jekta Shopping Centre, Tromsø		69,67566	18,9275
43	16.12.2014	City	Shopping area, parking lot, traffic, E6 - apprx. 400m.	Lillehammer	Strandtorget Kjøpesenter, 2609 Lillehammer	61,11355	10,45082

Figure I.1 Listing of noise measurement locations.

J Maps and photos of locations

In this section, the maps (i.e. flight photos) are all excerpted from “norgeskart.no” (20), a web-site administrated by the Norwegian Mapping Authority (Statens Kartverk), “kartverk.no” (21), ©Kartverket.

J.1 Location_2

Figure J.1 Map and view at location 2, Skedsmohallen, Lillestrøm. Red dot on map indicates antenna position.

J.2 Location_3

Figure J.2 Map and view at location 3, Volla, Lillestrøm. Red dot on map indicates antenna position.

J.3 Location_4

Figure J.3 Map and view at location 4, Toppenhaug, Drammen. Red dot on map indicates antenna position.

J.4 Location_5

Figure J.4 Map and view at location 5, Slottsfjellet, Tønsberg. Red dot on map indicates antenna position.

J.5 Location_6

Figure J.5 Map at location 6, Borre track and field, Horten. Red dot on map indicates antenna position.

J.6 Location_7

Figure J.6 Map at location 7, industrial area, Horten. Red dot on map indicates antenna position.

J.7 Location_8

Figure J.7 Map and view at location 8, Bruserudveien, Vestfold. Red dot on map indicates antenna position.

J.8 Location_13

Figure J.8 Map and view at location 13, Hammeren, Sørum. Red dot on map indicates antenna position.

Figure J.9 View at location 13.

J.9 Location_16

Figure J.10 Map and view at location 16, Såkroken, Sørum. Red dot on map indicates antenna position.

J.10 Location_17

Figure J.11 Map and view at location 17, Skar, Maridalen. Red dot on map indicates antenna position.

J.11 Location_18

Figure J.12 Map and view at location 18, Lørenhagan, Sørum. Red dot on map indicates antenna position.

J.12 Location_19

Figure J.13 Map and view at location 19, Aursmoen. Red dot on map indicates antenna position.

J.13 Location_20

Figure J.14 Map and view at location 20, Tævsjøen parking lot, Aursmoen. Red dot on map indicates antenna position.

J.14 Location_23

Figure J.15 Map and view at location 23, Budor-/Nordbygdveien, Løten. Red dot on map indicates antenna position.

J.15 Location_24

Figure J.16 Map and view at location 24, Bjørkerudveien, Løten. Red dot on map indicates antenna position.

J.16 Location_34

Figure J.17 Map and view at location 34, City Nord, Bodø. Red dot on map indicates antenna position.

J.17 Location_35

Figure J.18 Map and view at location 35, Prestvannet, Tromsø. Red dot on map indicates antenna position.

J.18 Location_36

Figure J.19 Map and view at location 36, Pyramiden Amfi, Tromsdalen. Red dot on map indicates antenna position. Notice the communication tower in the background.

J.19 Location_37

Figure J.20 Map and view at location 37, Jekta shopping, Tromsø. Red dot on map indicates antenna position.

J.20 Location_43

Figure J.21 Map at location 43, Strandtorget shopping, Lillehammer. Red dot on map indicates antenna position.

About FFI

The Norwegian Defence Research Establishment (FFI) was founded 11th of April 1946. It is organised as an administrative agency subordinate to the Ministry of Defence.

FFI's MISSION

FFI is the prime institution responsible for defence related research in Norway. Its principal mission is to carry out research and development to meet the requirements of the Armed Forces. FFI has the role of chief adviser to the political and military leadership. In particular, the institute shall focus on aspects of the development in science and technology that can influence our security policy or defence planning.

FFI's VISION

FFI turns knowledge and ideas into an efficient defence.

FFI's CHARACTERISTICS

Creative, daring, broad-minded and responsible.

Om FFI

Forsvarets forskningsinstitutt ble etablert 11. april 1946. Instituttet er organisert som et forvaltningsorgan med særskilte fullmakter underlagt Forsvarsdepartementet.

FFIs FORMÅL

Forsvarets forskningsinstitutt er Forsvarets sentrale forskningsinstitusjon og har som formål å drive forskning og utvikling for Forsvarets behov. Videre er FFI rådgiver overfor Forsvarets strategiske ledelse. Spesielt skal instituttet følge opp trekk ved vitenskapelig og militærteknisk utvikling som kan påvirke forutsetningene for sikkerhetspolitikken eller forsvarsplanleggingen.

FFIs VISJON

FFI gjør kunnskap og ideer til et effektivt forsvar.

FFIs VERDIER

Skapende, drivende, vidsynt og ansvarlig.

FFI's organisation

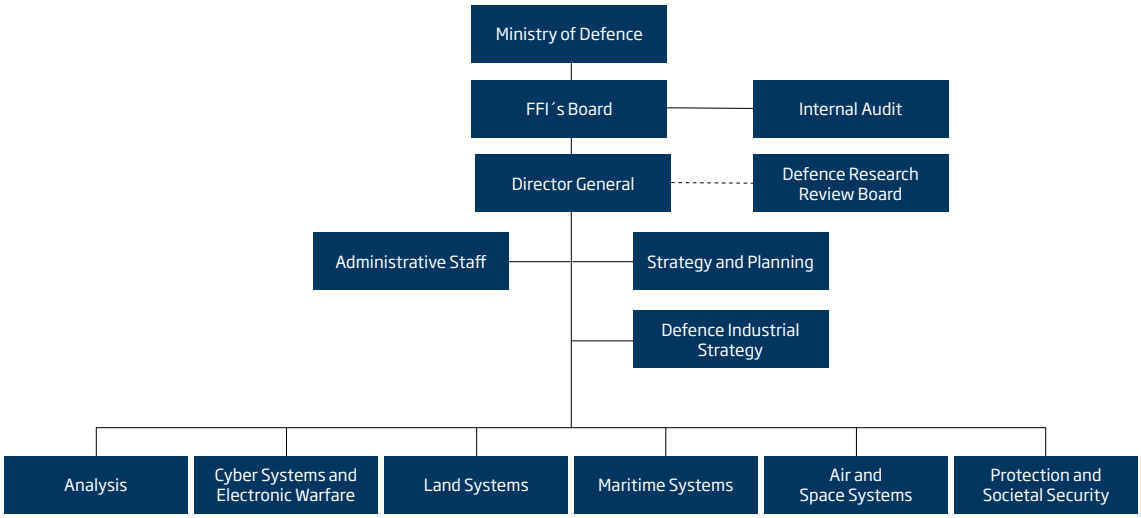

Forsvarets forskningsinstitutt
Postboks 25
2027 Kjeller

Besøksadresse:
Instituttveien 20
2007 Kjeller

Telefon: 63 80 70 00
Telefaks: 63 80 71 15
Epost: ffi@ffi.no

Norwegian Defence Research Establishment (FFI)
P.O. Box 25
NO-2027 Kjeller

Office address:
Instituttveien 20
N-2007 Kjeller

Telephone: +47 63 80 70 00
Telefax: +47 63 80 71 15
Email: ffi@ffi.no

FFI Forsvarets forskningsinstitutt
Norwegian Defence Research Establishment